CR-151346

(NASA-CR-151346) BALLOON STRATOSPHERIC RESEARCH FLIGHTS, APRIL 1976 TO DECEMBER 1976 (Lockheed Electronics Co.) 169 p HC A08/MF A01 CSCL 04A

N77-23645

Unclas G3/46 26089

ENVIRONMENTAL EFFECTS OFFICE

INTERNAL REPORT

BALLOON STRATOSPHERIC RESEARCH FLIGHTS

APRIL 1976 TO DECEMBER 1976

PREPARED BY

LOCKHEED ELECTRONICS CO., INC.

SERVICES SYSTEMS DIVISION

UNDER CONTRACT

NAS9-15200

FOR

National Aeronautics and Space Administration

LYNDON B. JOHNSON SPACE CENTER

Houston, Texas

MARCH 1977

LEC-9905

ENVIRONMENTAL EFFECTS OFFICE

INTERNAL REPORT

BALLOON STRATOSPHERIC RESEARCH FLIGHTS
APRIL 1976 TO DECEMBER 1976

SUBMITTED BY:

Norman C. Allen/LEC

APPROVED BY:

John F. Stanley/SC4

Andrew E. Potter, Jr./SC4

LEC-9905

CONTENTS

Section Page

FIGURES

TABLES

APPENDIXES

Appendix

1.0 GENERAL SUMMARY

The NASA/JSC Environmental Effects Office (EEO), in conjunction with several government and private agencies, conducted five balloon-parachute flights from the National Scientific Balloon Facility (NSBF) at Palestine, Texas, during the period from May 1976 through October 1976. These flights (see Table I) were designed to measure the vertical concentration profile of trace stratospheric species which form major links in the chlorine photochemical system of the upper atmosphere. As such, they represent a continuation of the previous six flights in this series which were instrumented to measure the vertical concentration profiles of atomic oxygen, the hydroxyl radical and ozone in the stratosphere. These earlier flights are fully documented in JSC Internal Report JSC-11846 (Balloon Stratospheric Research Flights - November 1974 to January 1976) dated October 1976.

This document contains an overview of the scientific goals of the program, a statement of program management and support functions, a brief description of the instrumentation flown, pertinent engineering and payload operations data, and a summary of the scientific data obtained for four flights during the period from May 1976 through October 1976. Results of the 14-meter parachute Test Flight, flown on 5-2-76, are described in a Quick-Look Flight Report (ref. TC-76-337, dated 5-10-76) prepared by NASA/JSC/EEO and are not discussed in this report.

TABLE I. BALLOON STRATOSPHERIC RESEARCH FLIGHTS
APRIL 1976 TO DECEMBER 1976

Flight	NCAR Flight No.	Type of Experiment	Date Launch Time Release Time	
7	954-P	1st Chlorine Oxide (ClO-1) Measurement (ClO/Aerosol-1)	4-4-76 (1) 1053 CST 1534 CST	NASA/JSC-NCAR-University of Michigan (2) - Langley Research Center/ University of Pittsburgh (4) - Wallops Flight Center (5)
8	961-P	Parachute Test Flight (14-meter Diameter Guide Surface and 16.75-meter Diameter Cross Parachute)	5-2-76 0655 CDT 1041 CDT (JSC) 1045 CDT (GSFC)	NASA/JSC-NCAR-GSFC (6) - University of Michigan (7)
9	965-P	2nd Chlorine Oxide (ClO-2) Measurement (ClO/Grab Sample-2)	5-15-76 0727 CDT 1200 CDT	NASA/JSC-NCAR-University of Michigan (2) & (3)
10	977-P	1st Atomic Chlorine/ Chlorine Oxide (Cl/ClO-1) Measurement (Cl-ClO-1)	7-28-76 0829 CDT 1241 CDT	NASA/JSC-NCAR-University of Michigan (2) - Wallops Flight Center (5)
11	990-P	2nd Atomic Chlorine/ Chlorine Oxide (Cl/ClO-2) Measurement ($Cl/ClO/O_3$)	10-2-76 0759 CDT 1215 CDT	NASA/JSC-NCAR-University of Michigan (2) - Wallops Flight Center (5)
12	1001-P	3rd Atomic Chlorine/ Chlorine Oxide (Cl/ClO-3) Ozone O_3 Total Air Temp (TAT)	12-8-76 0853 CDT 1200 CDT	NASA/JSC-NCAR-University of Michigan (2) - Wallops Flight Center (5)

(1) The first attempt to launch the 1st Chlorine Oxide (ClO) Measurement payload on 4-1-76 was aborted on the launch pad due to insufficient balloon lift.
(2) Resonance/fluorescence instrumentation ;(3) Grab sample instrumentation ; (4) Aerosol instrumentation ; (5) Ozonesondes ; (6) 16.75-meter cross parachute ; (7) Solar background (118.8 nm) counter instrumentation and multi-module instrument support frame

2.0 SCIENTIFIC RATIONALE AND GOALS

Over the past decade, as our understanding of the delicate photochemical balance of the Earth's upper atmosphere has expanded, it has become clear that irreversible harm can be done to this region of the atmosphere by contaminants released at the Earth's surface or in the lower atmosphere. Of particular concern is the depletion of stratospheric ozone (O_3) - an important natural resource due to its unique capability of screening the Earth's surface from ultraviolet radiation. Attempts to quantitatively predict photochemical perturbations of the ozone layer (and thus variations in the ultraviolet dosage reaching the surface) resulting from the injection and diffusion of gases into the stratosphere, have demonstrated that insufficient empirical knowledge exists regarding the concentration of various atomic and diatomic radicals in the stratosphere. These minor species are thought to control ozone through catalytic reaction cycles.*

Although our appreciation for potential problems has grown, our understanding of the fundamental physical and chemical processes which control the stratosphere is incomplete and seriously lacking in observational verification. In particular, most of the major atomic and diatomic species which are thought to couple the oxygen, hydrogen, nitrogen, and chlorine photochemical systems together have

* A description of ozone chemistry and ozone reduction by catalytic reaction cycles is given in JSC Internal Note JSC-09688 (Fundamentals of Stratospheric Ozone) dated June 1975.

never been observed. Thus, it is difficult to defend theories which attempt to correlate the injection of a stable compound with, for example, the depletion of stratospheric ozone.

The complexity of stratospheric photochemistry is illustrated in figure 1. The major chemical source terms, indicated by upward-pointing arrows, are relatively stable polyatomic molecules released from the earth's surface and within the troposphere. These species have chemical lifetimes on the order of weeks to months so that their upward flow and global distribution is, in general, governed by transport processes. The linking radicals are formed directly (and irreversibly) from the chemical source terms either by photolysis (dissociation by ultraviolet solar radiation) or chemical reaction. The radicals, in contrast to the source terms, have chemical lifetimes on the order of minutes and they thus reflect the chemical conditions in their immediate vicinity. The reservoir or sink terms, indicated by downward-pointing arrows, are formed by the recombination of the radicals. Like the source terms, they are rather stable chemically but may be recycled into the radical system by photolysis and chemical reaction or removed by downward and meridional transport.

The NASA/JSC Environmental Effects Project Office, in conjunction with several government and private agencies, is studying the vertical concentration profiles of those radicals which form major links in the photochemical systems of the stratosphere. The goal of the

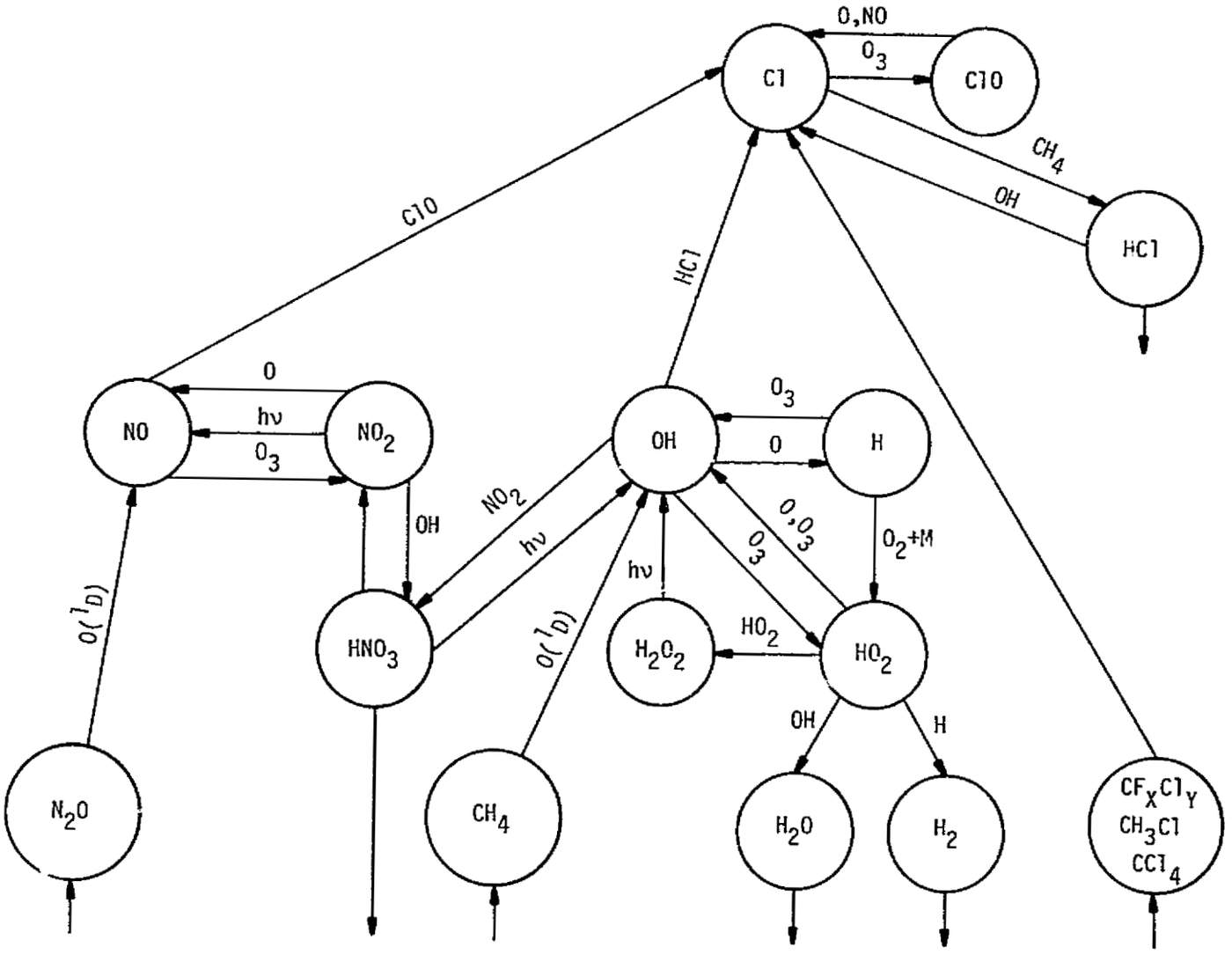

Figure 1.— Oxygen, hydrogen, nitrogen and chlorine photochemical systems.

research is to determine simultaneously the absolute concentration of one or more radicals in each of the major stratospheric systems. This will allow for empirical verification of calculated ozone depletion resulting from the presence of hydrogen, nitrogen, and chlorine source gases in the stratosphere. The data gathered are indicative of the current state of the stratosphere and will establish an invaluable basis for measurement of future changes in the concentration of the critical trace species. Among the most important constituents are atomic oxygen, ozone, hydrogen, chlorine, and the oxides of hydrogen, nitrogen, and chlorine - all of which are under study at the present time. This report documents five balloon-parachute flights conducted to measure the concentration of atomic chlorine (Cl) and/or chlorine oxide (ClO) at various levels in the stratosphere. Reference measurements of stratospheric ozone (conducted *via* radiosonde), ancillary measurement of stratospheric aerosols, and the collection of stratospheric gases using a grab sample technique are also documented.

3.0 PROGRAM MANAGEMENT

The JSC Science and Applications Directorate is responsible for the overall direction and evaluation of the balloon-parachute stratospheric measurements program.

4.0 PROGRAM SUPPORT

The JSC/Environmental Effects Office (EEO) conducts the balloon-parachute flight operations. Prime overall technical and operational support of the payload is provided by Lockheed Electronics Company, Inc. (LEC), under terms of a scientific and engineering support services contract to JSC. The National Center for Atmospheric Research (NCAR) provides prime operational support such as launch operations, payload tracking, recovery operations, range safety, facilities, and meteorological data.

The University of Michigan working under contract to the EEO has responsibility for the resonance fluorescence and grab sample instrumentation. Data reduction and analysis for measurements obtained with this instrumentation are the joint responsibility of the University of Michigan and the EEO. The University of Pittsburgh under the sponsorship of Langley Research Center is responsible for ancillary aerosol particle counter instrumentation flown on the first ClO flight and also for reduction and analysis of the aerosol data. Wallops Flight Center is responsible for operation of the reference ozone (radiosonde) instrumentation and for data reduction of the resulting ozone measurements.

In addition to scientific and managerial administration of the program, NASA/JSC also provides logistics and technical support for the flights. The JSC/Logistics Division is responsible for transportation of payload

and support equipment to the NCAR facility. The JSC/Space Environment Test Division assists in demonstrating the capability of the instrumentation to withstand the thermal and vacuum conditions encountered during balloon flights. The JSC/Space Vehicle Battery Facility is responsible for the preparation and delivery of the flight and spare battery and for the up-looking motion picture camera. The JSC/Photographic Division provides documentary photography for launch, flight, and recovery.

5.0 BALLOON OBSERVATION OF STRATOSPHERIC SPECIES (BOSS) FLIGHTS

5.1 FIRST CHLORINE OXIDE (ClO-1) MEASUREMENT

(NCAR FLIGHT NO. 954-P)

4 April 1976

5.1.1 SUMMARY

This balloon-parachute flight was the sixth flight of the laminar flow through/resonance fluorescence instrument (principal investigator: Dr. James Anderson, University of Michigan) and took place on 4 April 1976. The purposes of the flight were to measure the vertical concentration profile of chlorine oxide (ClO) in the 25 to 45 km altitude range and to obtain an *in situ* grab sample of stratospheric gas at an altitude of approximately 20 km. An ancillary experiment was again flown as part of the payload to perform counting measurements (as a function of altitude) of stratospheric aerosols with surface-ionizable constituents.

The first attempt to launch the ClO instrument payload was made at 1015 CST on 1 April 1976 and is recorded as NCAR Flight Number 952-P. This launch failed due to insufficient balloon lift. An investigation of the failure identified the problem as being the direct result of incorrectly recording the weight of the flight package. The two most significant digits were transposed such that the weight was recorded as 570 pounds (not 750 pounds as was correct). As a result, insufficient helium was loaded into the balloon and the flight was aborted on the launch pad immediately after release from the launch vehicle. Minimal damage was incurred by the payload but the framework protecting the grab sample bottle was crushed and the frangible tube on the experiment was broken allowing contaminating gases to enter the sample bottle. This experiment was changed out prior to the next launch attempt.

A successful launch of the ClO instrument payload was achieved at 1053 CST on 4 April 1976 from the NSBF at Palestine, Texas. Hardware consisted of a 4.3×10^5 cubic meter balloon, 9.75-meter guide surface parachute, NCAR telemetry system, JSC flight support module, the resonance fluorescence instrument modified to measure the concentration of ClO, a grab sample bottle, and an aerosol particle counter to monitor the presence of particulates larger and/or richer in surface ionizable constituents than a pre-set discrimination level. The University of Michigan was responsible for the resonance fluorescence and the University of Pittsburgh, under the sponsorship of Langley Research Center, was responsible for the aerosol particle counter instrumentation and for reduction and analysis of the aerosol data.

The payload weighed approximately 290 kg, and consisted of telemetry, balloon control, descent-observation, and scientific instrumentation. A sketch of the payload showing the placement antennae and instrumentation is shown in figure 2. The modifications made in the placement of antennae and the antennae support structures for the previous flight of this series (the Third Hydroxyl OH($X^2\pi$) Flight) were adopted for the present flight. Figure 3 is a photograph of the payload hanging from the launch vehicle taken a few minutes prior to lift-off.

Instrumentation carried as part of the payload consisted of NCAR and JSC telemetry instrumentation, NCAR balloon control instrumentation, NCAR and JSC pressure transducers to measure the altitude of the payload, two vertical reference gyros to measure payload attitude, a

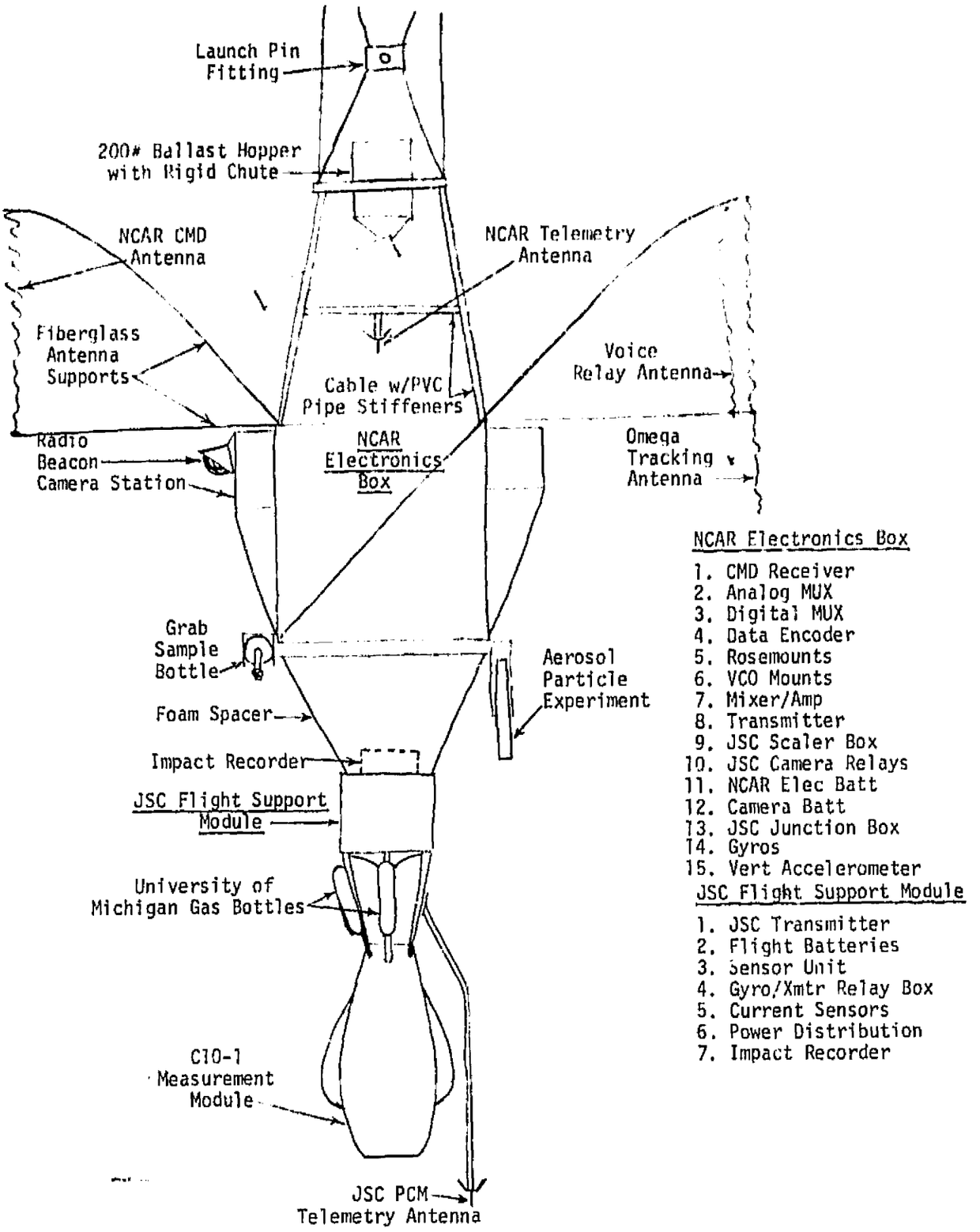

Figure 2. Sketch of the First Chlorine Oxide (ClO-1) Payload

NASA
S- 76- 24292

Figure 3. First Chlorine Oxide (ClO-1) Payload Ready for Launch

z-axis accelerometer to determine the loading forces when the parachute is deployed, a single up-looking motion picture camera (64 frames/sec using a 10 mm lens) to observe parachute opening and descent characteristics, the laminar flow through/resonance fluorescence instrument to measure the concentration of chlorine oxide, and an aerosol particle counter to monitor the presence of particulates. A grab sample bottle experiment from the University of Michigan was originally planned, but it was damaged in the pad abort on 4/1/76; consequently, it was not operational during this flight. Two ozone radiosondes were scheduled to be launched in conjunction with the flight to make correlative measurements of the concentration of stratospheric ozone.

Function, manufacturer, model, and serial numbers for support instrumentation are itemized in Appendix A. Pertinent electrical and mechanical drawings are listed in Appendix B. A description of the telemetry systems and channel allocations is given in Appendix C. Photographic documentation for the flight is itemized in Appendix D.

The payload reached a float altitude of 44.5 km (146 k ft) at approximately 1400 CST after a normal ascent. However, the payload did not respond to commands to activate the resonance fluorescence instrument.

A series of command transmissions (including sending commands from the tracking aircraft, sending commands with different code addresses and sending all programmed commands including FLIGHT TERMINATE failed to produce any response from the payload. The flight was terminated

automatically by the on-board backup timer at 1534:44 CST with housekeeping data being received until 1541 CST. Due to the failure of the payload to respond to commands, none of the scientific objectives of the flight were achieved.

The payload landed in a clearing approximately 32 minutes after payload release about 25 nm NW of Jackson, Mississippi. The recovery crew found that the ballast hopper contained 25 kg of ballast at the impact site. Comparing this value with the command/ballast log indicated that the failure occurred betweeen 1310 and 1320 CST (about 2 hours, 20 minutes into the flight) at an altitude of approximately 38 km (125 k ft). The payload was recovered and returned to the NSBF at Palestine on 5 April 1976. Post flight analysis by NSBF, JSC/EEO and LEC personnel during the period from 6-9 April 1976 isolated the failure to the on-board PCM command decoder system. A complete description of the investigation is contained in a report from JSC/EEO to NASA Headquarters entitled "ClO Flight Failures and Corrective Action" Reference TC-76-314 dated April 26, 1976.

5.1.2 PAYLOAD OPERATIONS

5.1.2.1 Ascent Phase

After the abortive attempt to launch the first chlorine oxide ClO payload on 1 April (designated as NCAR Flight No. 952-P), a successful launch occurred at 1053 CST, 4 April 1976, and was accomplished using

the dynamic launch technique. The flight profile for the First Chlorine Oxide ClO Flight is illustrated in figure 4. The balloon system ascended at an average rate of 4.0 meters per second to a float altitude of 44.5 km. The altitude of the payload was measured by three pressure transducers: a high range (0.1-0 psi), a medium range (1-0 psi) and a low range (15-0 psi). Figure 5 is a plot of the altitude data obtained from these three sensors during the ascent and float phases of the flight. Except for the data at ~44.5 km, the portions of the curves where the indicated altitude is nearly constant with time indicate the saturation levels of the pressure transducers. An apparent discrepancy exists between the high and medium sensors of about 1.2 km.

5.1.2.2 Descent Phase

The payload failed to respond to commands and the payload was released automatically by the backup on-board timer at 1534:44 CST. The z-axis accelerometer measured the loading forces while two vertical reference gyros monitored the descent attitude of the system. Payload altitude as measured by the three pressure transducers during descent is plotted in figure 6. The discrepancy in the altitude data as measured by the three sensors is apparent. The velocity/altitude profile of the descending payload is shown in figure 7. The velocities on this flights are comparable to those of previous flights. The vertical force on the payload during parachute deployment is illustrated in figure 8. The payload reached terminal velocity in about 33 seconds

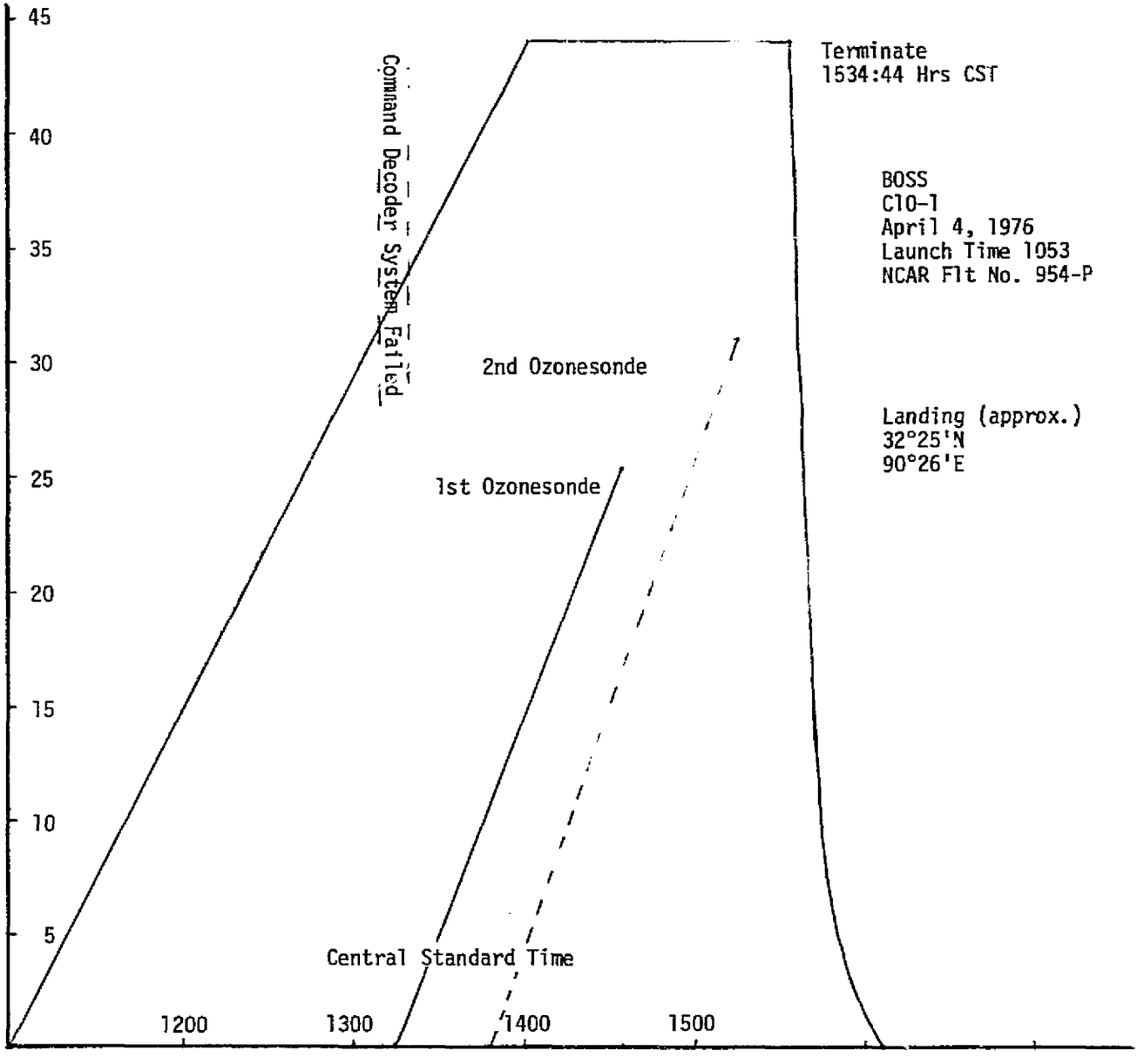

Figure 4. Flight Profile for the First Chlorine Oxide (ClO-1) Flight

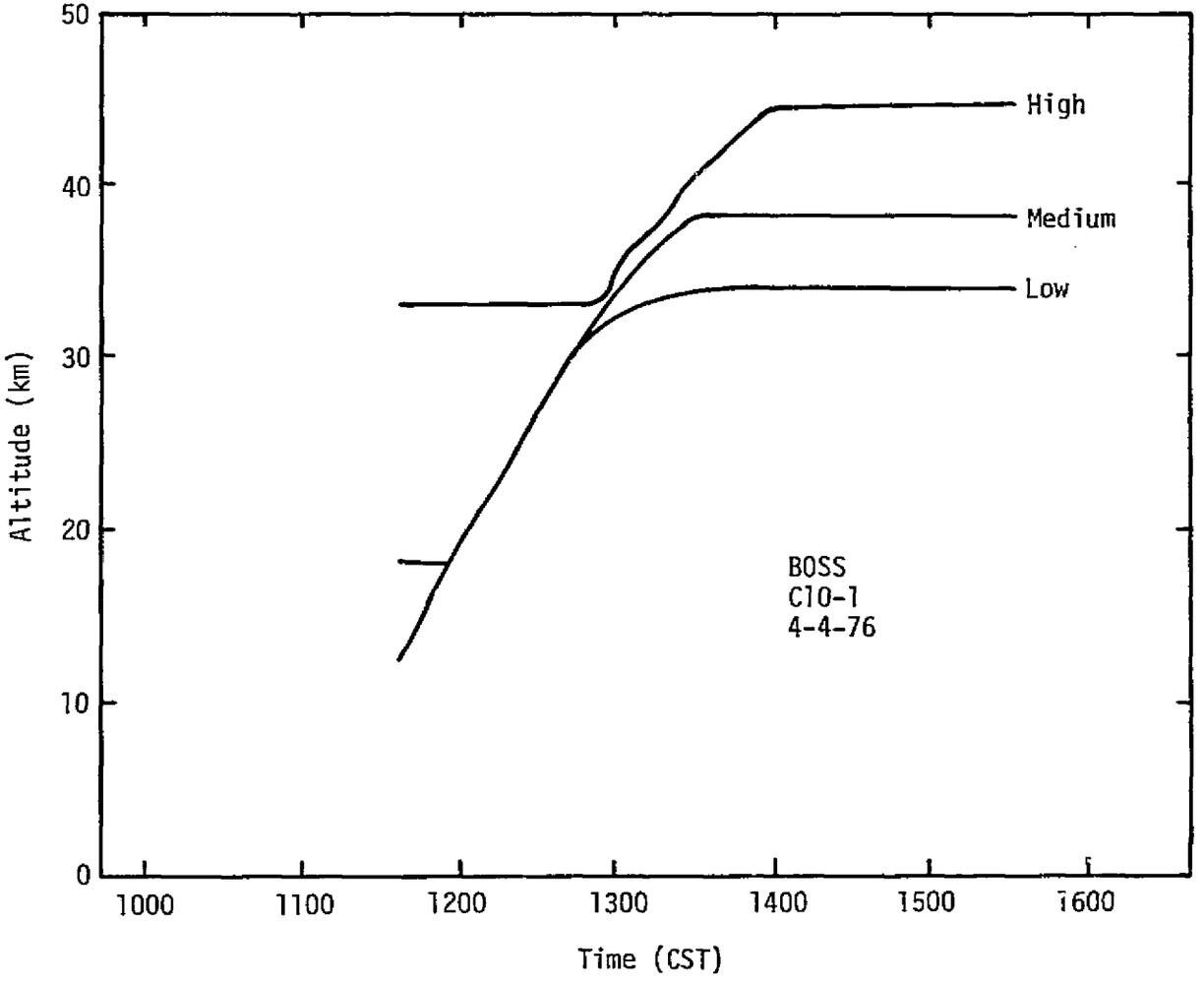

Figure 5. Altitude/time profiles for the ascending payload during the first Chlorine Oxide (ClO-1) flight as measured by three pressure transducers.

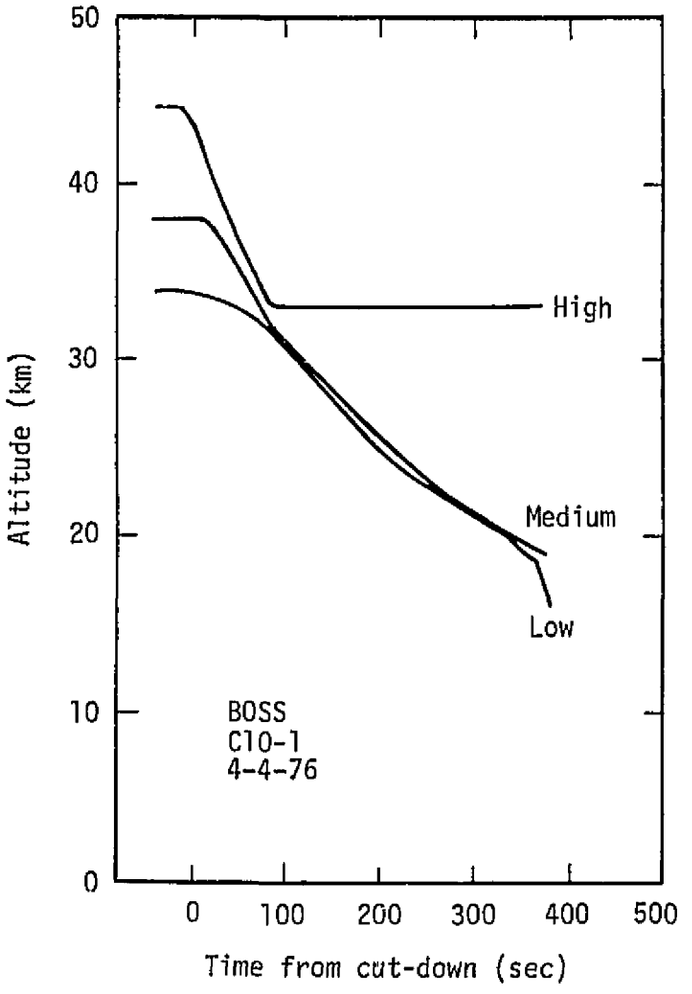

Figure 6. Altitude/time profiles for the descending payload during the first Chlorine Oxide (C10-1) flight as measured by three pressure transducers.

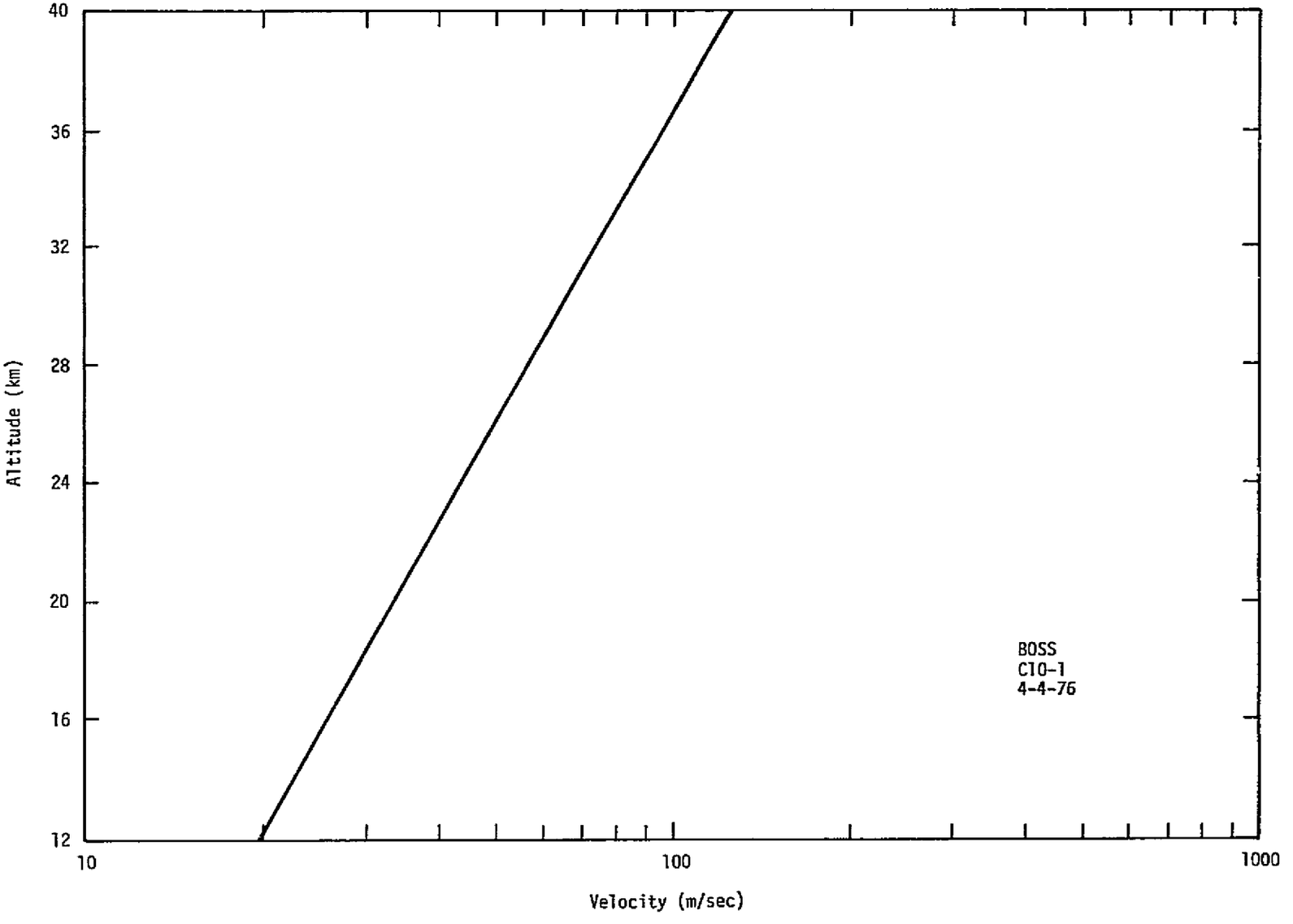

Figure 7. Velocity/altitude profile of descending payload for the First Chlorine Oxide (C10-1) flight

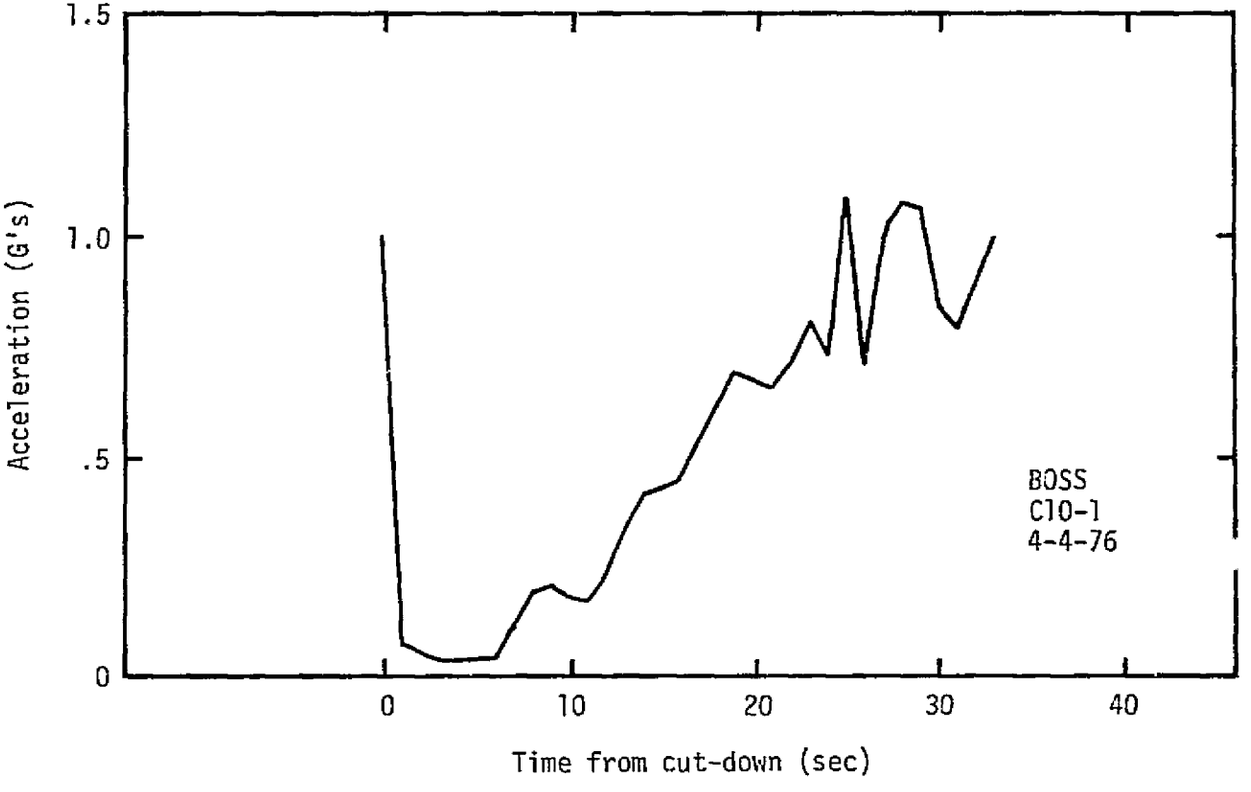

Figure 8. Vertical force on payload after parachute deployment for the first Chlorine Oxide (C10-1) flight

as is normal for this parachute. Figure 9 shows the probability that the angular deviation of the payload from vertical is less than a given angle as a function of angle during the first 7 minutes of descent. The payload was within 10 degrees of vertical 40% of the time and was within 15 degrees of vertical 75% of the time. This flight had somewhat more oscillation in the descent than the previous flight of this series but the degree of stability is still roughly comparable to the stability exhibited by the parachute system in the past.

5.1.2.3 Power and Temperature Profiles

Due to the command system failure, the ClO experiment could not be turned ON and very little power was consumed. The total power used by the complete payload was 10.5 ampere-hours with the ClO experiment accounting for only 2.68 ampere-hours of this total. The integrated power consumption is plotted as a function of time in figure 10. Figure 11 is a thermal history of the battery and transmitter for the flight. The curves show a warm launch temperature and the normal drop in temperature as the payload gained altitude.

5.1.3 POSTFLIGHT ACTIVITIES

The parachute/payload landed in a clearing approximately 32 minutes after payload release 25 nm NW of Jackson, Mississippi. The recovery crew found that the ballast hopper contained 25 kg of ballast at the impact site. Comparing this value with the command/ballast log indicated that the failure occurred between 1310 and 1320 CST at an altitude

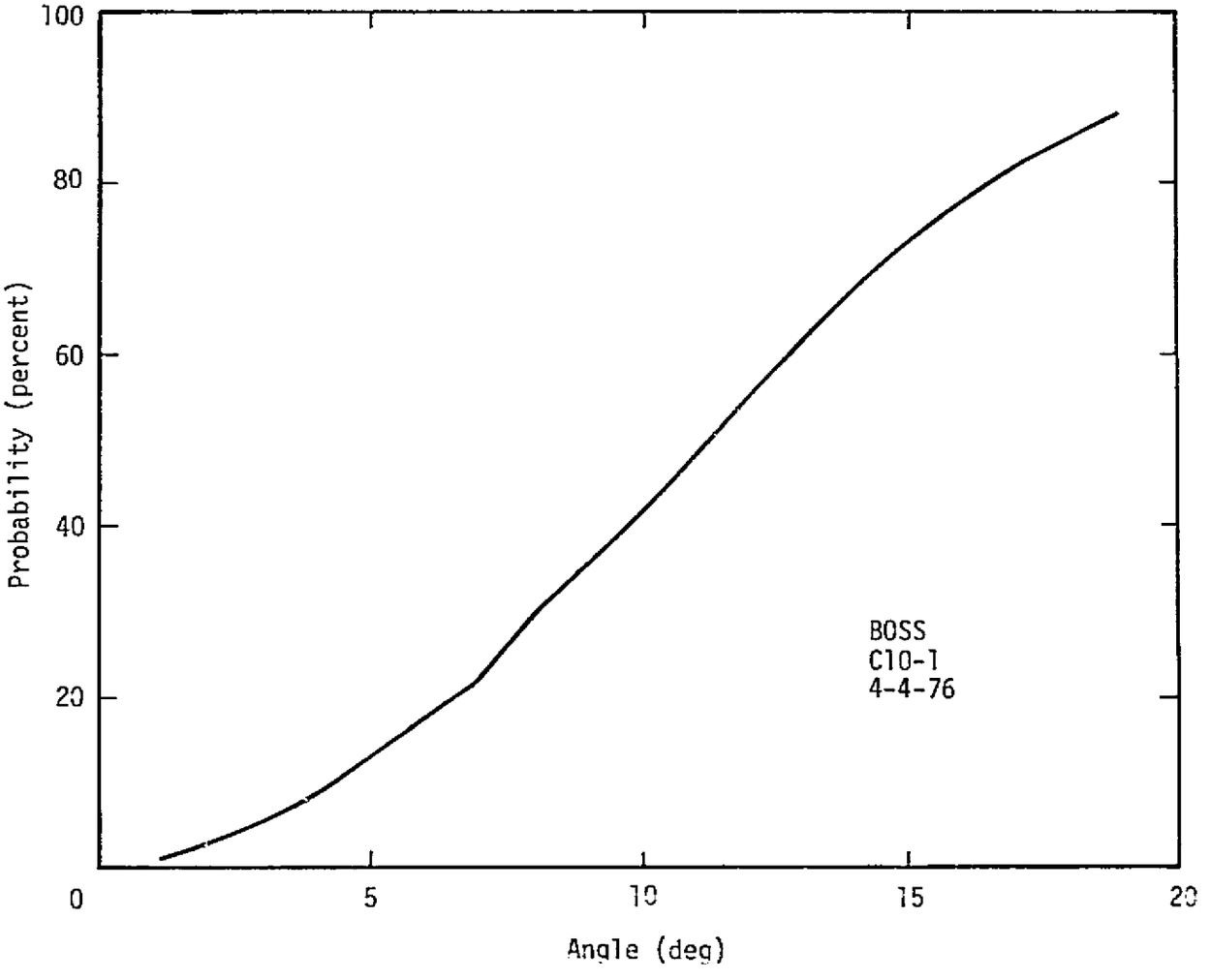

Figure 9. Probability (percent) that the angular deviation of the payload from vertical is less than a given angle as a function of angle for the first 7 minutes during descent of the first Chlorine Oxide (C10-1) flight.

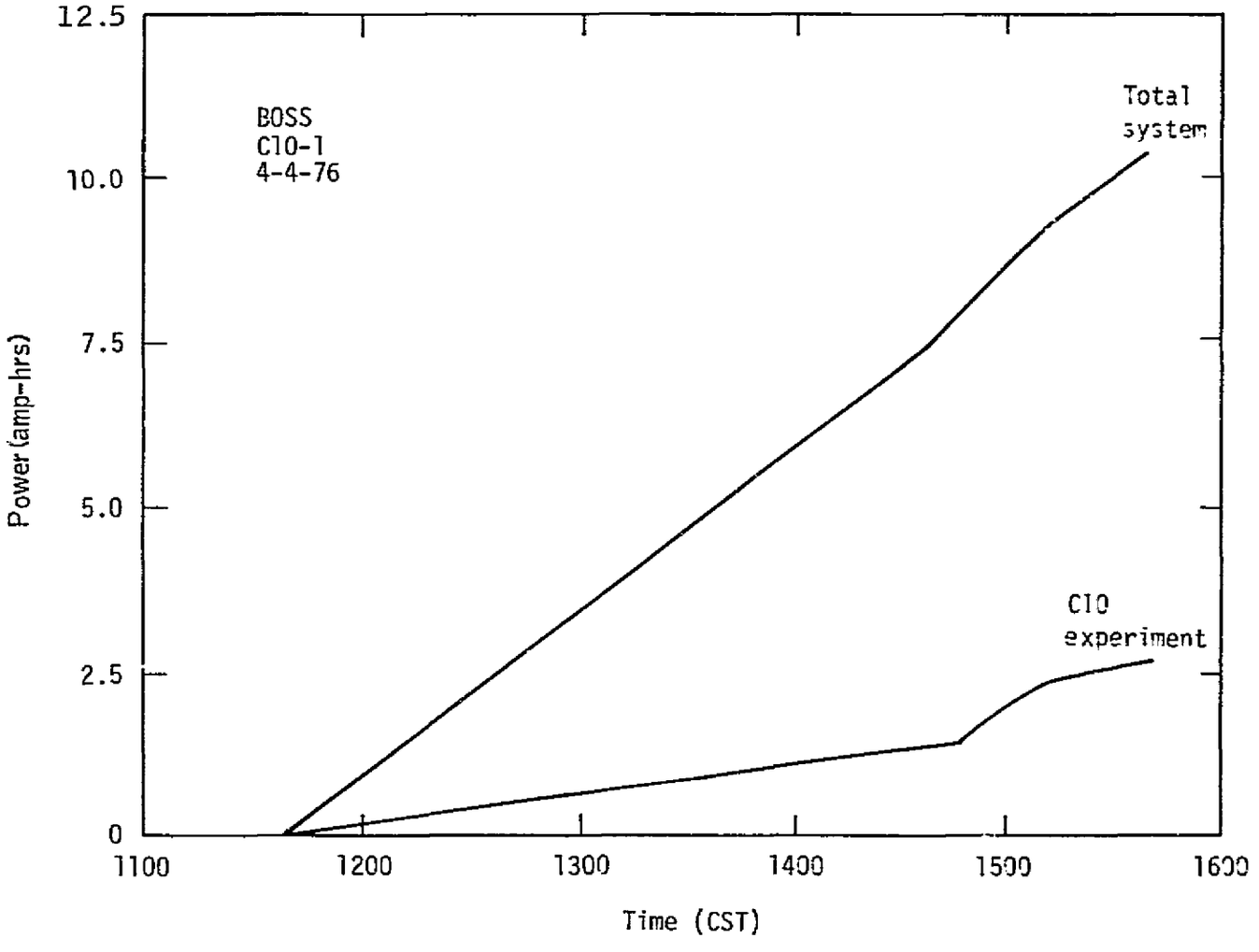

Figure 10. Payload power consumption for the first Chlorine Oxide (C10-1) flight

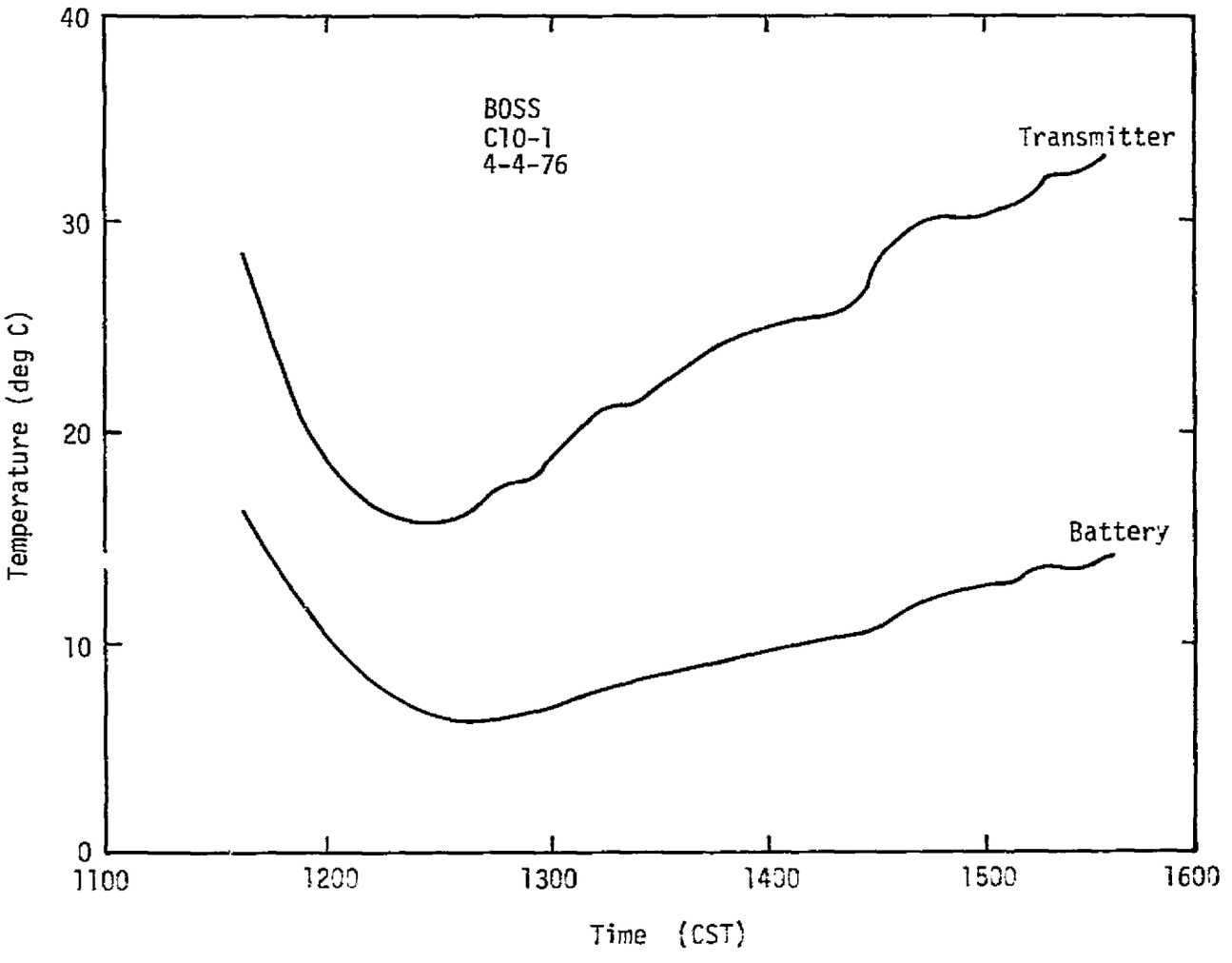

Figure 11. Thermal history of the battery and transmitter for the first Chlorine Oxide (C10-1) flight

of approximately 38 km (125 k ft). The payload was recovered in good condition and returned to the NSBF at Palestine the evening of 5 April 1976. On 6 April 1976 an investigation of the failure was initiated. Results of this investigation were reported to EEPO in an LEC document authored by W. C. Gibson dated 12 April 1976.

5.1.4 DATA RESULTS

Due to the failure of the payload to respond to commands, no data was received from the resonance fluorescence instrument to allow the construction of a vertical concentration profile for ClO. Likewise, no data was received from the aerosol particle counter. None of the scientific objectives of the flight were achieved.

Wallops launched ozonesondes to determine ozone profiles. Results of these measurements are shown in figure 12.

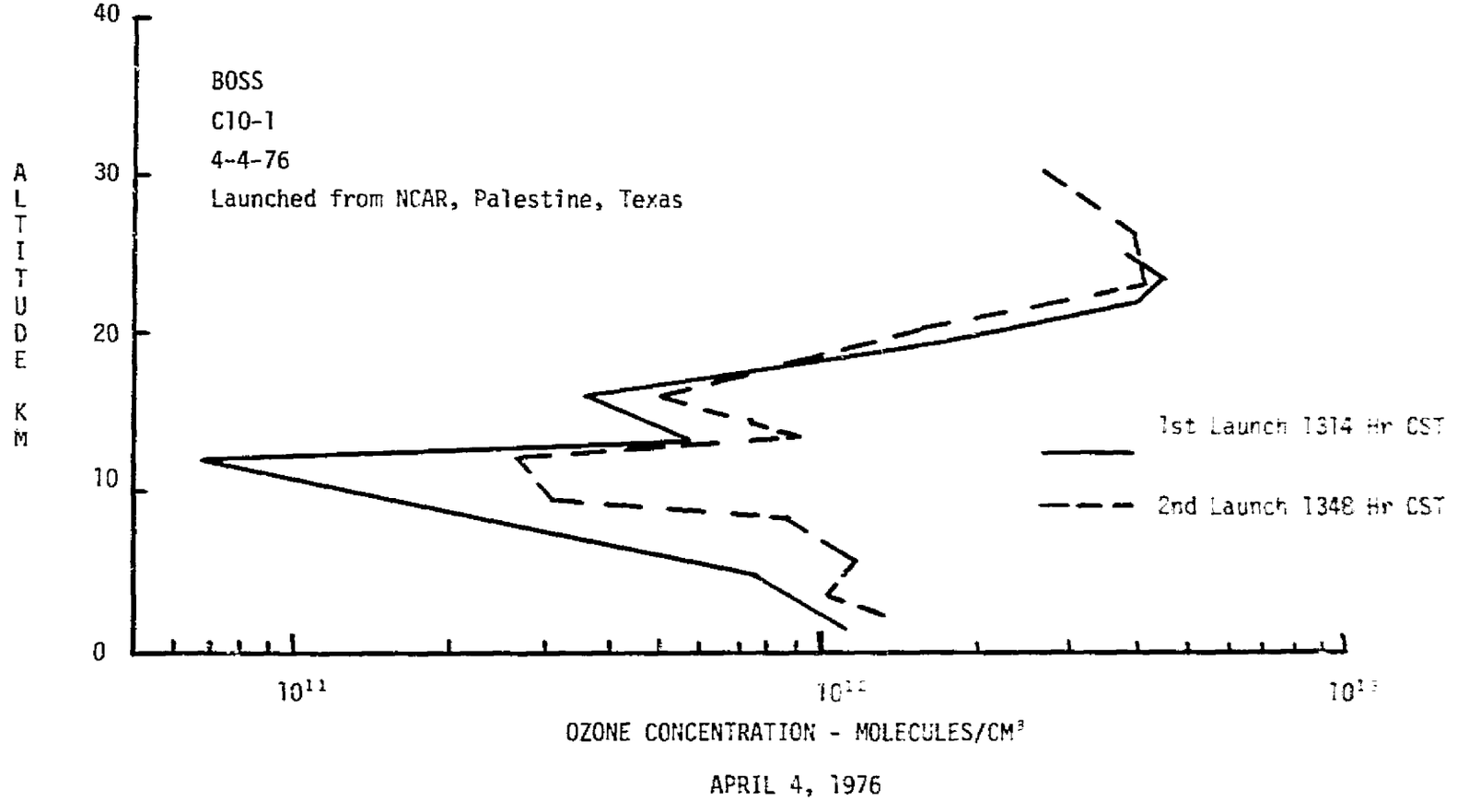

Figure 12. Concentration of Ozone Determined by Radiosonde During the First Chlorine Oxide (C10-1) Flight

5.2 SECOND CHLORINE OXIDE (ClO-2) MEASUREMENT

(NCAR FLIGHT NO. 965-P)

15 May 1976

5.2.1 SUMMARY

This balloon-parachute flight was the seventh flight of the laminar flow through/resonance fluorescence instrument (principal investigator: Dr. James Anderson, University of Michigan) and took place on 15 May 1976. The purposes of the flight were to measure the vertical concentration profile of chlorine oxide (ClO) in the 25 to 45 km altitude range and to obtain an *in situ* grab sample of stratospheric gas at an altitude of approximately 20 km.

The flight was launched at 0727 CDT from the NSBF at Palestine, Texas. The morning launch was chosen such that the payload could be released from the balloon at midday at which time the theoretical diurnal concentration cycle of ClO would be stable. Hardware consisted of a 4.3×10^5 cubic meter balloon, 9.75-meter guide surface parachute, NCAR telemetry system, JSC flight support module, the resonance fluorescence instrument modified to measure the concentration of ClO, and the *in situ* grab sample bottle. The University of Michigan was responsible for the resonance fluorescence and grab sample instrumentation. Thus the hardware was essentially identical to that flown on the previous flight of this series with the exception that the aerosol particle counter experiment was deleted.

The resonance fluorescence instrument was launched with only the photomultiplier tubes (PMTs) and engineering data monitors operating. The payload condition and background readings from the PMTs were checked

during ascent and appeared to be satisfactory. All payload systems functioned as expected including the NCAR PCM command system. The payload reached a float altitude of 45 km (148 k ft) at approximately 1030 CDT after a normal ascent. The command to release the payload was sent from the NCAR tower at 1200 noon CDT to begin the data gathering phase of the mission. ClO concentration data was obtained from 41 km (134.5 k ft) to 27 km (88.5 k ft). The grab sample bottle experiment was activated on schedule and apparently worked normally. The bottle and entrapped sample were returned to the University of Michigan for study.

The overall performance of both JSC and NCAR telemetry systems during the flight was excellent and good quality data was transmitted to each of the three ground tracking stations used for this flight. A sketch of the payload is shown in Figure 13 and a photo of the launch is shown in Figure 14.

5.2.2 PAYLOAD OPERATIONS

5.2.2.1 Ascent Phase

The flight profile for the Second Chlorine Oxide ClO Flight is illustrated in figure 15. Launch occurred at 0727 CDT, 15 May 1976, and was accomplished using the dynamic launch technique. The 4.5×10^5 cubic meter balloon and payload were launched very cleanly from the NCAR launch vehicle. There was no visible release interference, ground contact, or excessive swinging of the payload. The parachute and suspension system appeared to be correctly rigged and straight. The balloon system ascended at an average rate of 4.1 meters per second

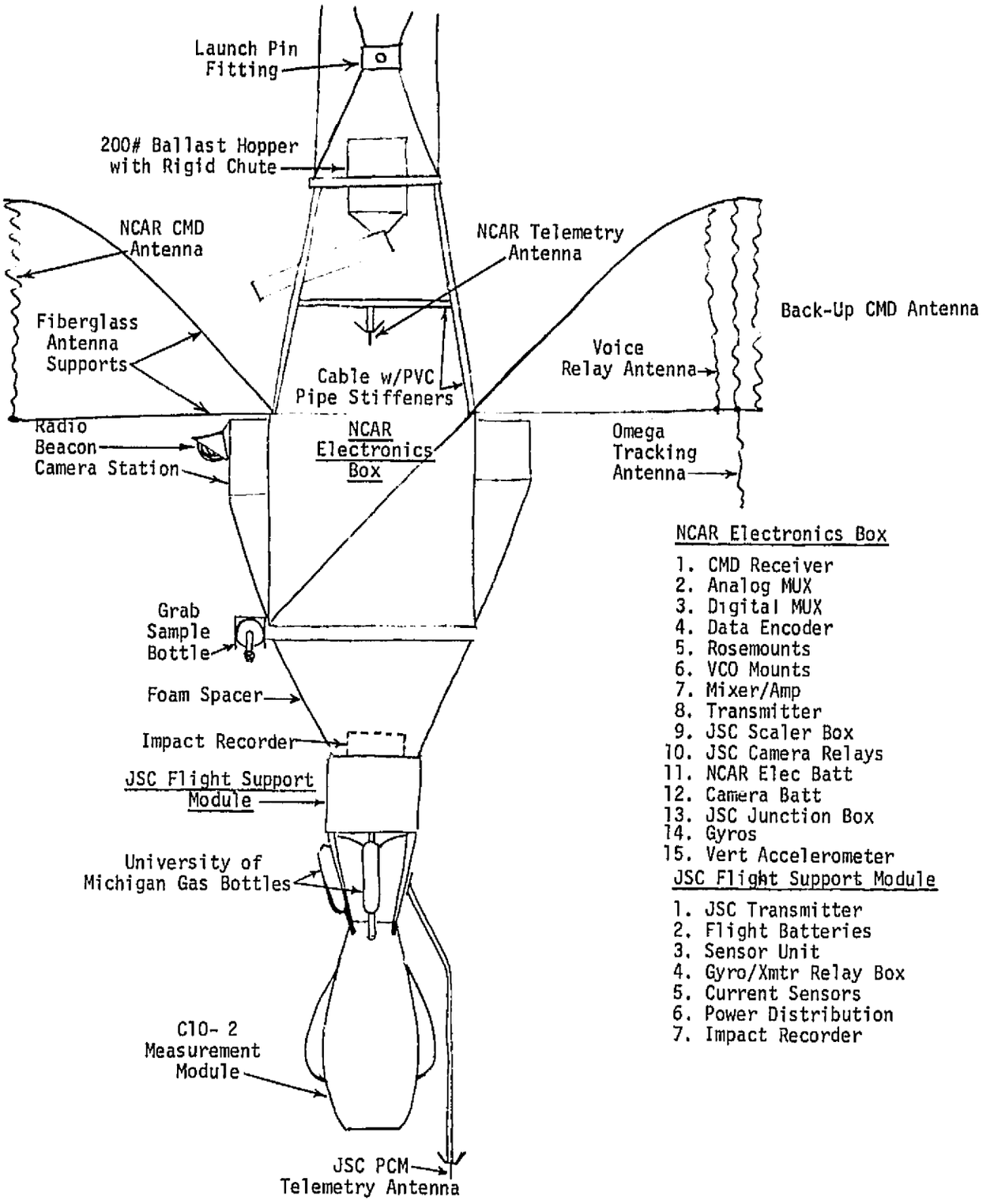

Figure 13. Sketch of the Second Chlorine Oxide (ClO-2) Payload

NASA
S- 76- 29171

Figure 14. Second Chlorine Oxide (ClO-2) Payload Ready for Launch

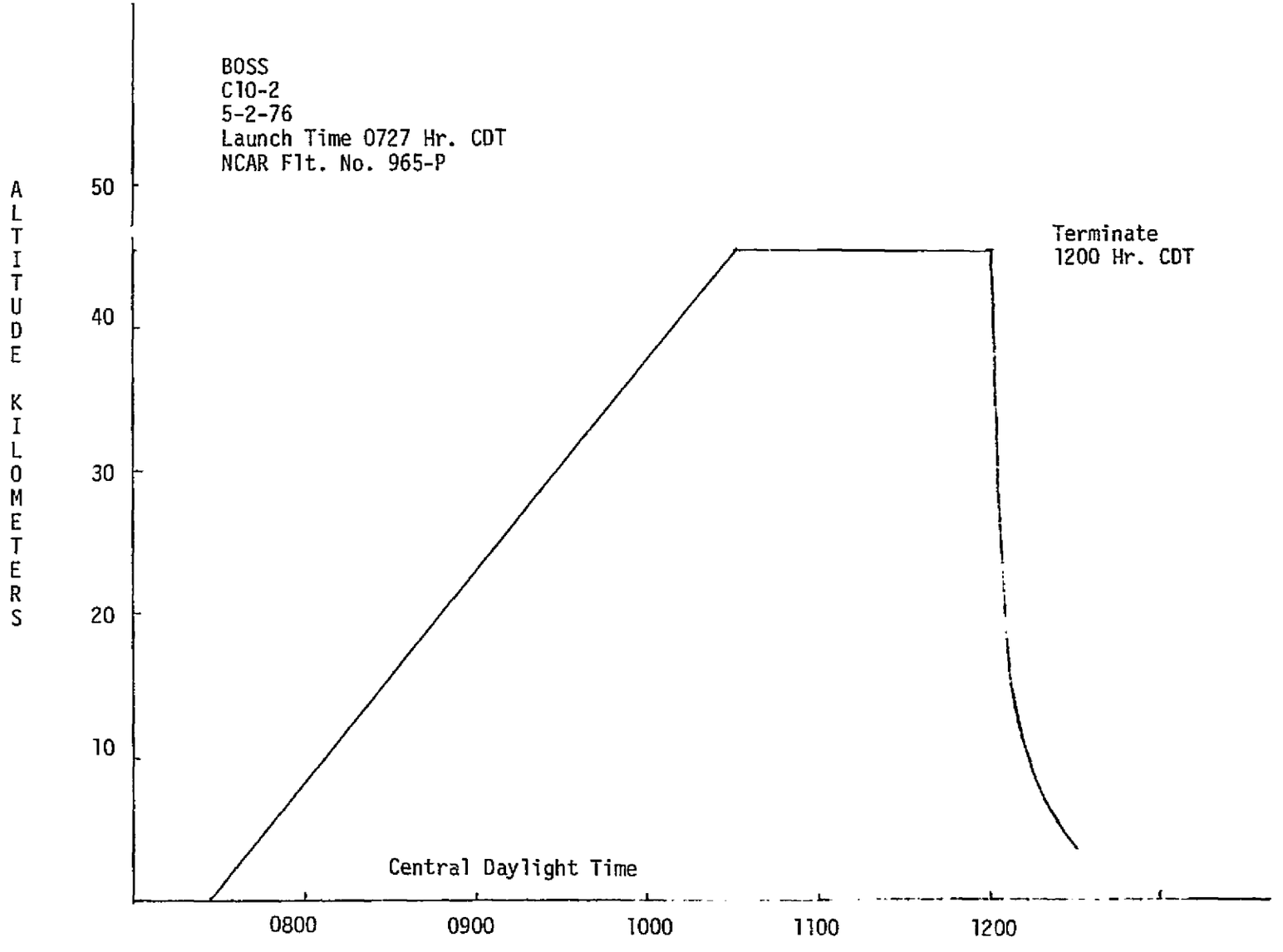

Figure 15. Flight Profile for the Second Chlorine Oxide (ClO-2) Flight

to a float altitude of 45 km. The altitude of the payload was measured by three pressure transducers: a high range (0.1-0 psi), a medium range (1-0 psi) and a low range (15-0 psi). Figure 16 is a plot of the altitude data obtained from these three sensors during the ascent phase of the flight. Except for the data at ~45 km, the portions of the curves where the indicated altitude is nearly constant with time indicate the saturation levels of the pressure transducers. As in the previous flight, an apparent discrepancy exists in the altitude data. The magnitude of this discrepancy is about 2 km for the low and medium range sensors. Because the payload was to be released around noon and nothing of significance appeared to be happening, the recorder was turned OFF at about 1030 CDT and turned ON again at 1128 CDT.

5.2.2.2 Descent Phase

The payload was released on command from the NCAR tower at 1200 noon CST and the data gathering phase of the mission began. An onboard motion picture camera and accelerometer observed parachute deployment and measured the loading forces while two vertical reference gyros monitored the descent attitude of the system. Payload altitude as measured by the three pressure transducers during descent is plotted in figure 17. The discrepancy in the altitude data as measured by the low and medium sensors is apparent. The velocity/altitude profile of the descending payload is shown in figure 18. The velocities encountered on the present flight are comparable to those of previous

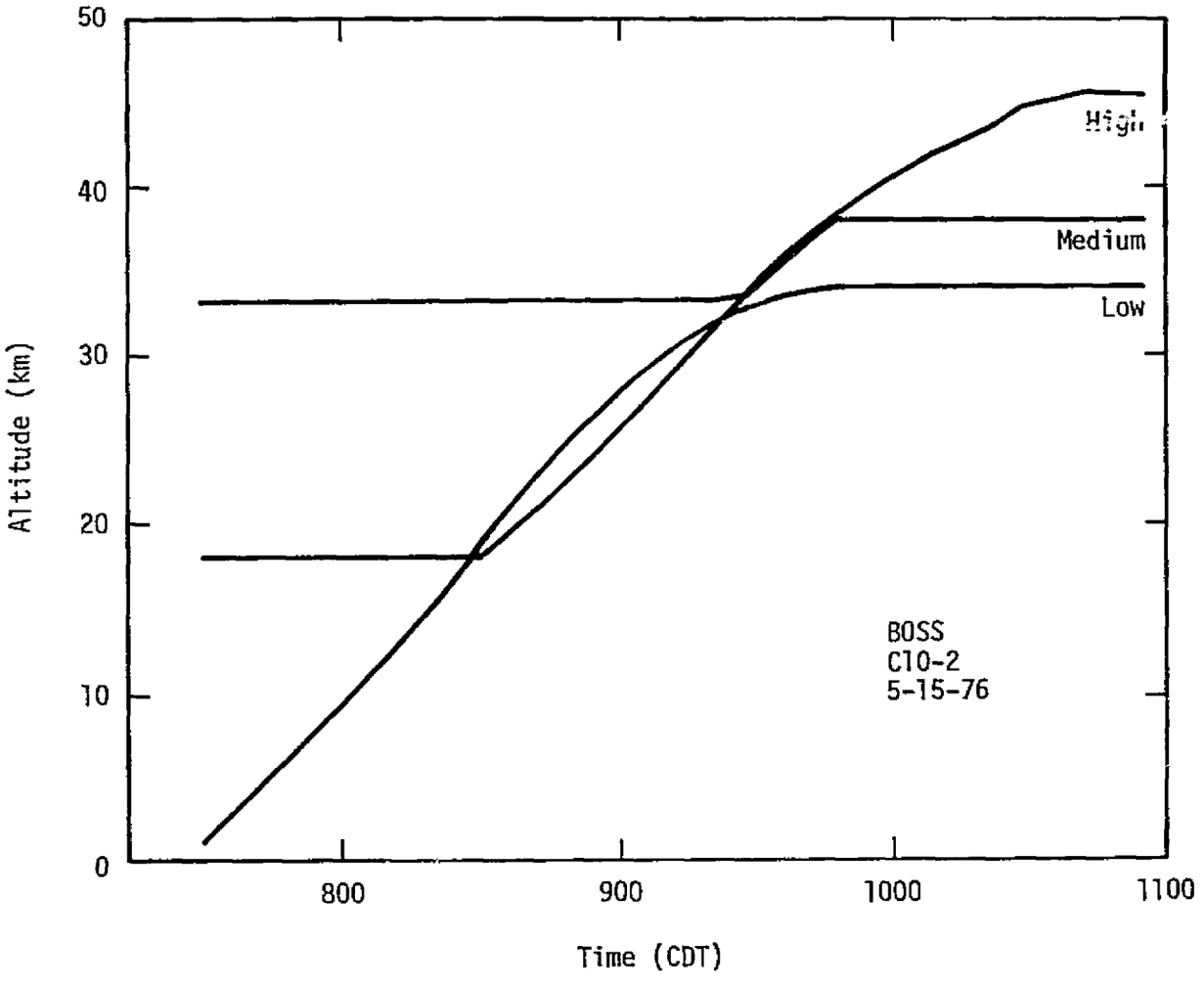

Figure 16. Altitude/time profiles for the ascending payload during the second Chlorine Oxide (ClO-2) flight as measured by three pressure transducers.

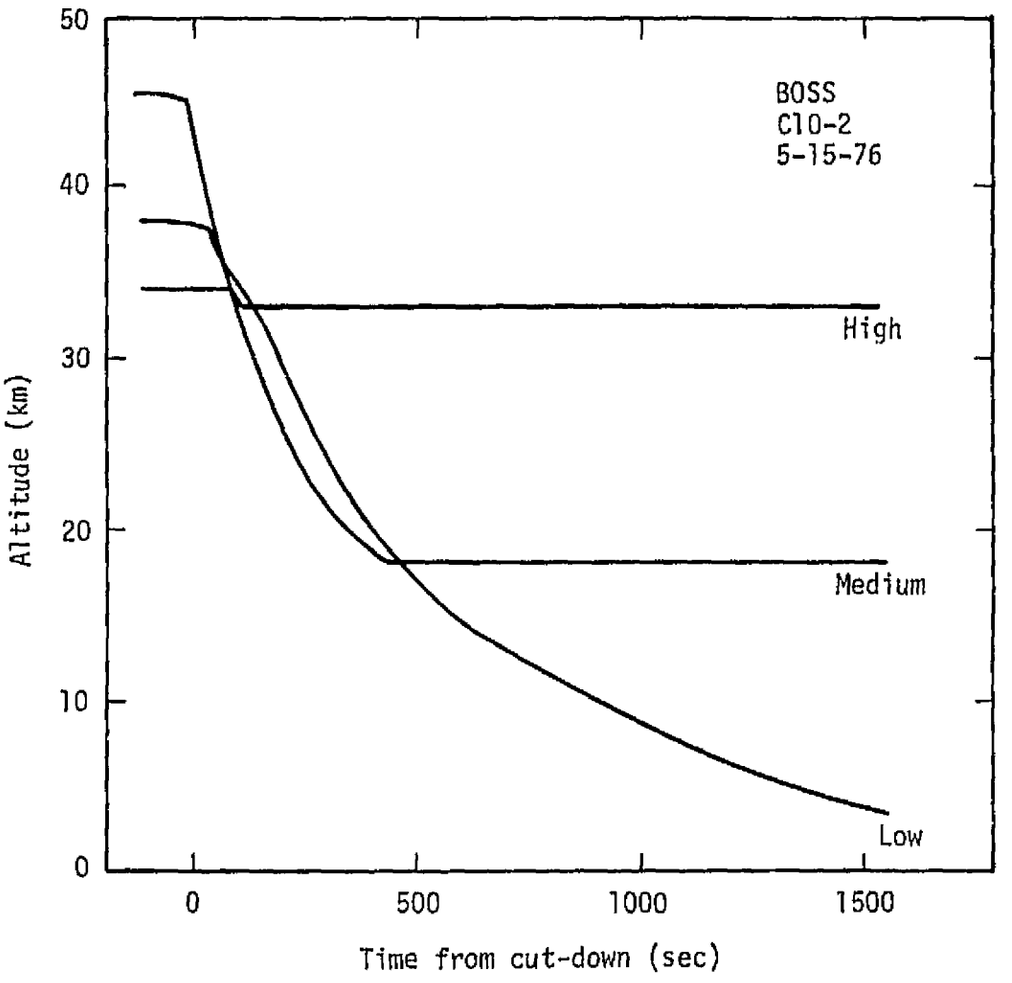

Figure 17. Altitude/time profiles for the descending payload during the second Chlorine Oxide (ClO-2) flight as measured by three pressure transducers.

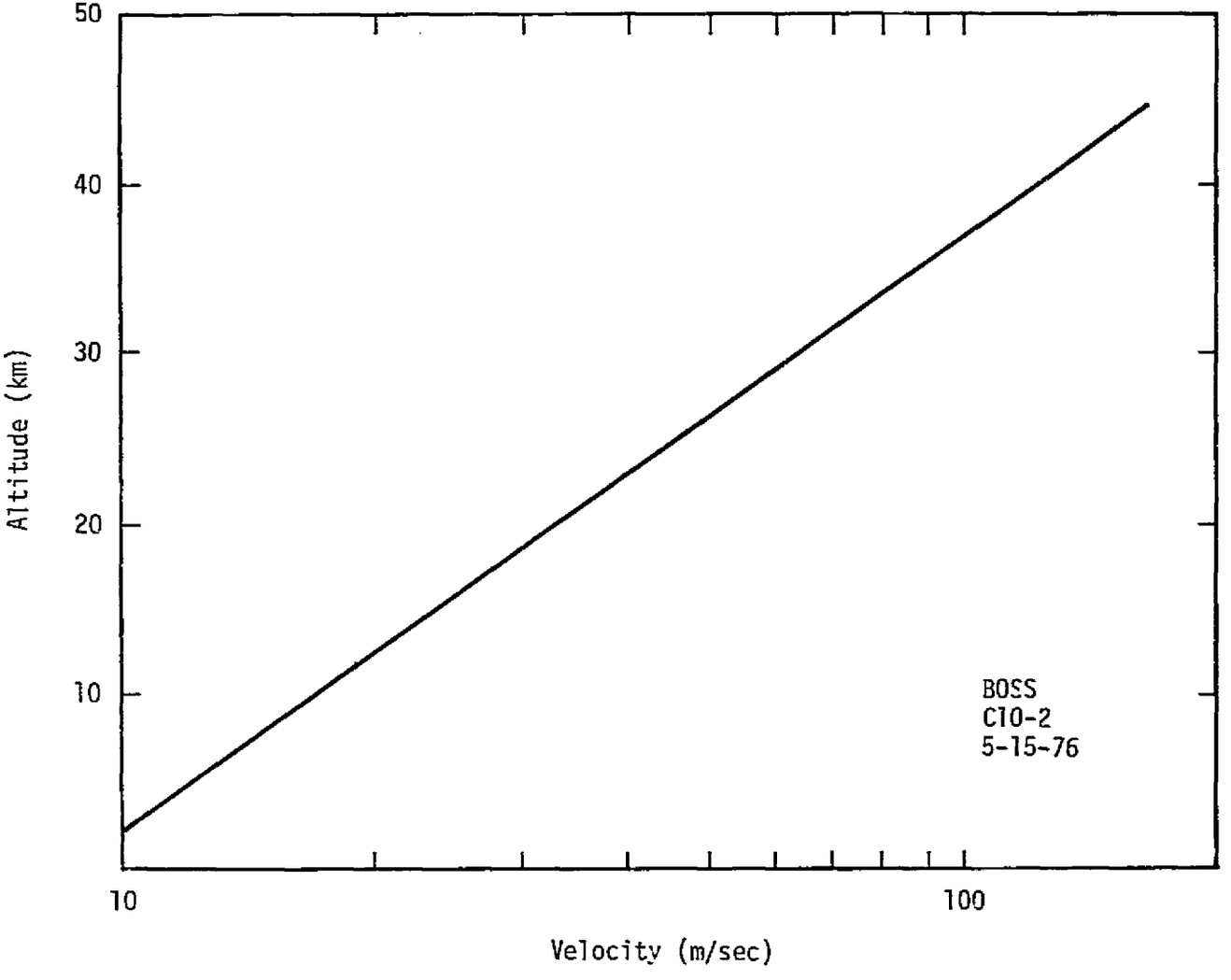

Figure 18. Velocity/altitude profile of descending payload for the second Chlorine Oxide (C10-2) flight.

flights. The vertical force on the payload during parachute deployment is illustrated in figure 19. The payload reached terminal velocity in about 30 seconds as is normal for this parachute. Figure 20 shows the probability that the angular deviation of the payload from vertical is less than a given angle as a function if angle during the first 20 minutes of descent. The payload was within 10 degrees of vertical 40% of the time and was within 15 degrees of vertical 75% of the time. This degree of stability is comparable to the stability exhibited by the parachute system in the past.

5.2.2.3 Power and Temperature Profiles

Figure 21 shows the payload power consumption integrated as a function of time for the flight. The magnetron on the resonance fluorescence instrument was turned ON at 1159 and turned OFF 9 minutes later and resulted in the large increase in power consumption around the time of cut down. Total power used by the complete payload was 16.9 ampere hours with the ClO experiment accounting for ~ 2 ampere hours of this total.

Figure 22 is a thermal history of the battery and transmitter for the flight. Figure 23 is a similar plot showing the temperature of the uplooking motion picture camera. A comparison of these two figures shows when power was supplied to the heaters on the camera.

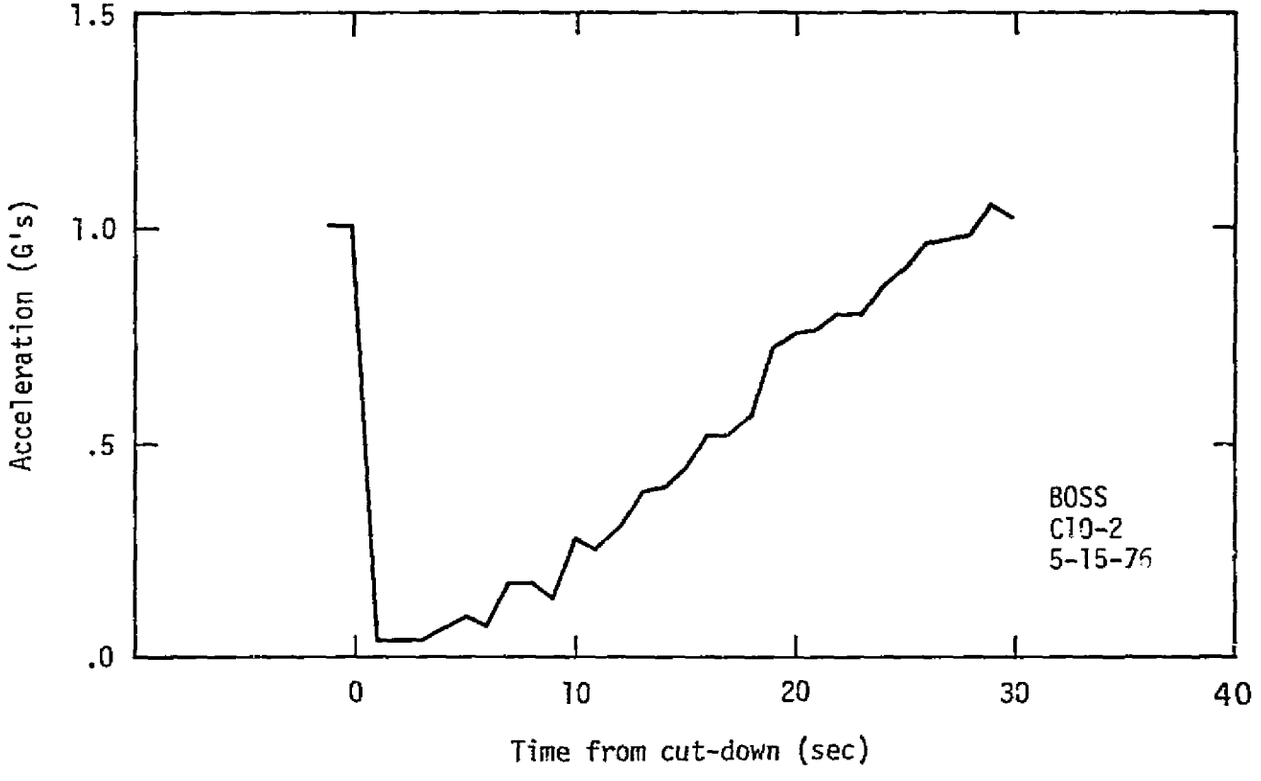

Figure 19. Vertical force on payload after parachute deployment for the second Chlorine Oxide (ClO-2) flight

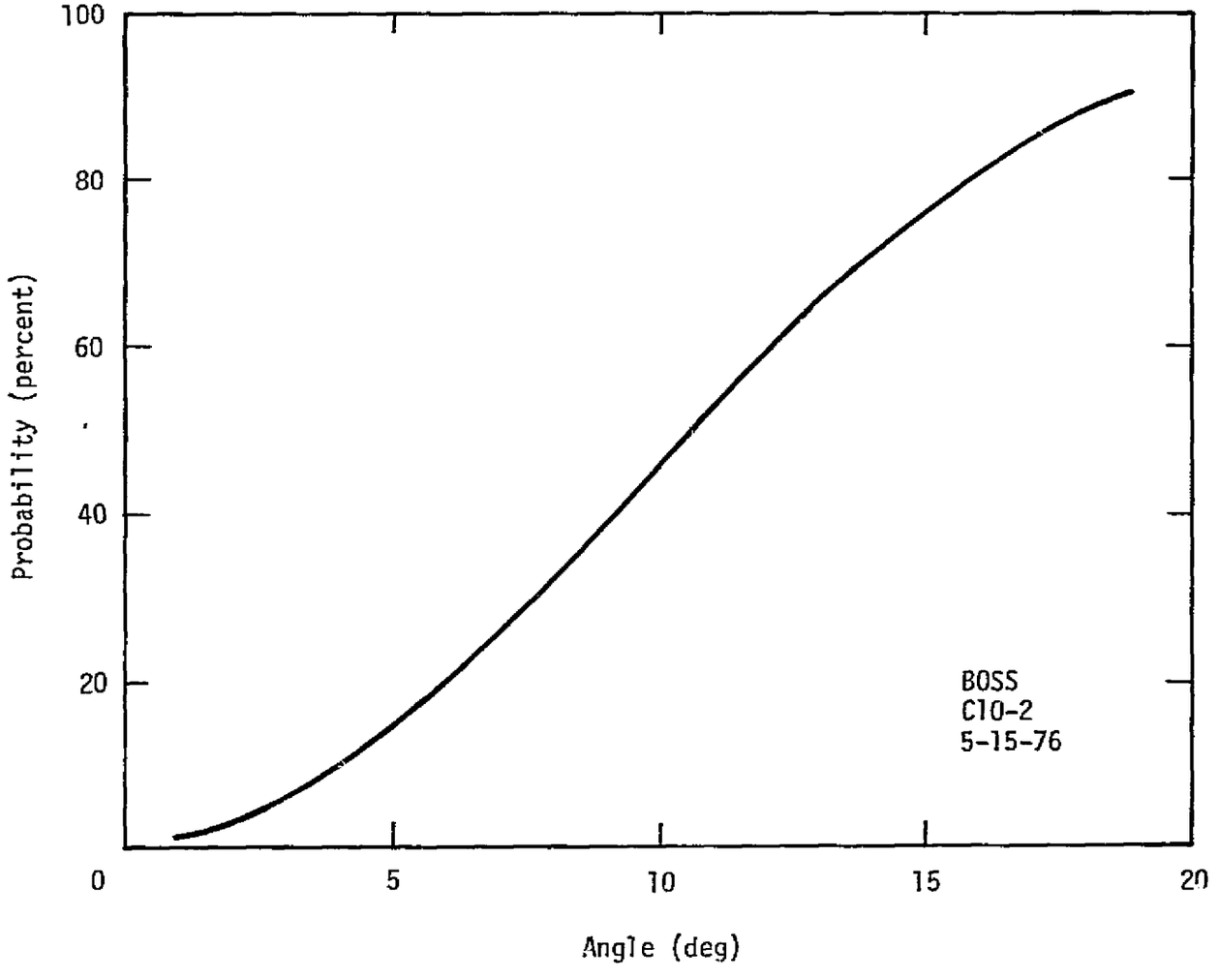

Figure 20. Probability (percent) that the angular deviation of the payload from vertical is less than a given angle as a function of angle for the first 20 minutes during descent of the second Chlorine Oxide (ClO-2) flight.

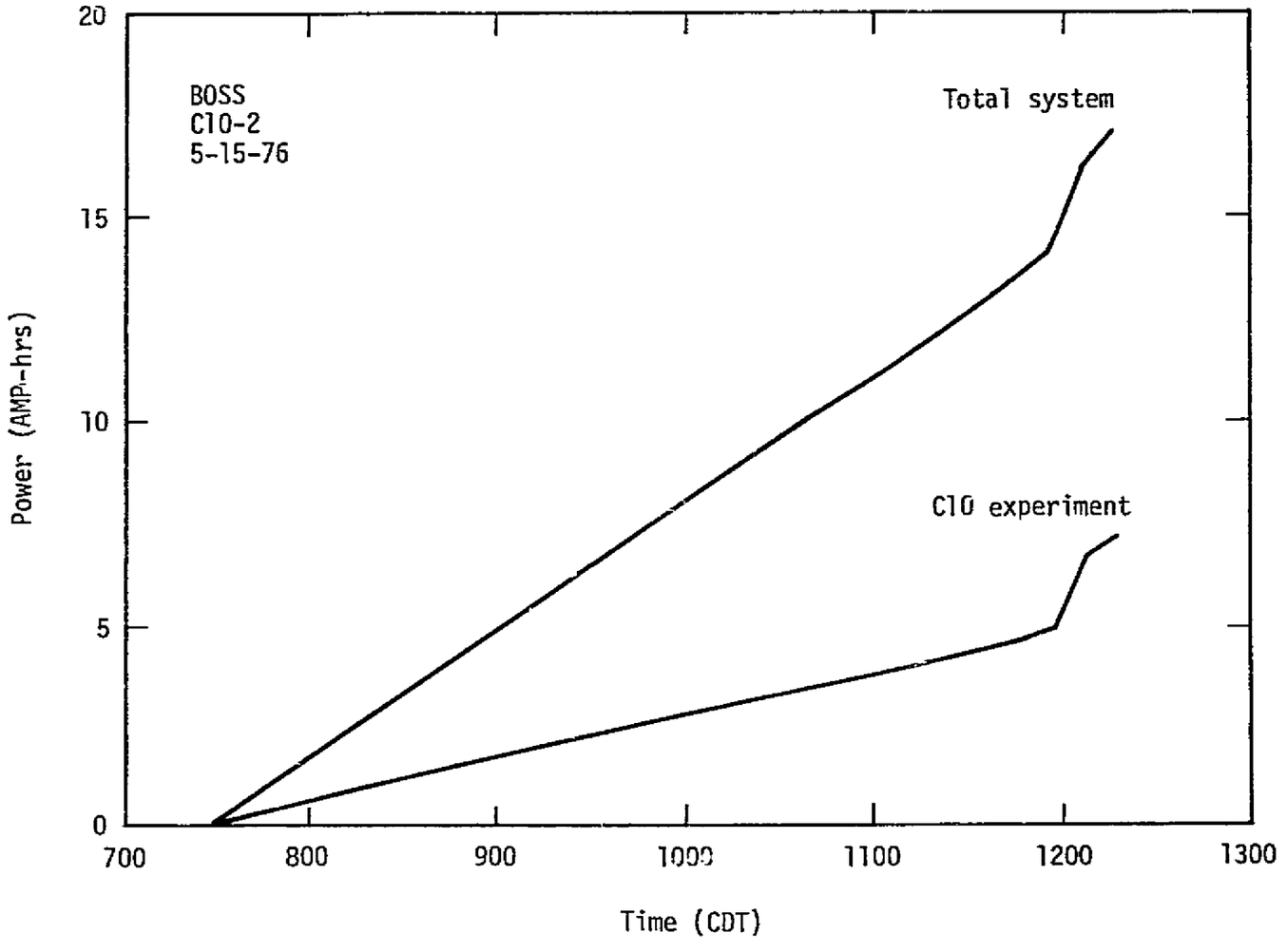

Figure 21. Payload power consumption for the second Chlorine Oxide (C10-2) flight.

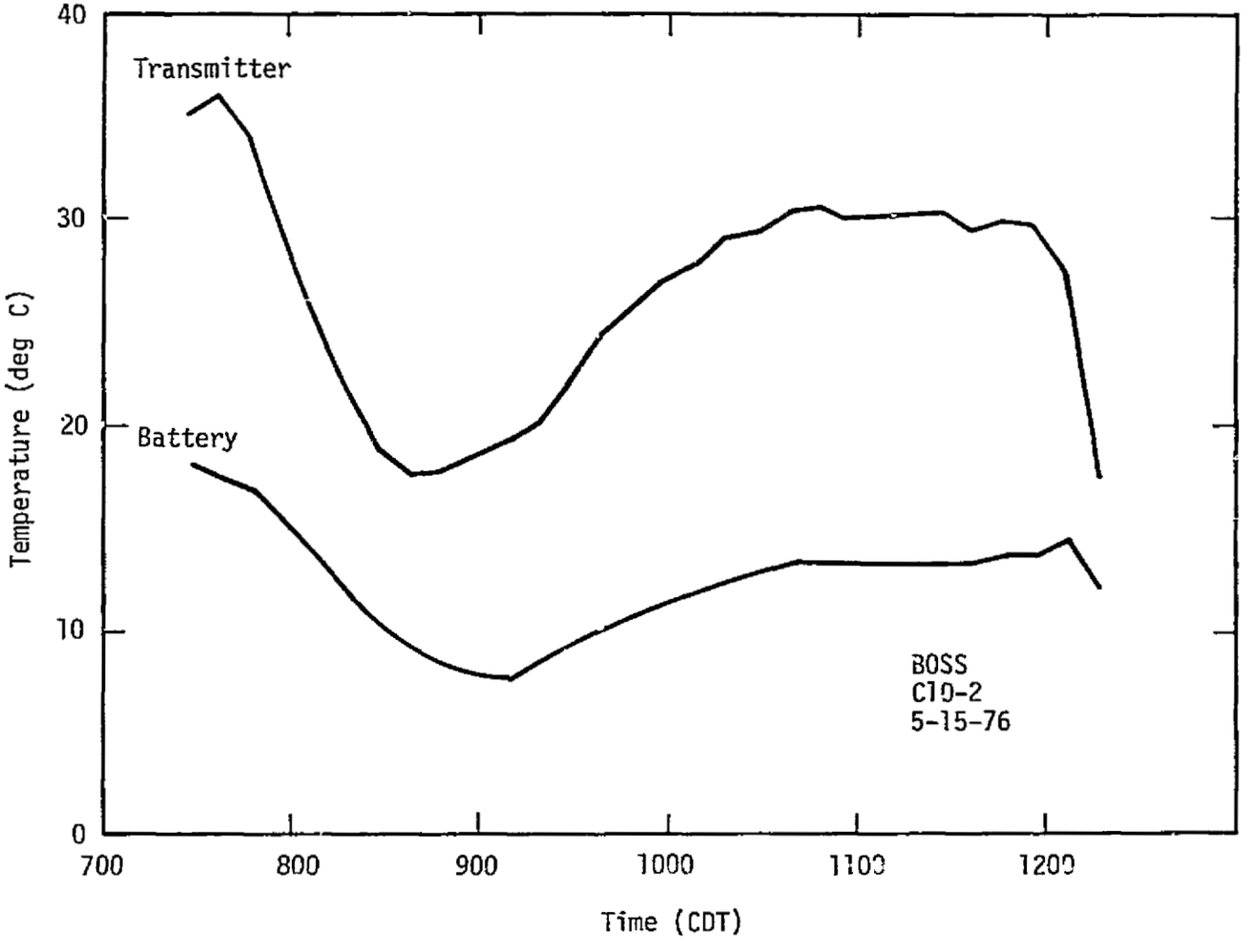

Figure 22. Thermal history of the battery and transmitter for the second Chlorine Oxide (C10-2) flight

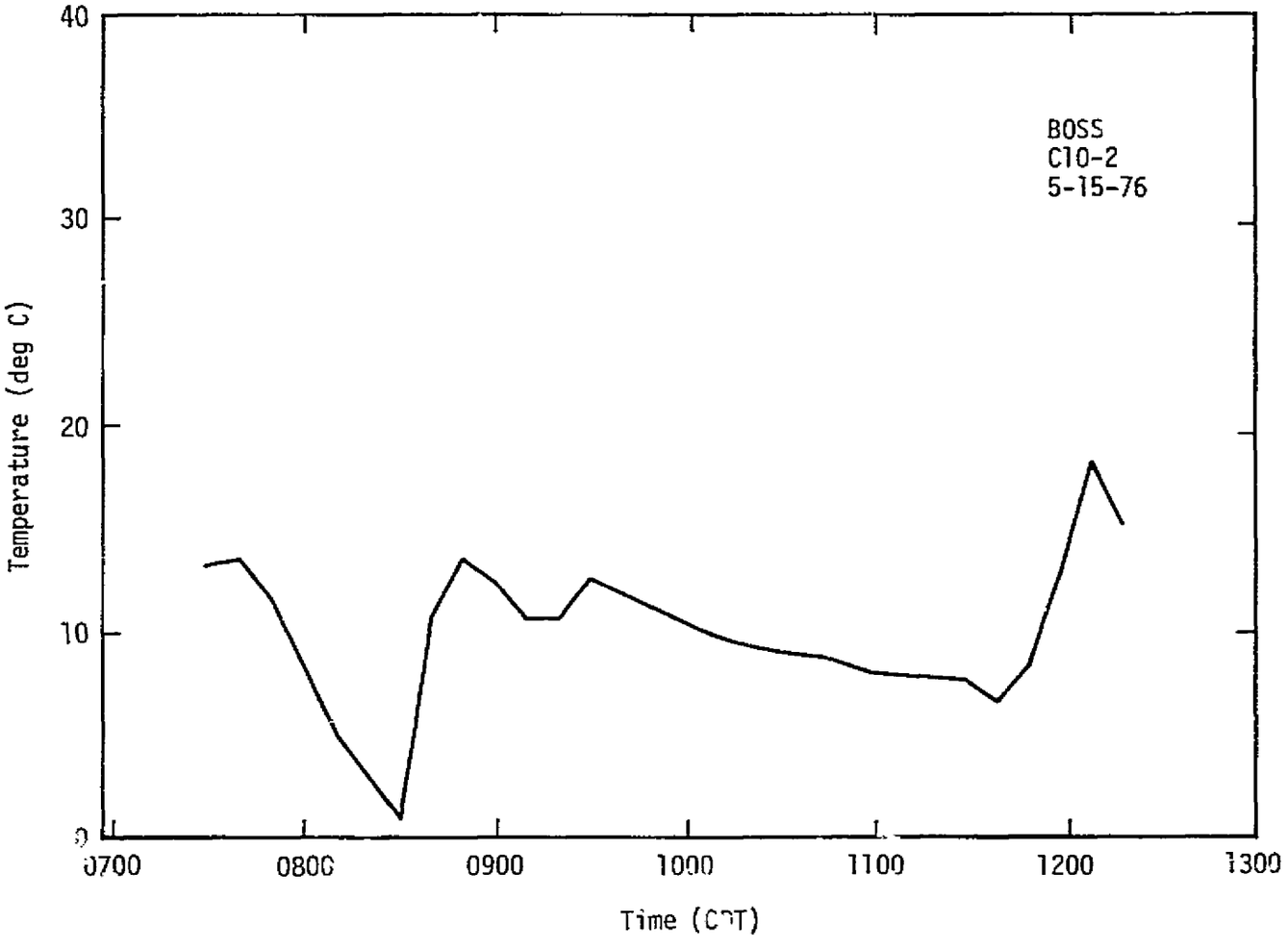

Figure 23. Thermal history of the uplooking motion picture camera for the second Chlorine Oxide (ClO-2) flight

5.2.3 POSTFLIGHT ACTIVITIES

The parachute/payload landed in an open field only 19 nm from the NSBF at Palestine, Texas at 1233 CDT. There was no apparent damage to the instrument or support systems upon impact and the payload was recovered and returned to the NSBF less than 90 minutes after landing.

5.2.4 DATA RESULTS

5.2.4.1 Resonance Fluorescence Experiment

Concentration profile data obtained from this flight is available from the Principal Investigator, Dr. J. Anderson, at the University of Michigan.

5.2.4.2 Grab Sample Experiment

A grab sample system was flown by investigators from University of Michigan to demonstrate the operation and performance of a specific flight hardware design. The objective was to develop a grab sample capability on all future flights to measure N_2O, Freon 11 and Freon 12 at an altitude of 20 Km. This flight verified that the sample was taken at the intended altitude. The contents were examined only for methane by investigators at the University of Michigan using gas chromatography-flame ionization detection (CG-FID) technique. Additional information can be obtained on this flight experiment by contacting R. Cicerone, B. Kennedy or D. Steadman at the University of Michigan.

5.3 First Atomic Chlorine/Chlorine Oxide (Cl/ClO-1) Measurement

5.3.1 SUMMARY

This balloon-parachute flight was the eighth flight of the laminar flow through/resonance fluorescence instrumentation (principal investigator: Dr. James Anderson, University of Michigan) and took place on 28 July 1976. The purpose of the flight was to measure the vertical concentration profiles of chlorine oxide (ClO) and atomic chlorine (Cl) in the stratosphere.

The flight was launched at 0829 CDT from the NSBF at Palestine, Texas. The morning launch was chosen such that the payload could be released from the balloon when the theoretical diurnal concentration cycle of Cl and ClO would be stable (approximately the same period in the cycle as the previous flight in this series). To accomplish the simultaneous measurement of the concentration of two stratospheric species, the University of Michigan mechanically and electrically reconfigured the scientific portion of the payload to use two resonance fluorescence instrument pods. The additional pod and supporting structure increased the payload weight necessitating the use of a 14-meter guide surface parachute. Additional support hardware consisted of a 4.4×10^5 cubic meter balloon, NCAR telemetry system, and the JSC flight support module. Figure 24 identifies various subsystems and components and figure 25 shows the payload ready for launch.

The resonance fluorescence instruments were launched in a low power configuration with only the photomultiplier tubes (PMTs) and engineering

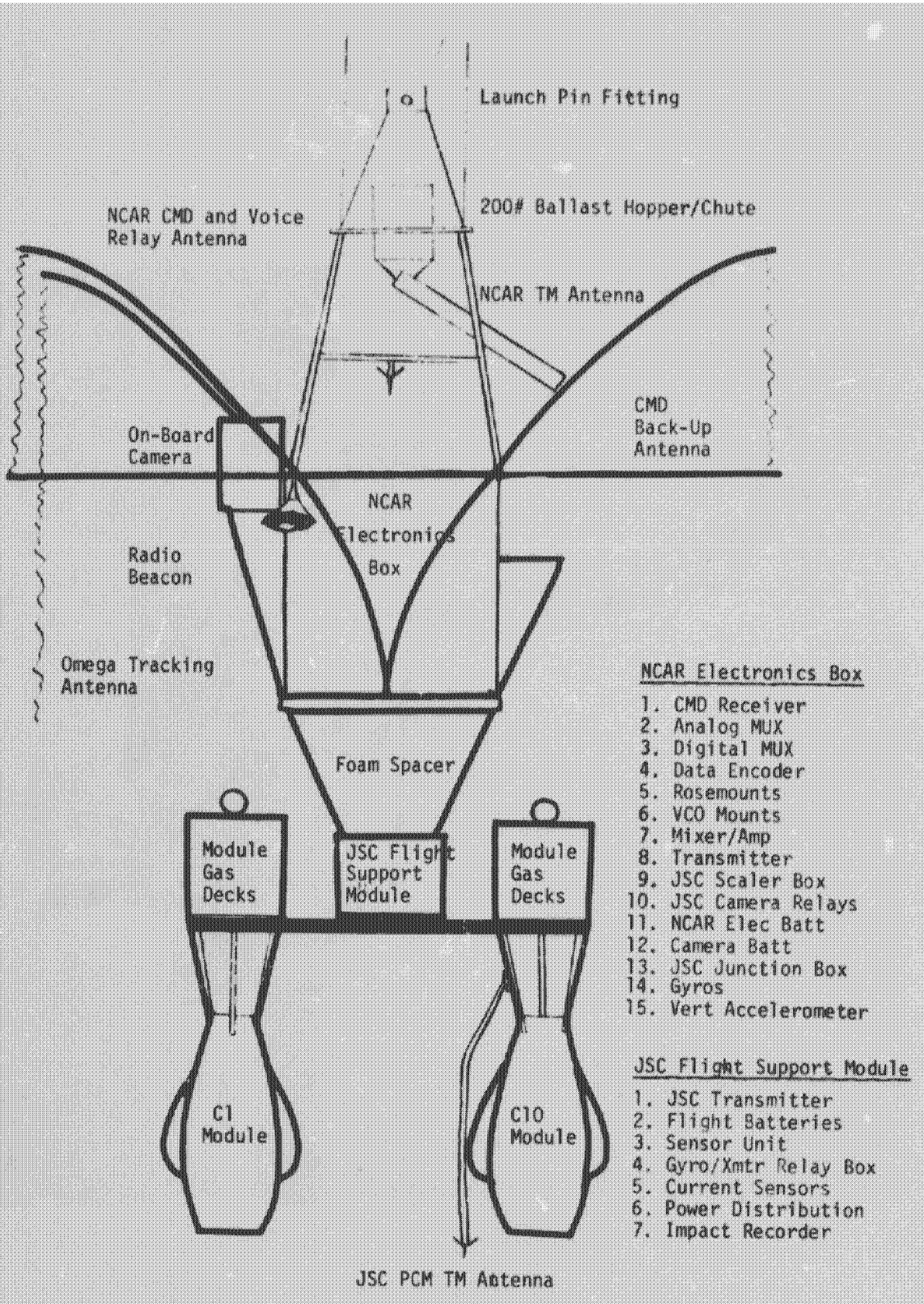

Figure 24. Sketch of the First Atomic Chlorine/Chlorine Oxide (Cl/ClO-1) Payload

NASA
S- 76- 27806

Figure 25. Photo of the First Atomic Chlorine/Chlorine Oxide (Cl/ClO-1) Payload Ready for Launch

data monitors operating. The payload condition and background readings from the PMTs were checked during ascent and appeared to be satisfactory. Instrument activation prior to cut down was normal with all functions responding as planned. The payload reached a float altitude of 43 km (141 k ft) at approximately 1045 CDT after a normal ascent. The command to release the payload was sent from the NCAR tower at 1200 noon CDT to begin the data gathering phase of the mission. ClO concentration data was obtained from 41 km (134.5 k ft) to 27 km (88.6 k ft) and $Cl(^2P)$ concentration data was obtained from 42 km (137.8 k ft) to 35 km (114.8 k ft).

The overall performance of both JSC and NCAR telemetry systems during the flight was excellent and good quality data was transmitted to each of the three ground tracking stations used for this flight.

The parachute/payload landed in an open field approximately 20 nm east of Brownwood, Texas at 1241 CDT. The dual pod attachment structure apparently failed on impact as predicted. This structural failure occurred at specific points and was intentional to reduce the landing impact effects on the electronics package. The only apparent damage to any payload system was mechanical damage to exposed cabling. The payload was recovered and returned to the NSBF at Palestine on 29 July 1976.

5.3.2 PAYLOAD OPERATIONS

5.3.2.1 Ascent Phase

The flight profile for the First Atomic Chlorine/Chlorine Oxide Cl/ClO Flight is illustrated in figure 26. Launch occurred at 0829 CDT, 28 July 1976, and was accomplished using the dynamic launch technique. The 4.4×10^5 cubic meter balloon and payload were launched from the NCAR launch vehicle with no visible release interference, ground contact or excessive swinging of the payload. The balloon system ascended at an average rate of 5.3 meters per second to a float altitude of 43 km. The altitude of the payload was measured by three pressure transducers: a high range (0.1-0 psi) a medium range (1-0 psi) and a low range (15-0 psi). The temperatures of the low and medium range sensors were monitored during the flight to determine if the thermal environment was responsible for the discrepancies in the altitude data seen on the two previous flights. As shown in figure 26, the thermistors had essentially identical temperature readings throughout the flight and the range in temperature was well within acceptable limits. Figure 27 is a plot of the altitude data obtained from the three pressure transducers during the ascent phase of the flight. Despite the small temperature differences measured, the discrepancy in the altitude data remains. Except for the data at ~43 km, the portions of the curves where the indicated altitude is nearly constant with time indicate the saturation levels of the pressure transducers.

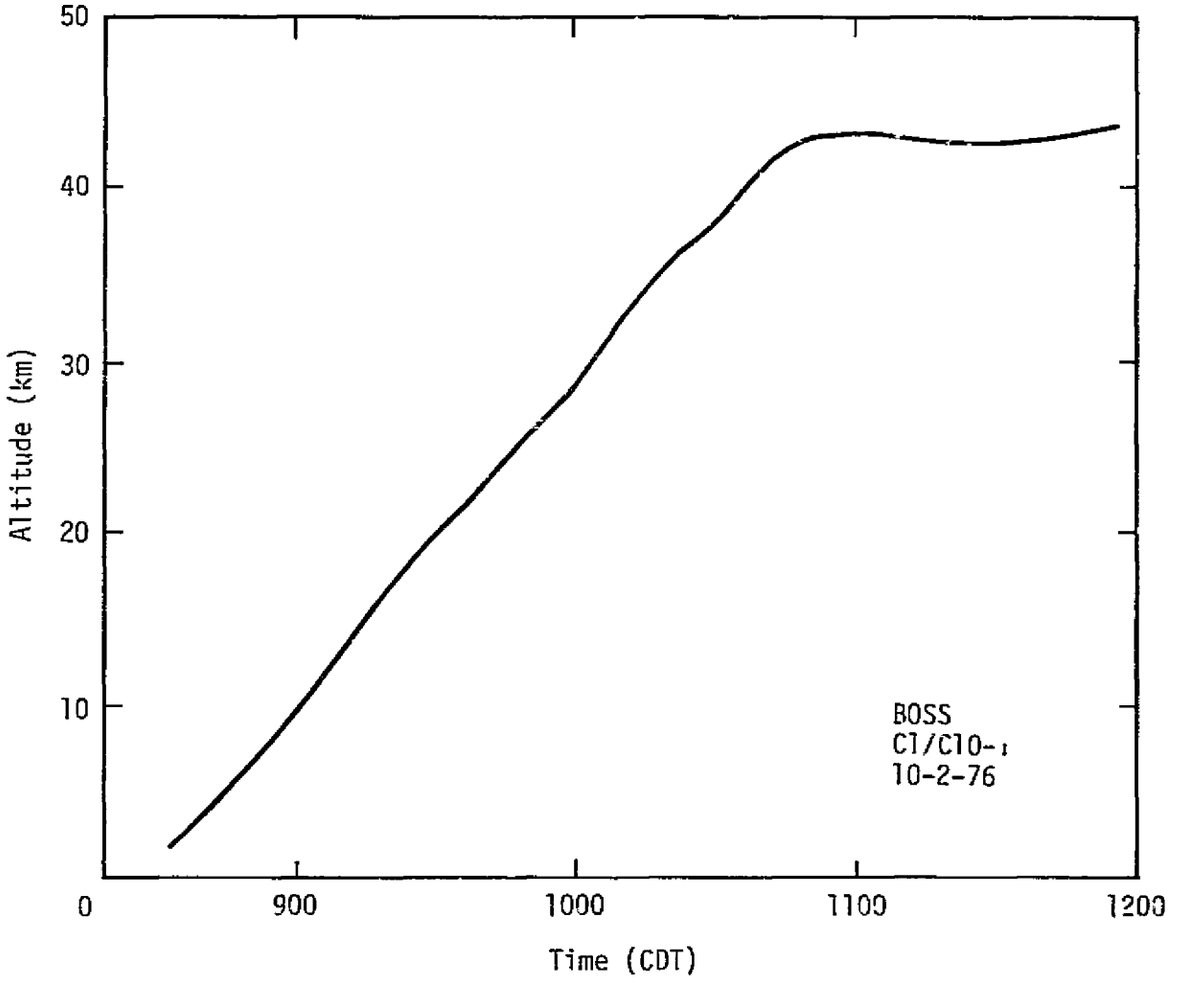

Figure 26. Best estimate of altitude/time profile for the ascending payload during the first Atomic Chlorine/Chlorine Oxide (Cl/ClO-1) flight

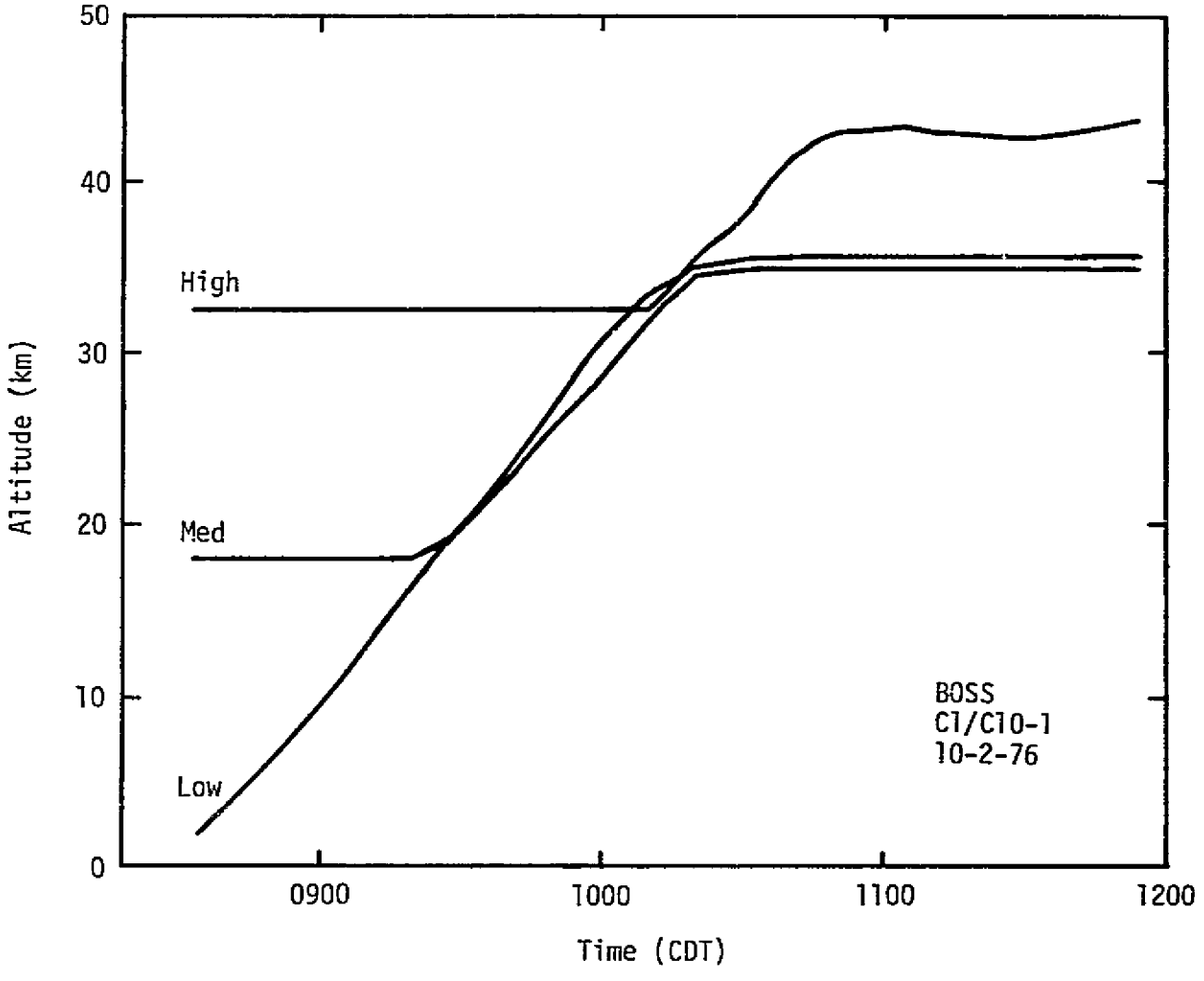

Figure 27. Altitude/time profiles for the ascending payload during the first Atomic Chlorine/Chlorine Oxide (CL/ClO-1) flight as measured by three pressure transducers.

5.3.2.2 Descent Phase

The payload was released on command from the NCAR tower at 1200 noon CST and the data gathering phase of the mission began. Solar zenith angle at the time of cut down was 16 degrees and the payload latitude was 31.4 degrees North. An onboard motion picture camera and accelerometer observed parachute deployment and measured the loading forces while two vertical reference gyros monitored the descent attitude of the system. The best estimate of payload altitude determined from the discordant pressure transducers during the descent is plotted in figure 28. The velocity/altitude profile of the descending payload is shown in figure 29. The velocities encountered on the present flight are somewhat lower overall when compared to previous flights. The vertical force on the payload during deployment of the 14 meter diameter parachute is illustrated in figure 30. The payload reached terminal velocity in about 24 seconds (considerably faster than on previous flights, which used a 9.75 meter diameter guide surface parachute). Figures 31, 32 and 33 show the probability that the angular deviation of the payload is less than a given angle as a function of angle for several time intervals during the descent. Figure 31 shows the payload attitude probabilities during the first 6 minutes of descent (payload within 10 degrees of vertical 55% of the time). Figure 32 shows the payload attitude probabilities during the next 6 minutes of descent (payload within 10 degrees of vertical 45% of the time. Figure 33 is a similar plot for the first 19 minutes

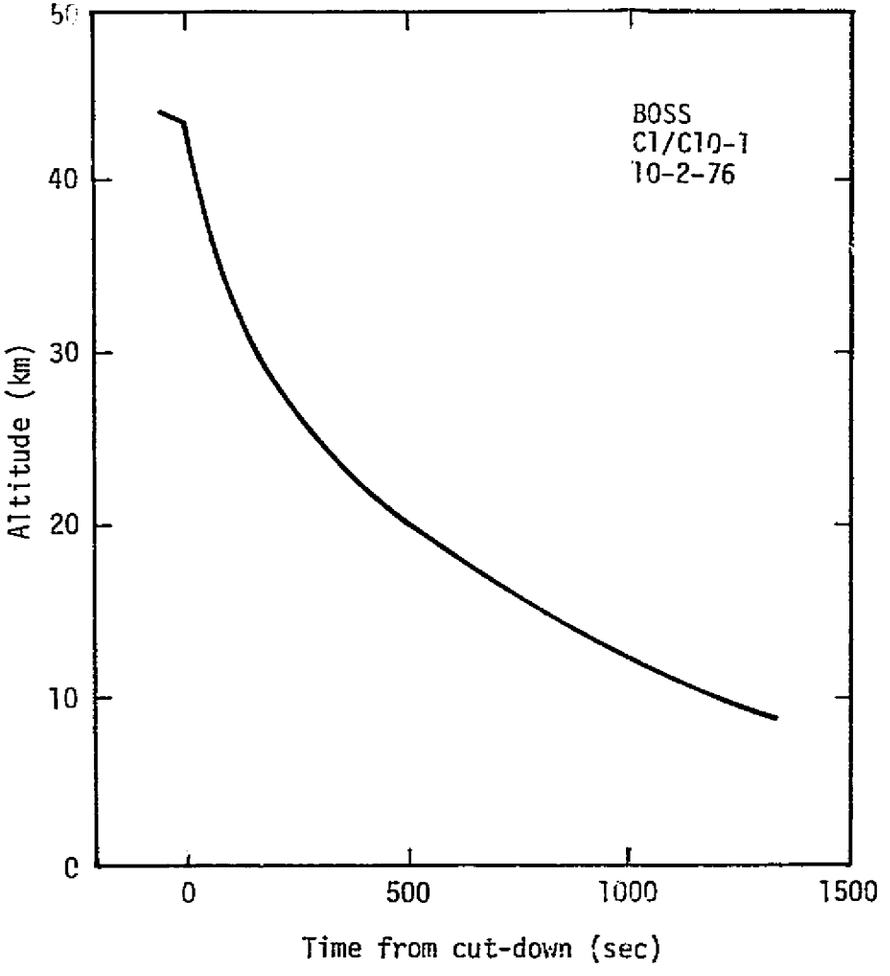

Figure 28. Best estimate of altitude/time profile for the descending payload during the first Atomic Chlorine/Chlorine Oxide (Cl/ClO-1) flight

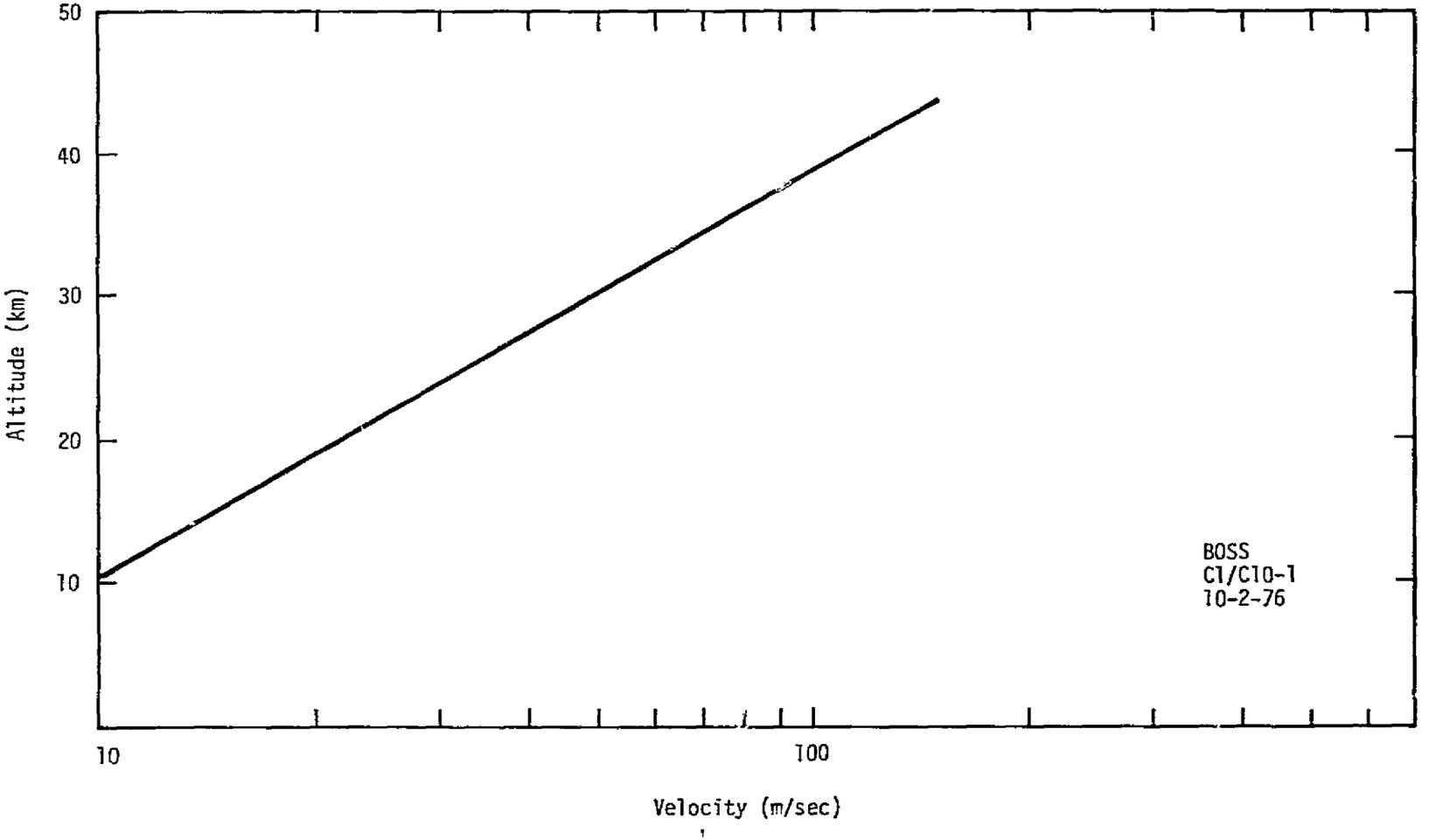

Figure 29. Velocity/altitude profile of descending payload for the first Atomic Chlorine/Chlorine Oxide (Cl/ClO-1) flight

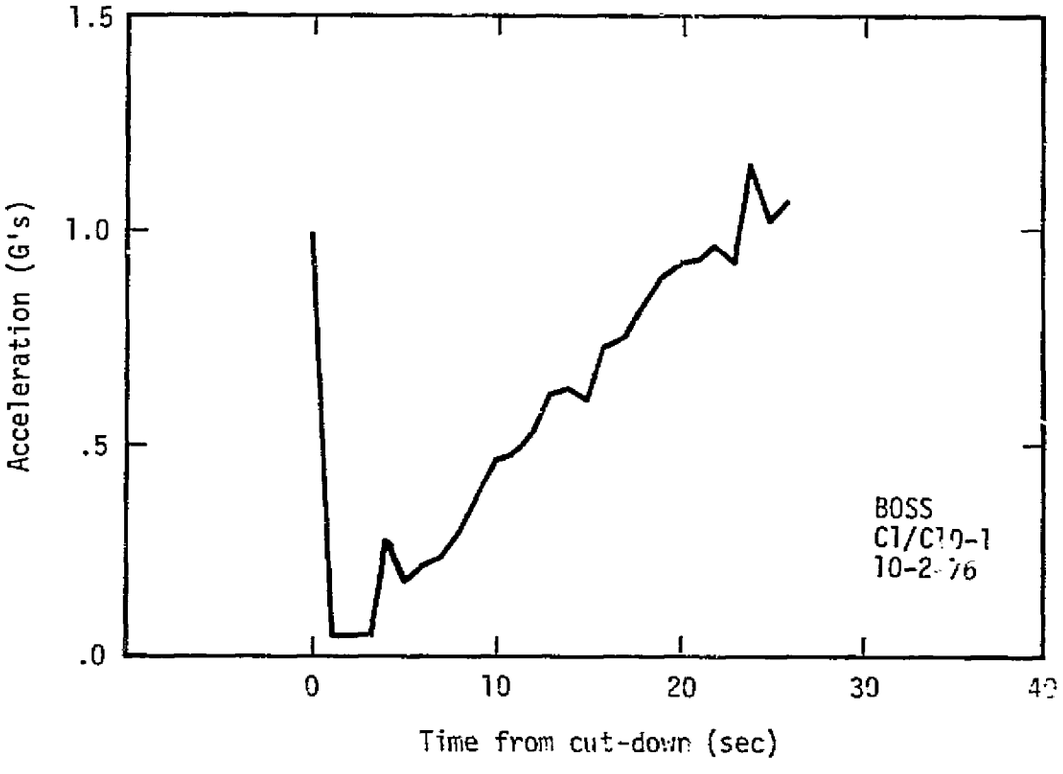

Figure 30. Vertical force on payload after parachute deployment for the first Atomic Chlorine/Chlorine Oxide (Cl/ClO-1) flight

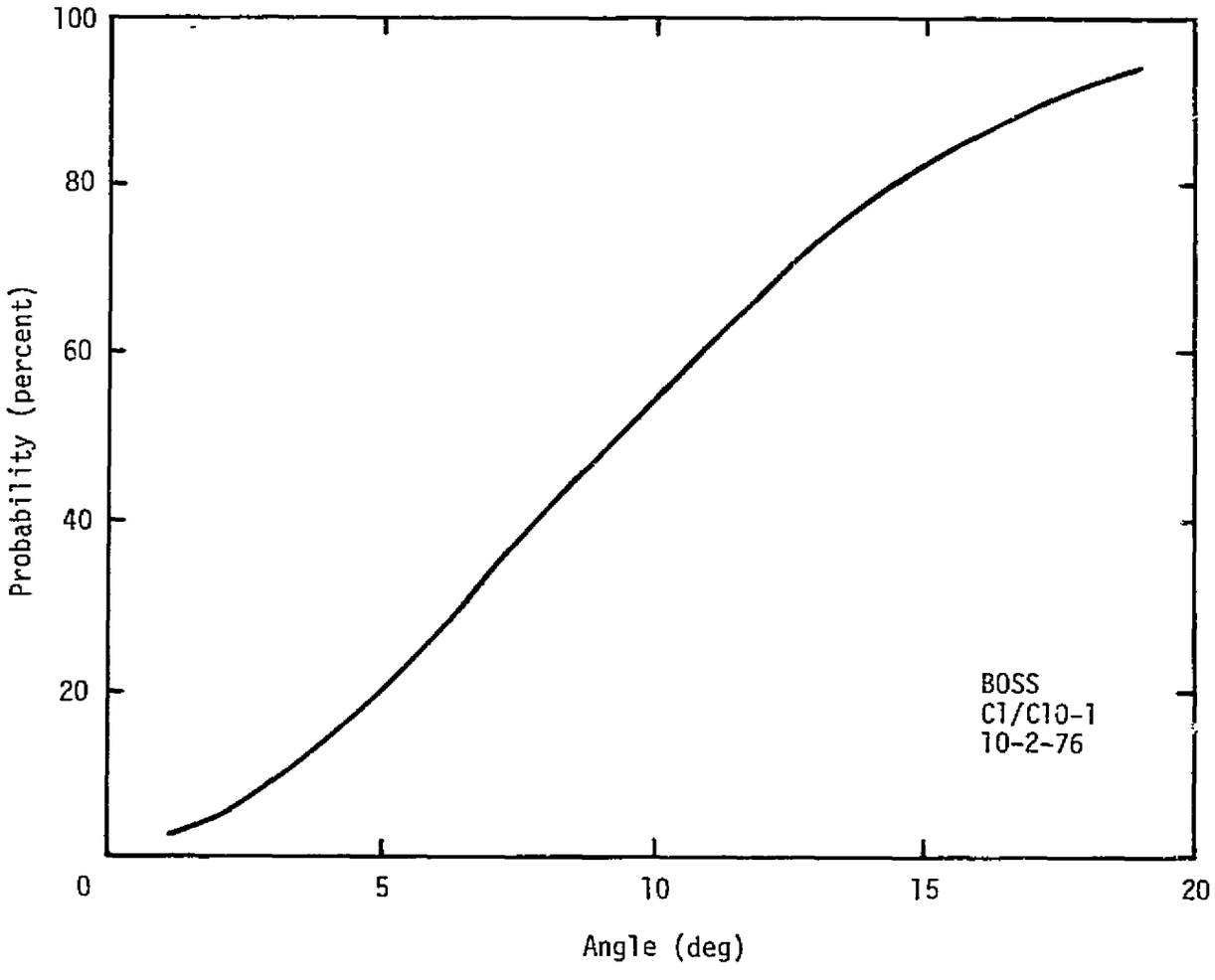

Figure 31. Probability (percent) that the angular deviation of the payload from vertical is less than a given angle as a function of angle for the first 6 minutes during descent of the first Atomic Chlorine/Chlorine Oxide (Cl/ClO-1) flight

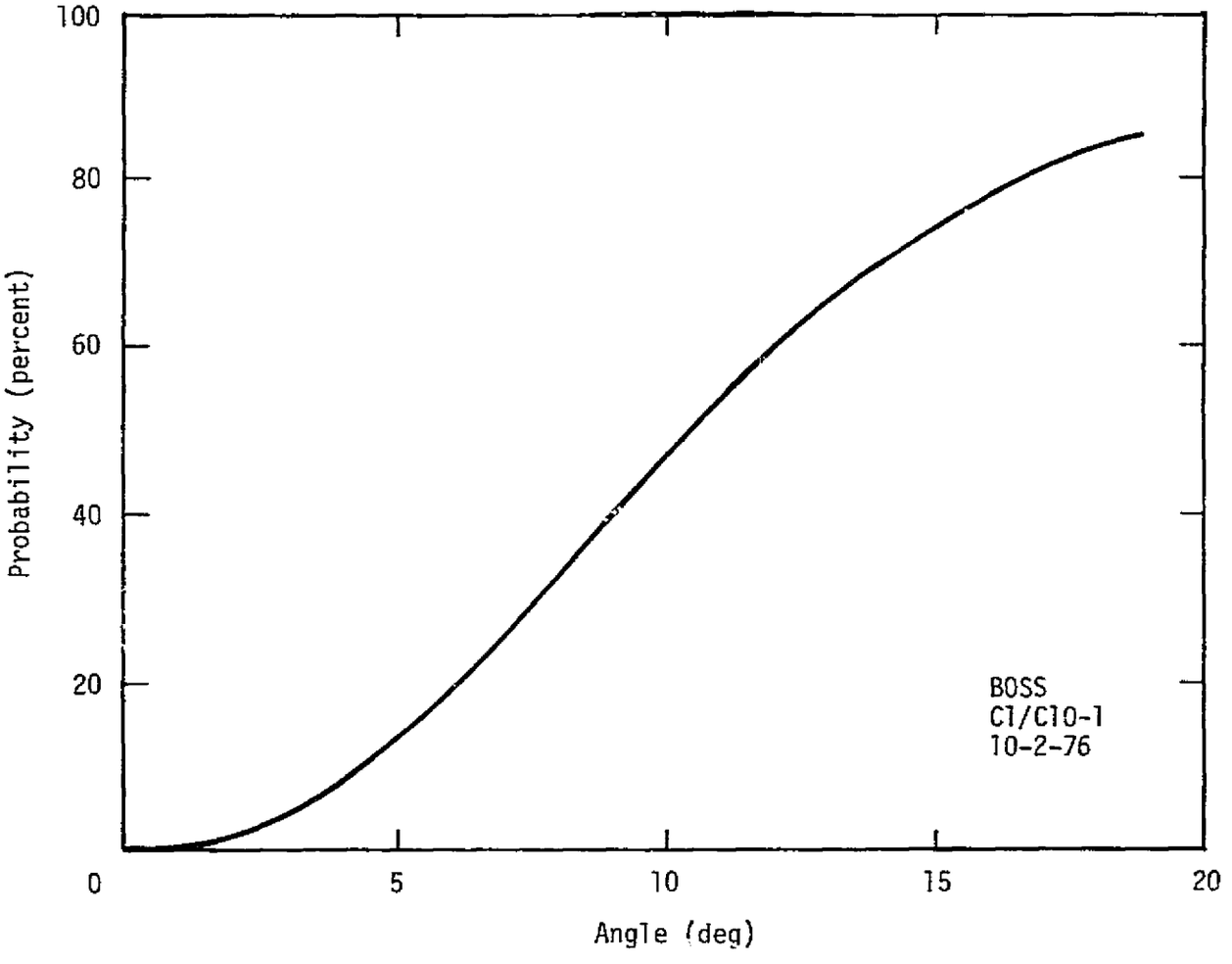

Figure 32. Probability (percent) that the angular deviation of the payload from vertical is less than a given angle as a function of angle for the second 6 minutes during descent of the first Atomic Chlorine/Chlorine Oxide (Cl/ClO-1) flight

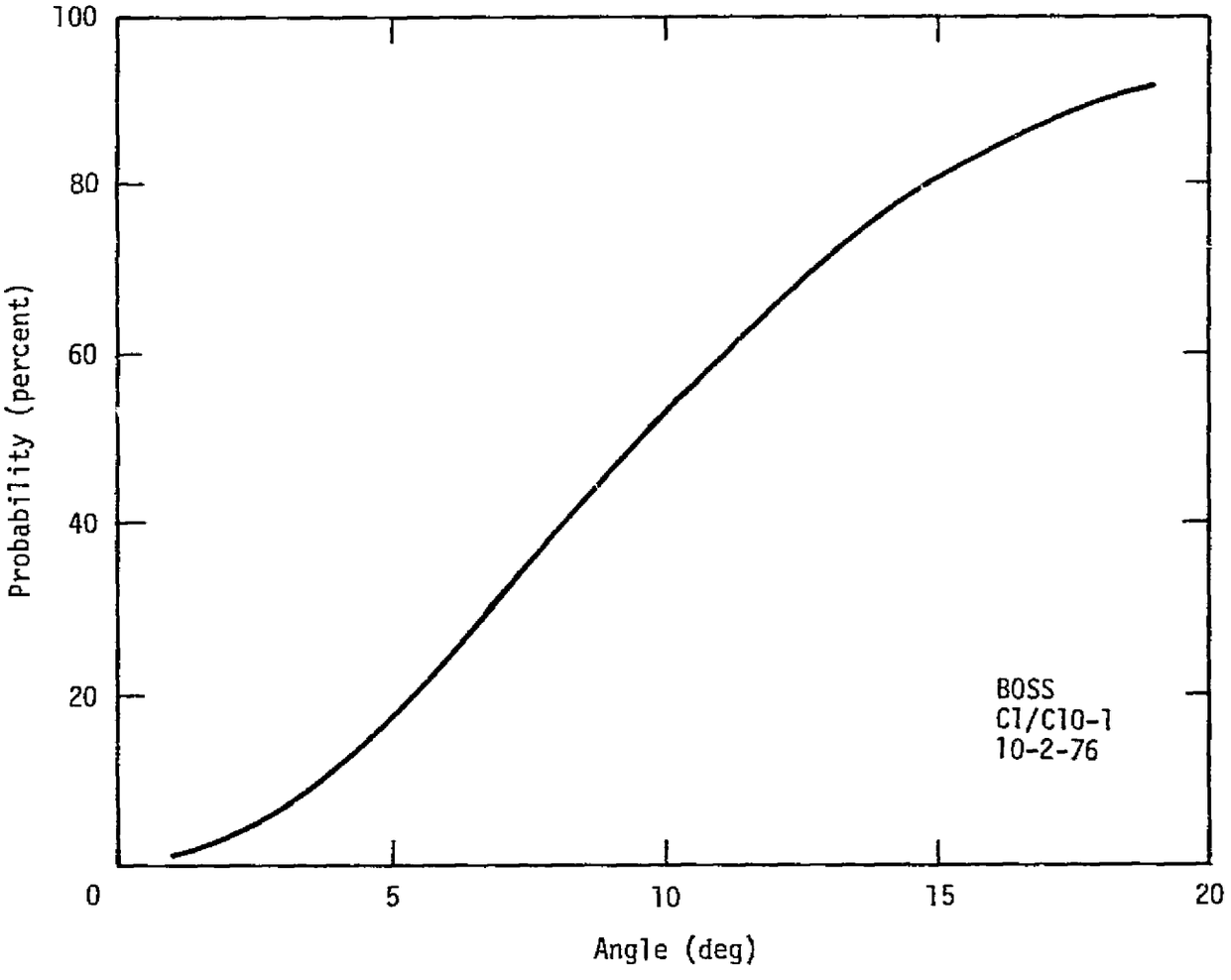

Figure 33. Probability (percent) that the angular deviation of the payload from vertical is less than a given angle as a function of angle for the first 19 minutes during descent of the first Atomic Chlorine/ Chlorine Oxide (Cl/ClO-1) flight

after cutdown (payload within 10 degrees of vertical 53% of the time). Thus the attitude stability was excellent during the entire descent.

5.3.2.3 Power and Temperature Profiles

Figure 34 shows the payload power consumptions integrated as a function of time for the flight. Total power used by the complete payload was 14.1 ampere hours.

Figure 35 is a thermal history of the transmitter and the uplooking motion picture camera for the flight. A similar plot showing the temperatures of the low and medium pressure transducers for determining payload altitude was shown in figure 36.

5.3.3 POSTFLIGHT ACTIVITIES

The payload landed in a open field approximately 20 nautical miles east of Brownwood, Texas, at 1241 CDT. The dual-pod attachment structure apparently failed on impact at the predicted points to decrease the shock on the electronic components. The payload was returned to NSBF the following day and the only damage was to some exposed cabling.

5.3.4 DATA RESULTS

5.3.4.1 Resonance Fluorescence Experiment

The results of the resonance fluorescence measurements of atomic chlorine and chlorine oxide which were obtained on this flight are included in the scientific write-up which is attached to appendix E.

5.3.4.2 Ozonesonde Data

Personnel from Wallops Flight Center supported this stratospheric measurement flight by launching two ozonesondes from the National Weather Station at Longview, Texas. The first ozonesonde was launched at 1000 CDT and the second ozonesonde was launched at 1309 CDT. Concentration measurements obtained by these two ozonesondes appears in figure 37.

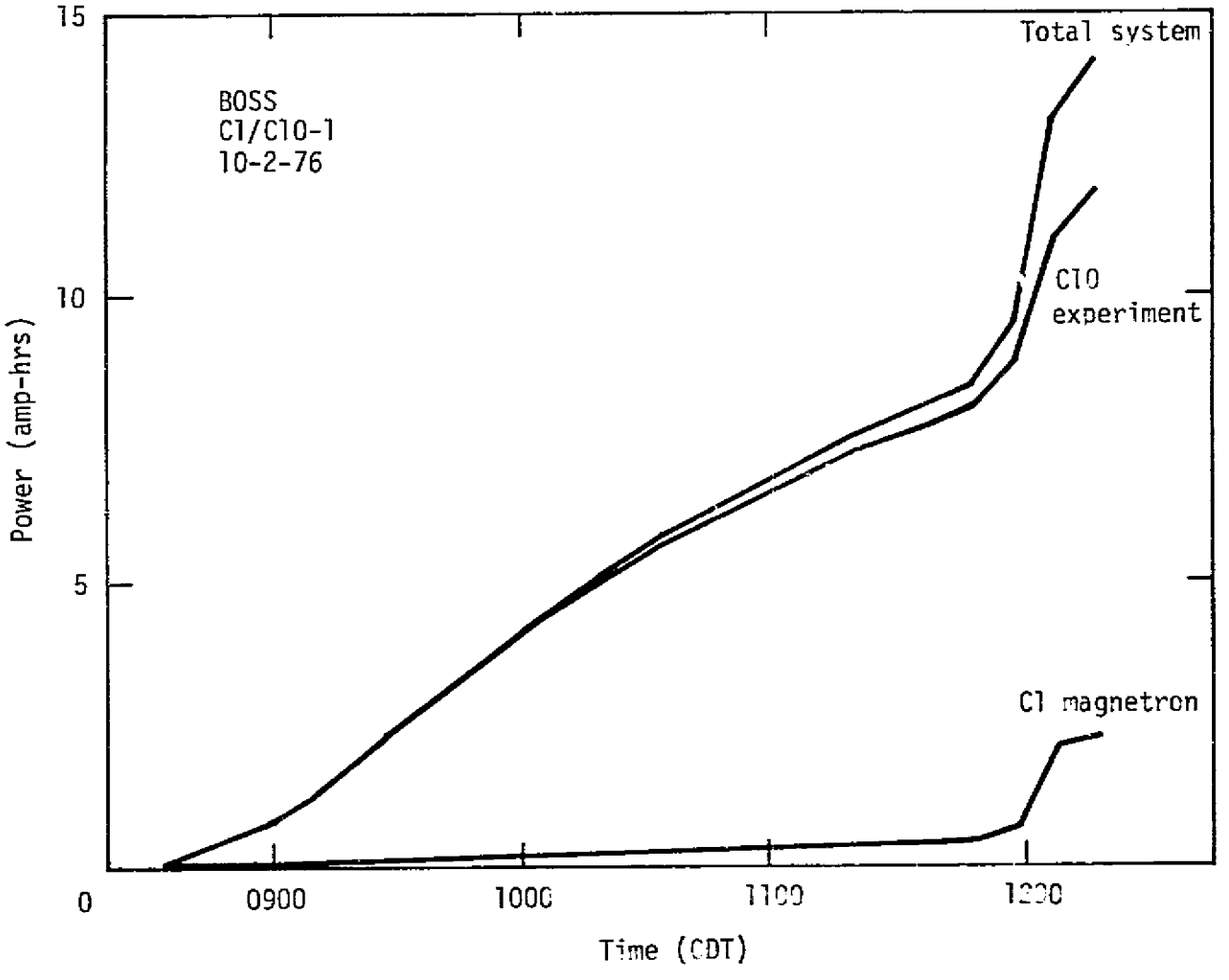

Figure 34. Payload power consumption for the first Atomic Chlorine/Chlorine Oxide (Cl/ClO-1) flight

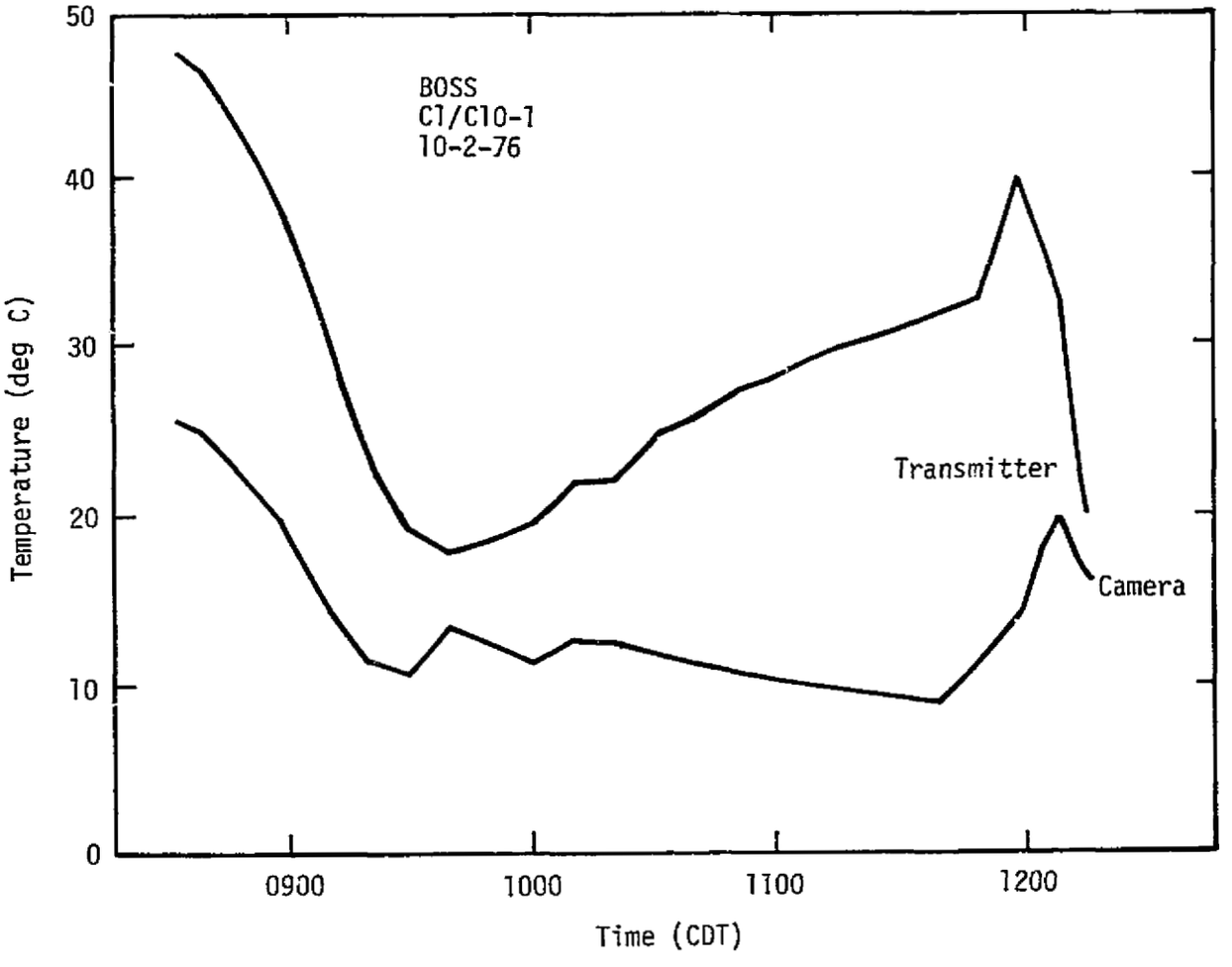

Figure 35. Thermal history of the transmitter and uplooking motion picture camera for the first Atomic Chlorine/Chlorine Oxide (Cl/ClO-1) flight

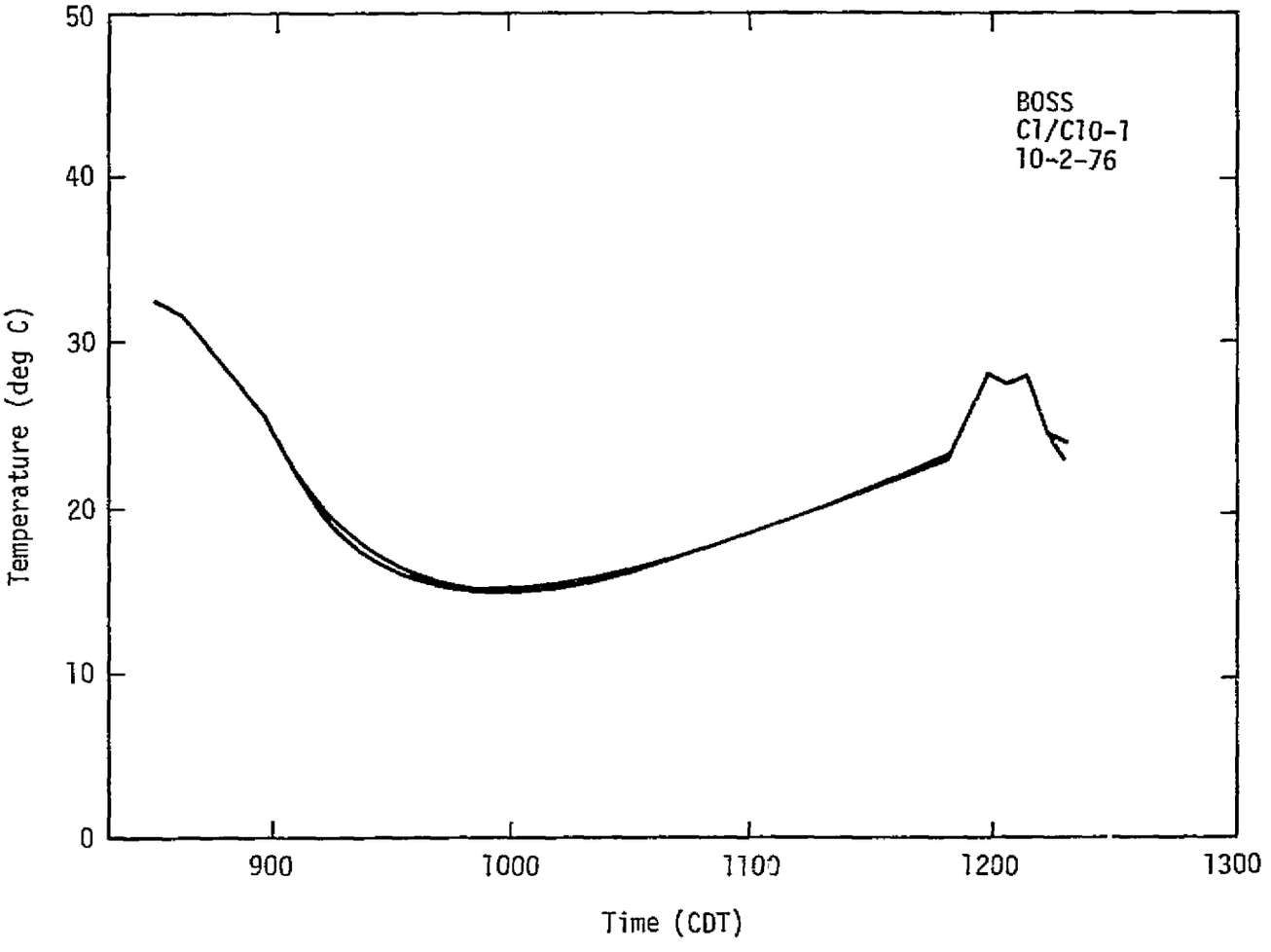

Figure 36. Thermal history of low and medium range pressure transducers for the first Atomic Chlorine/Chlorine Oxide (Cl/ClO-1) flight

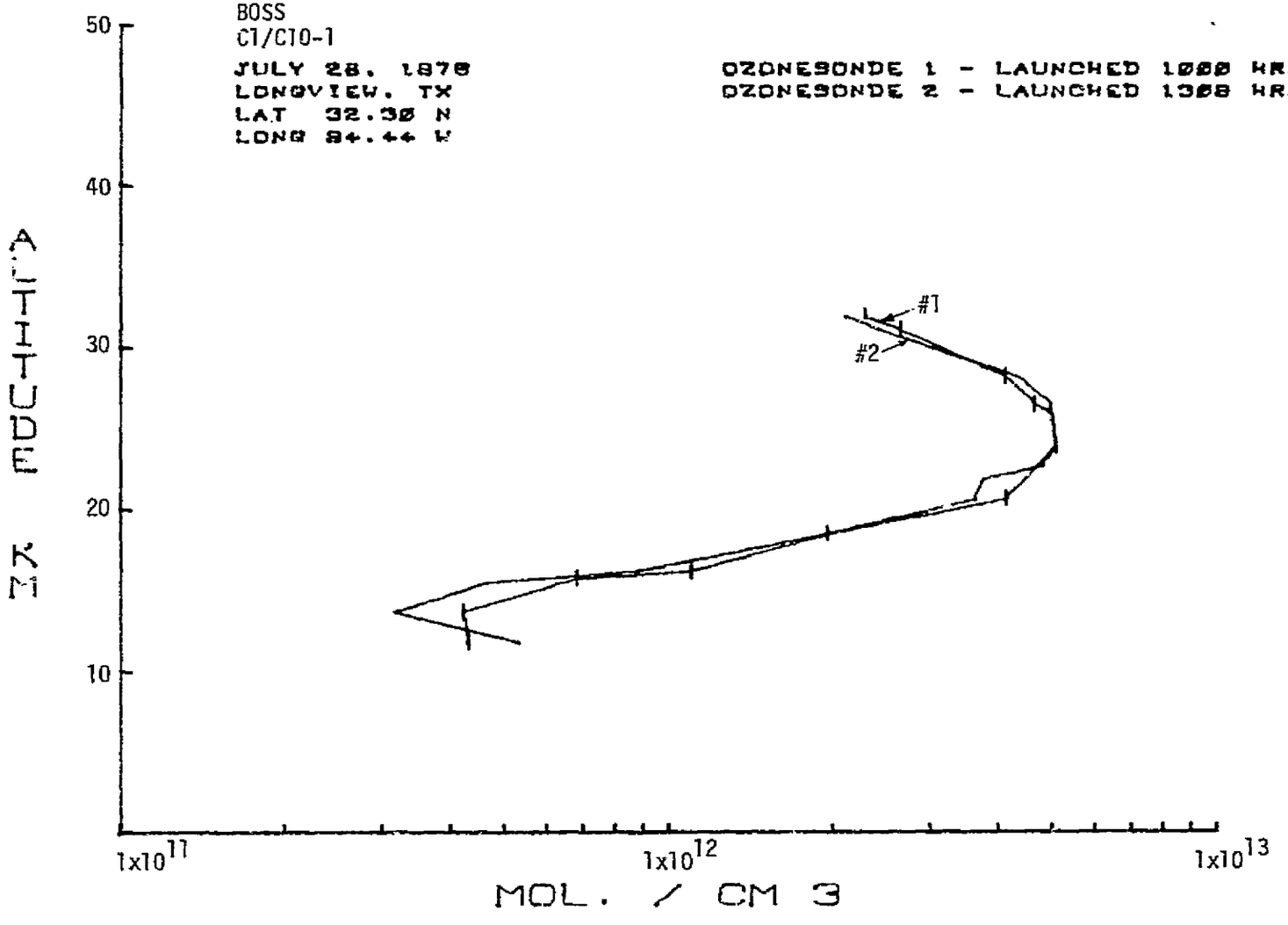

Figure 37. Concentration of ozone determined by radiosonde during the first Atomic Chlorine/Chlorine Oxide (Cl/ClO-1) flight

5.4 Second Atomic Chlorine/Chlorine Oxide (Cl/ClO-2) Measurement

5.4.1 SUMMARY

This balloon parachute flight was the ninth flight of the laminar flow through/resonance fluorescent instrumentation (principal investigator: Dr. James Anderson, University of Michigan) and took place on 2 October 1976. The purpose of this flight was to measure the vertical concentration profiles of atomic chlorine (Cl) and chlorine oxide (ClO) in the stratosphere. This flight was also utilized to perform a flight qualification test on a new design for an ultraviolet absorption ozone monitor and a total air temperature measuring device to supply temperature profiles to the chemical analysis.

The flight was launched at 0759 CDT from the National Science Balloon Facility at Palestine, Texas. The morning launch was again chosen to maximize the opportunity for low surface winds needed to launch the balloon and to drop around noon when the chlorine photochemistry has stabilized.

The two pod configuration for the laminar flow through/resonance fluorescence measurements was utilized and the ozone monitor and total air temperature systems were installed in the NCAR electronics box. The payload weight was 715 pounds and a 14 meter diameter guide surface parachute was used on this flight. The payload was carried aloft by a 4.4×10^5 m^3 helium filled balloon. A sketch of the payload and a listing of support hardware instrumentation is shown in figure 38. Figure 39 shows the payload hanging from the launch vehicle just prior to launch.

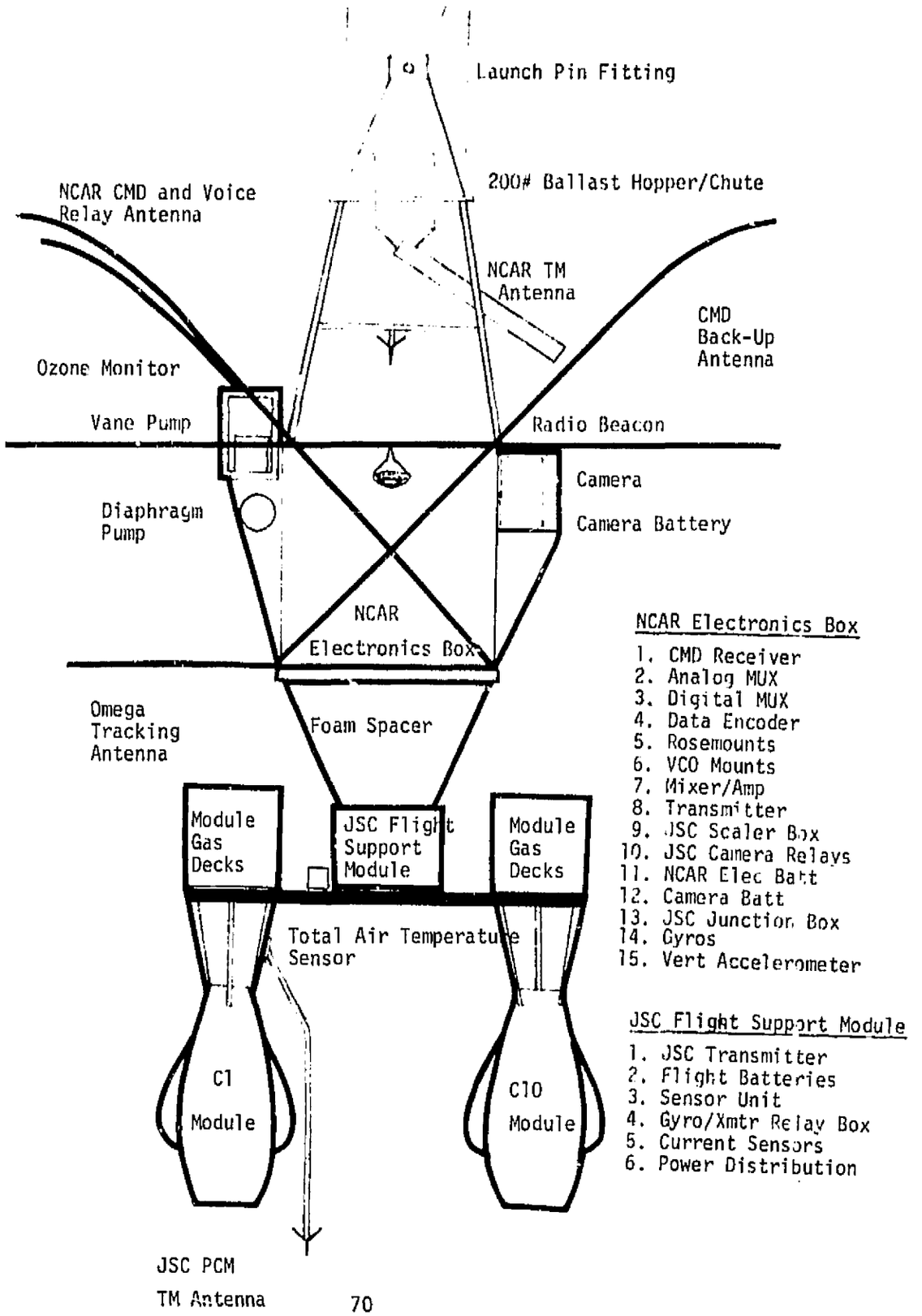

Figure 38. Sketch of the Second Atomic Chlorine/Chlorine Oxide (Cl/ClO-2) Payload

NASA
S- 76- 29721

Figure 59. Second Atomic Chlorine/Chlorine Oxide (Cl/ClO-2) Payload Ready for Launch

The payload reached a float altitude of approximately 43 km at 1107 CDT. The flight was terminated at 1215 CDT and the parachute/payload landed close to a residence on the outskirts of the town of Calvert, Texas which is north of Bryan. The dual pod attachment structure failed at the predicted points on impact. One of the vertical support struts to one of the University of Michigan pods also failed but did not damage the rest of the instrumentation.

5.4.2 PAYLOAD OPERATIONS

5.4.2.1 Ascent Phase

The flight profile for the second atomic chlorine/chlorine oxide (Cl/ClO-2) flight is illustrated in figure 40. Launch occurred at 0759 CDT, 2 October 1976, and was accomplished using the dynamic launch technique. The 4.4×10^5 m^3 balloon and payload were launched from the NCAR launch pad with no visible interference, ground contact, or accessive swinging of the payload. The payload obtained an altitude of approximately 43 km at 1107 CDT.

Operation of all systems during ascent was nominal except for the UV ozone monitor. This system exhibited an unusually high background noise level. Figure 41 shows the pressures indicated by the three onboard pressure transducers during the ascent phase of the flight.

5.4.2.2 Descent Phase

The payload was released on command from the NCAR tower at 1215 CDT.

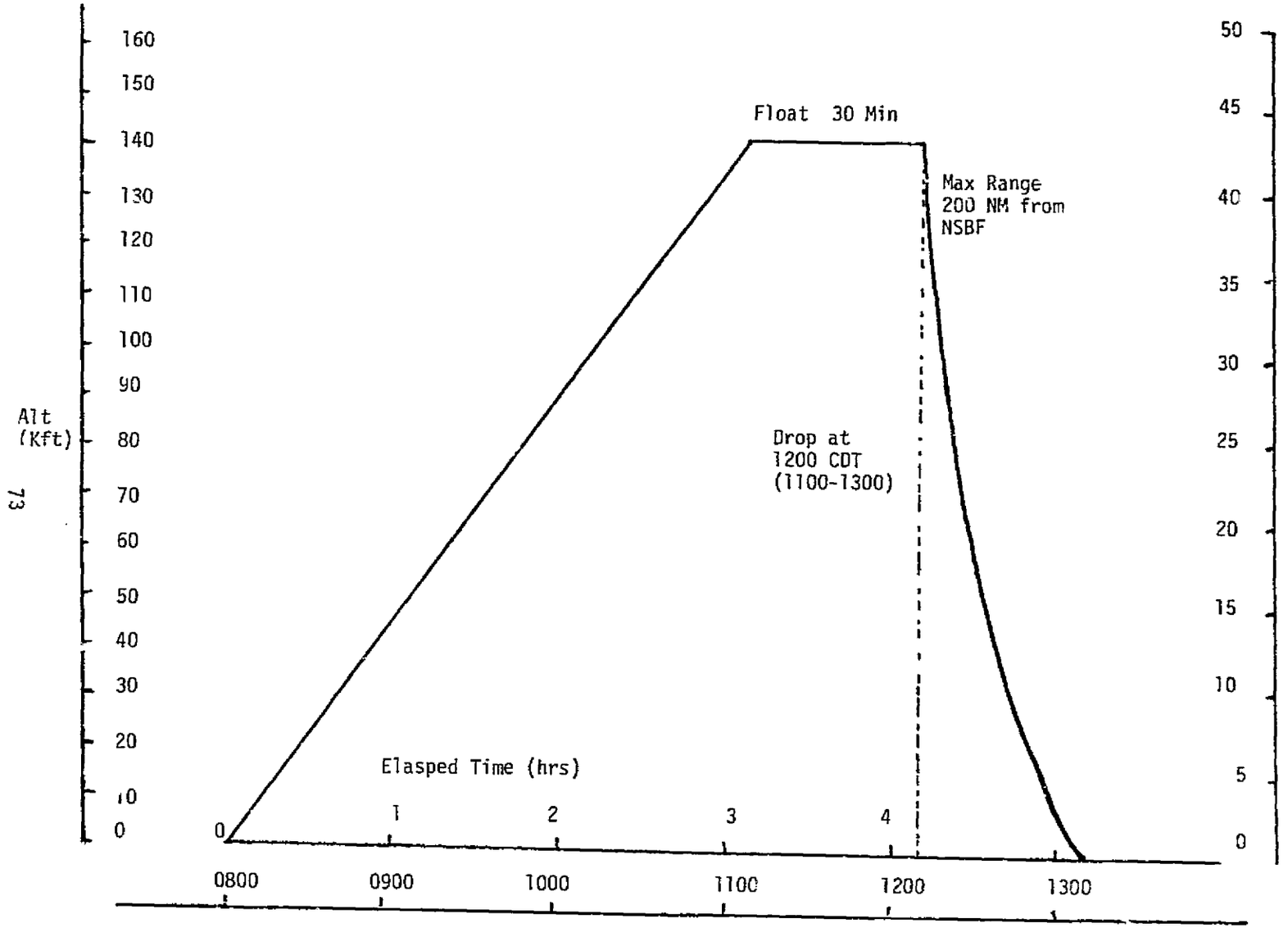

Figure 40. Second Cl/ClO Flight - Altitude Profiles

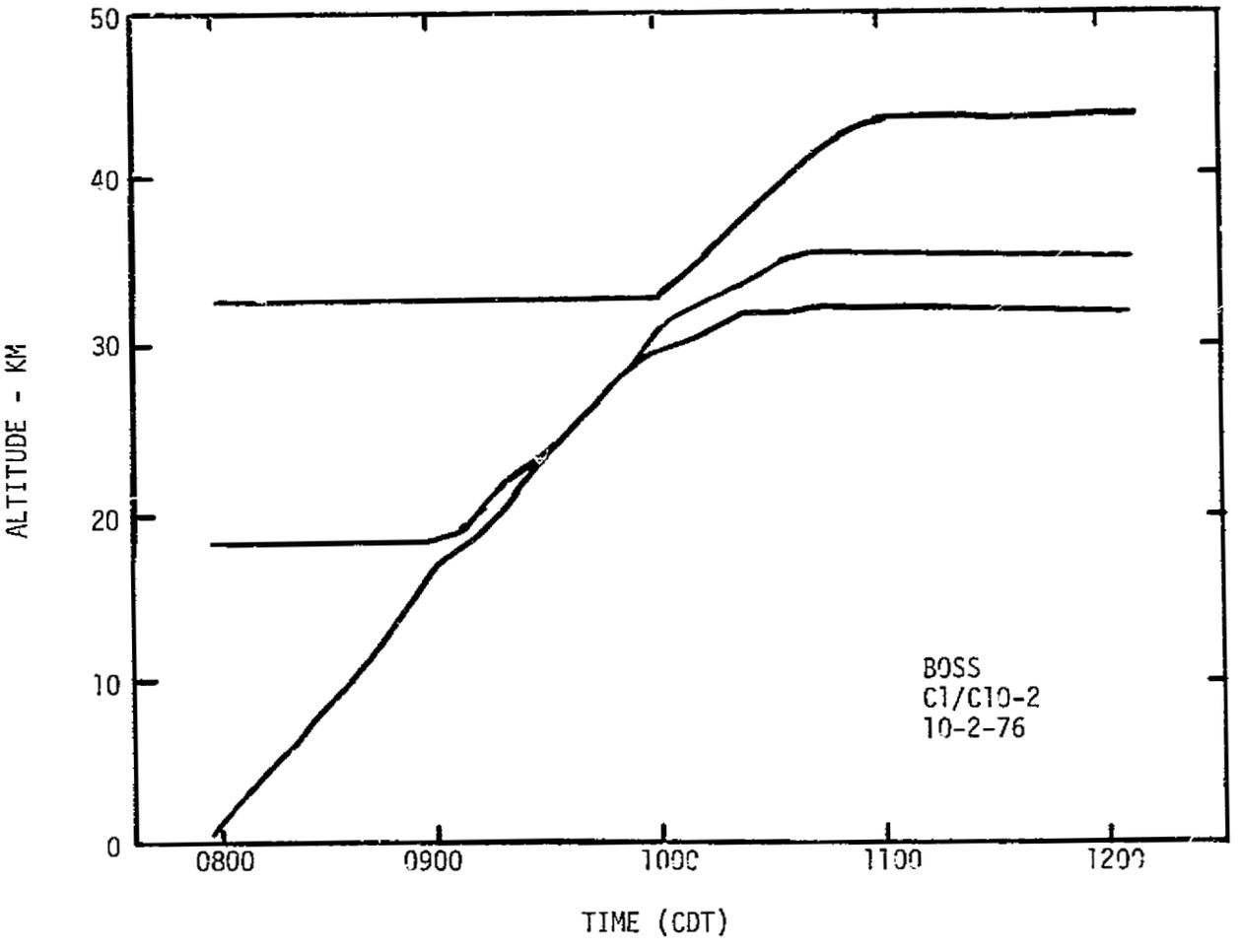

Figure 41. Altitude/time profiles for the ascending payload during the second Atomic Chlorine/Chlorine Oxide (Cl/ClO-2) flight as measured by three pressure transducers.

An onboard motion picture camera observed the parachute deployment, the accelerometer measured the G forces on parachute deployment, and two vertical reference gyros monitored the descent attitude of the system. The altitude profile as a function of time inferred from the pressure transducers is shown in figure 42. The velocity as a function of altitude for the descending payload is shown in figure 43. Vertical forces experienced by the payload during release and deployment of the 14 meter diameter parachute are shown in figure 44. Figure 45 shows the stability of the payload during the descent. This figure indicates the probability that the payload has less than the indicated angle during descent. Indications were that this payload was more unstable than the first Cl/ClO flight. This difference is attributed to higher wind shears and atmospheric turbulence since there were no variations in the rigging which would account for this difference.

5.4.2.3 Power and Temperature Profiles

Figure 46 shows the payload power consumption integrated as a function of time for the flight. Also shown in that figure are the separate power consumption profiles for the ozone monitor, and for the electronics systems. Total power consumption was approximately 35 ampere-hours. Figure 47 shows the temperature of the transmitter and the battery package. Figure 48 shows the skin temperature and the uplook TV camera during the flight.

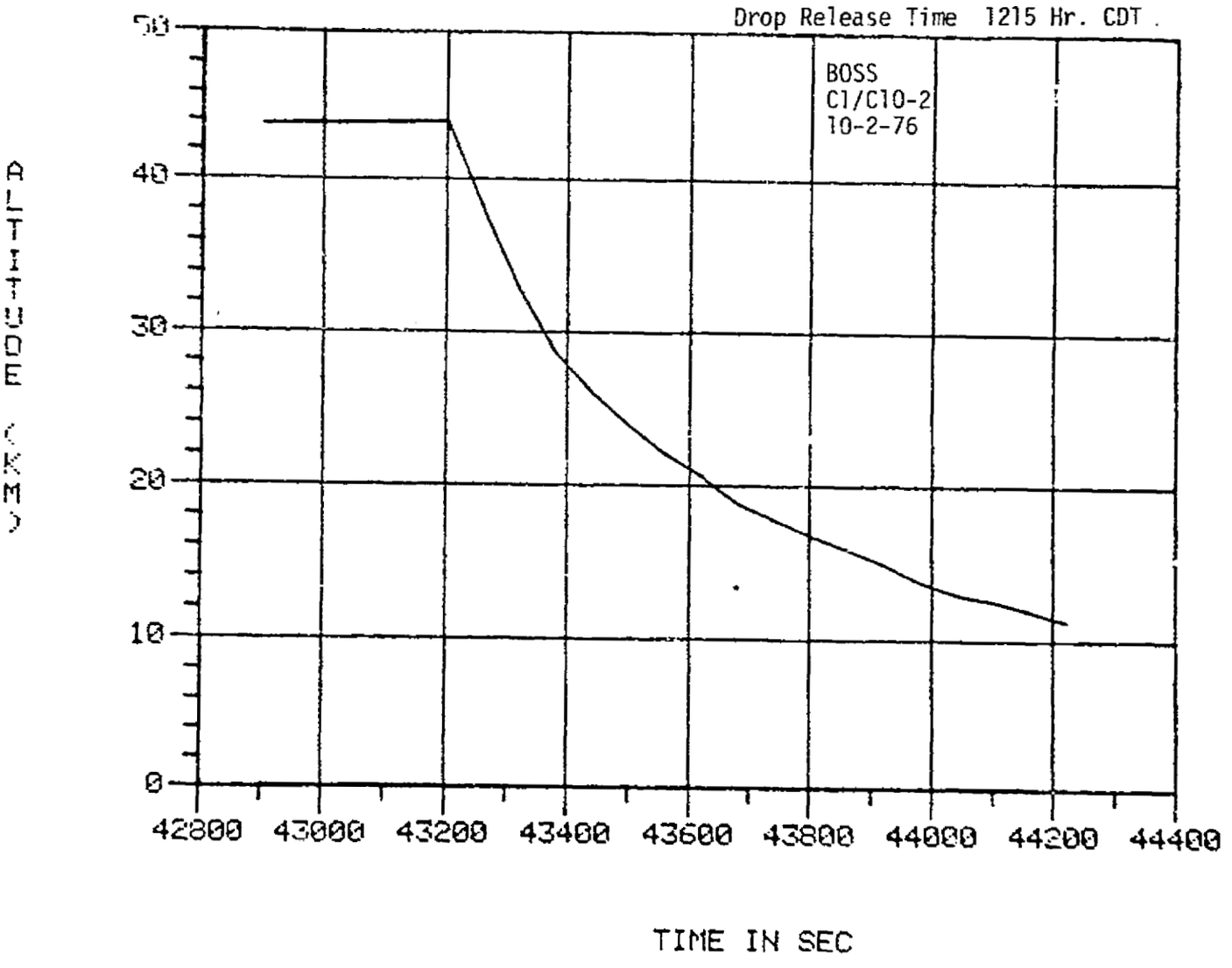

Figure 42. Altitude/Time Profiles for the Descending Payload During the Second Atomic Chlorine/Chlorine Oxide (Cl/ClO-2) Flight

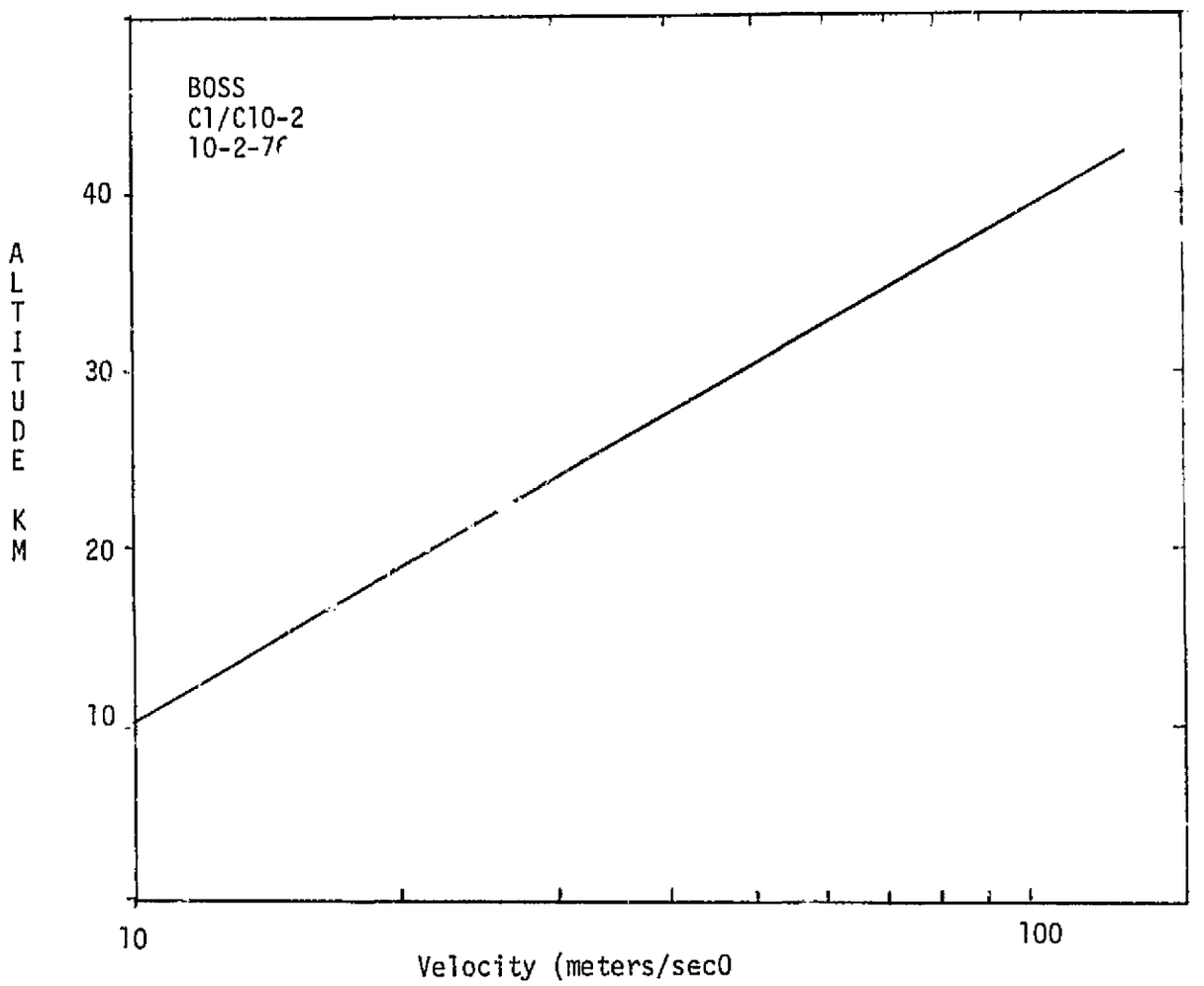

Figure 43. Velocity/Altitude Profile of Descending Payload for the Second Atomic Chlorine/Chlorine Oxide (Cl/ClO-2) Flight

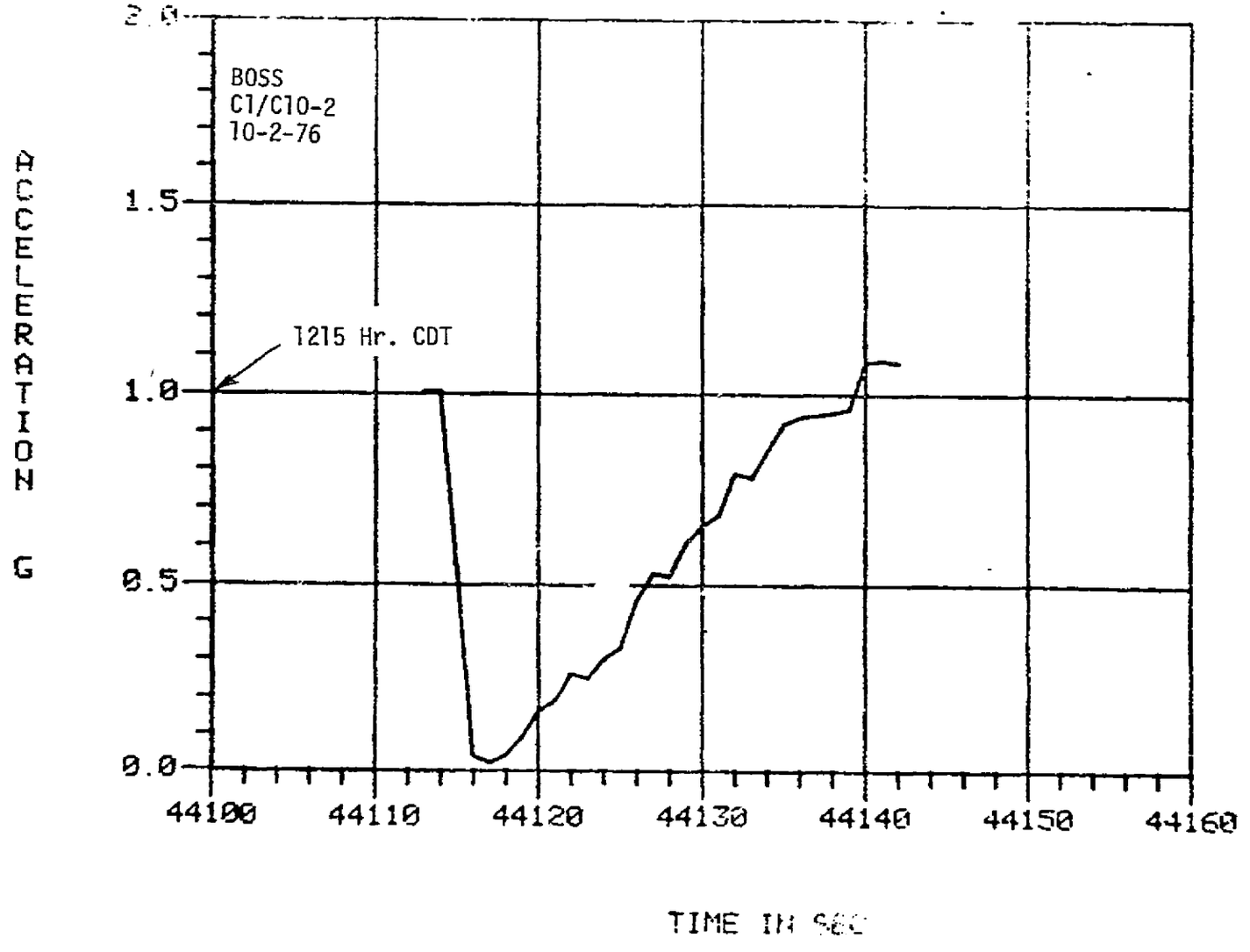

Figure 44. Vertical Force on Payload after Parachute Deployment for the Second Atomic Chlorine/Chlorine Oxide (Cl/ClO-2) Flight

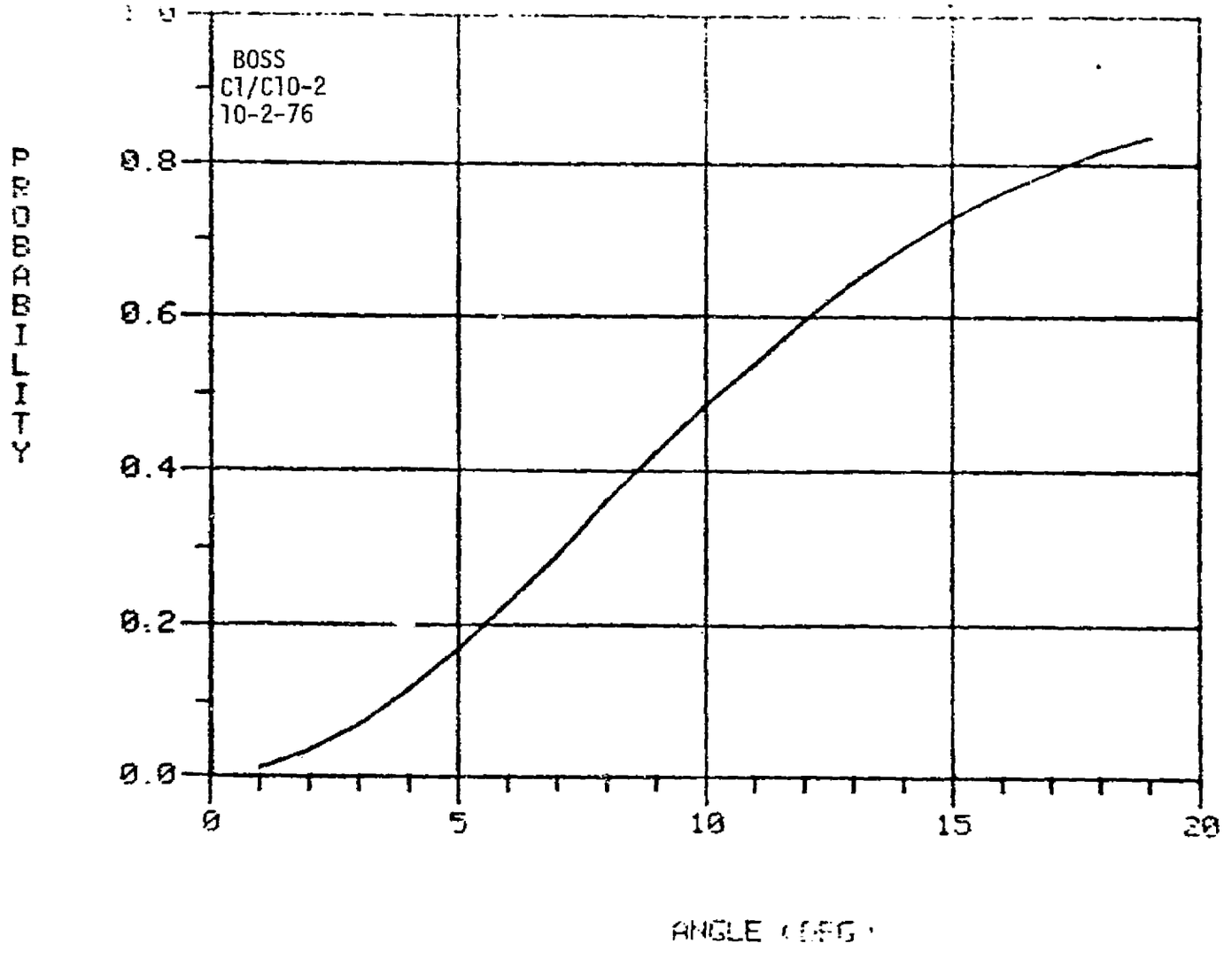

Figure 45. Probability that the Angular Deviation of the Payload from Vertical is less than a Given Angle as a Function of Angle During Descent of the Second Chlorine/Chlorine Oxide (Cl/ClO-2) Flight

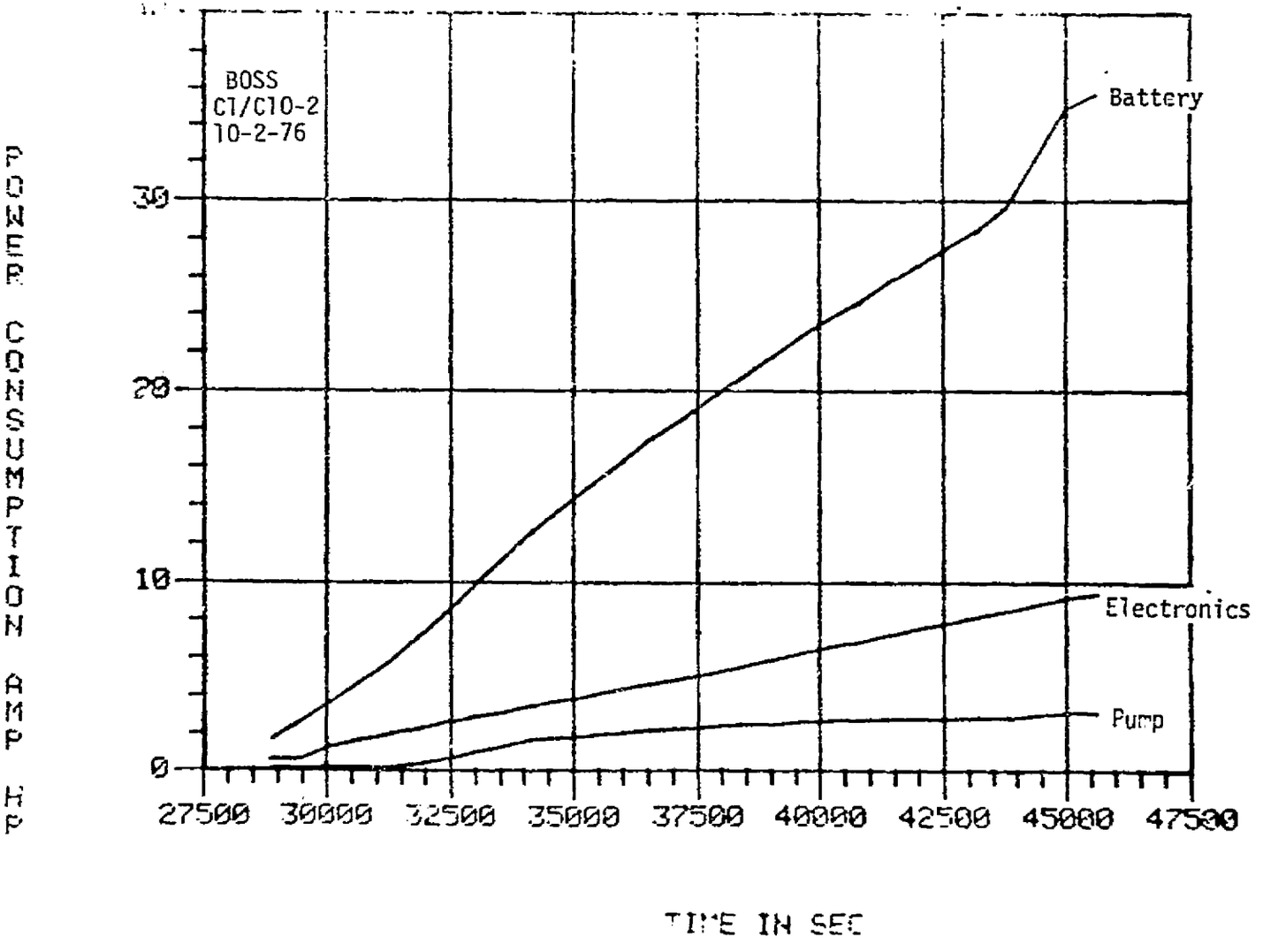

Figure 46. Payload Power Consumption for the Second Chlorine/Chlorine Oxide (Cl/ClO-2) Flight

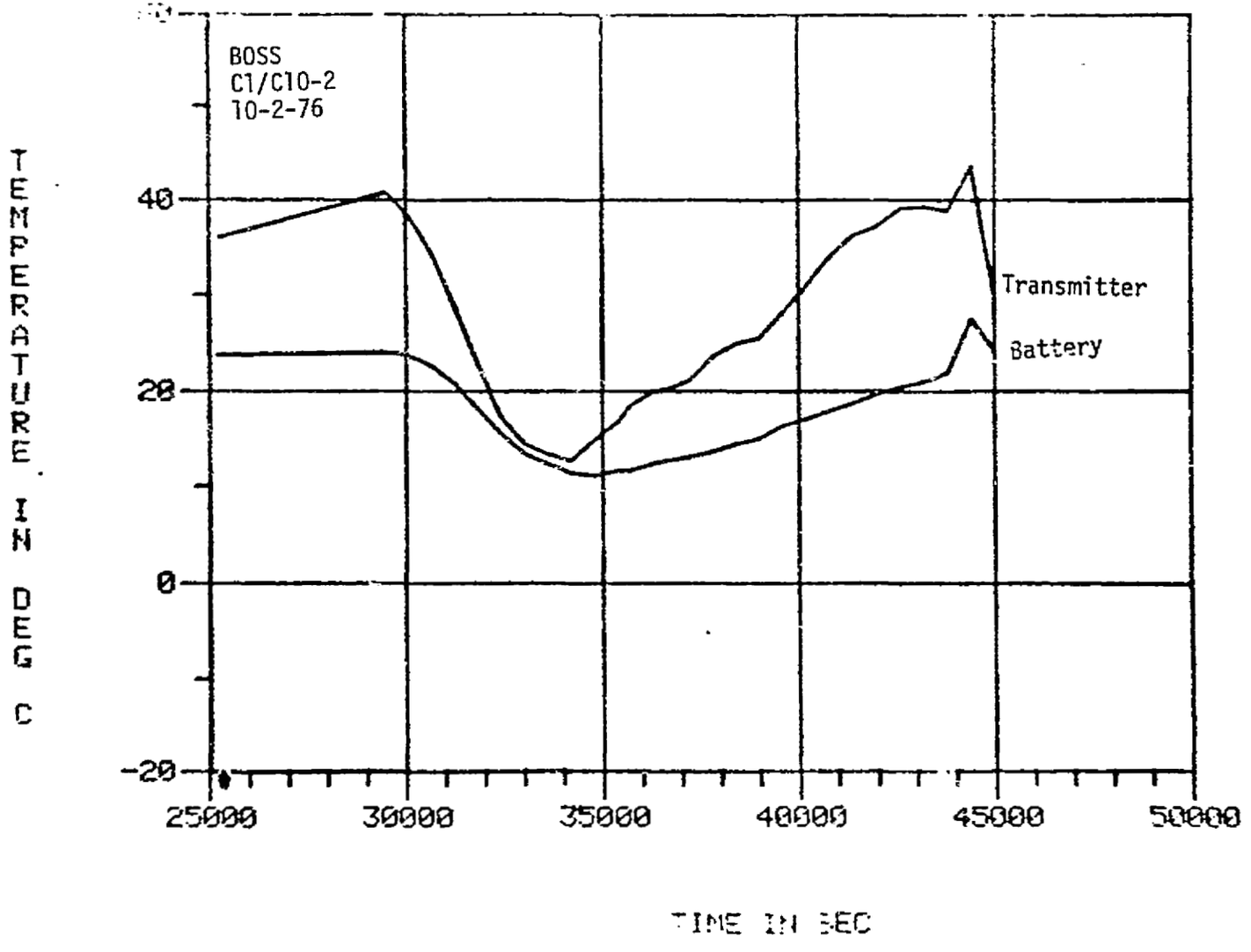

Figure 47. Thermal History of the Battery and Transmitter for the Second Atomic Chlorine/Chlorine Oxide (Cl/ClO-2) Flight

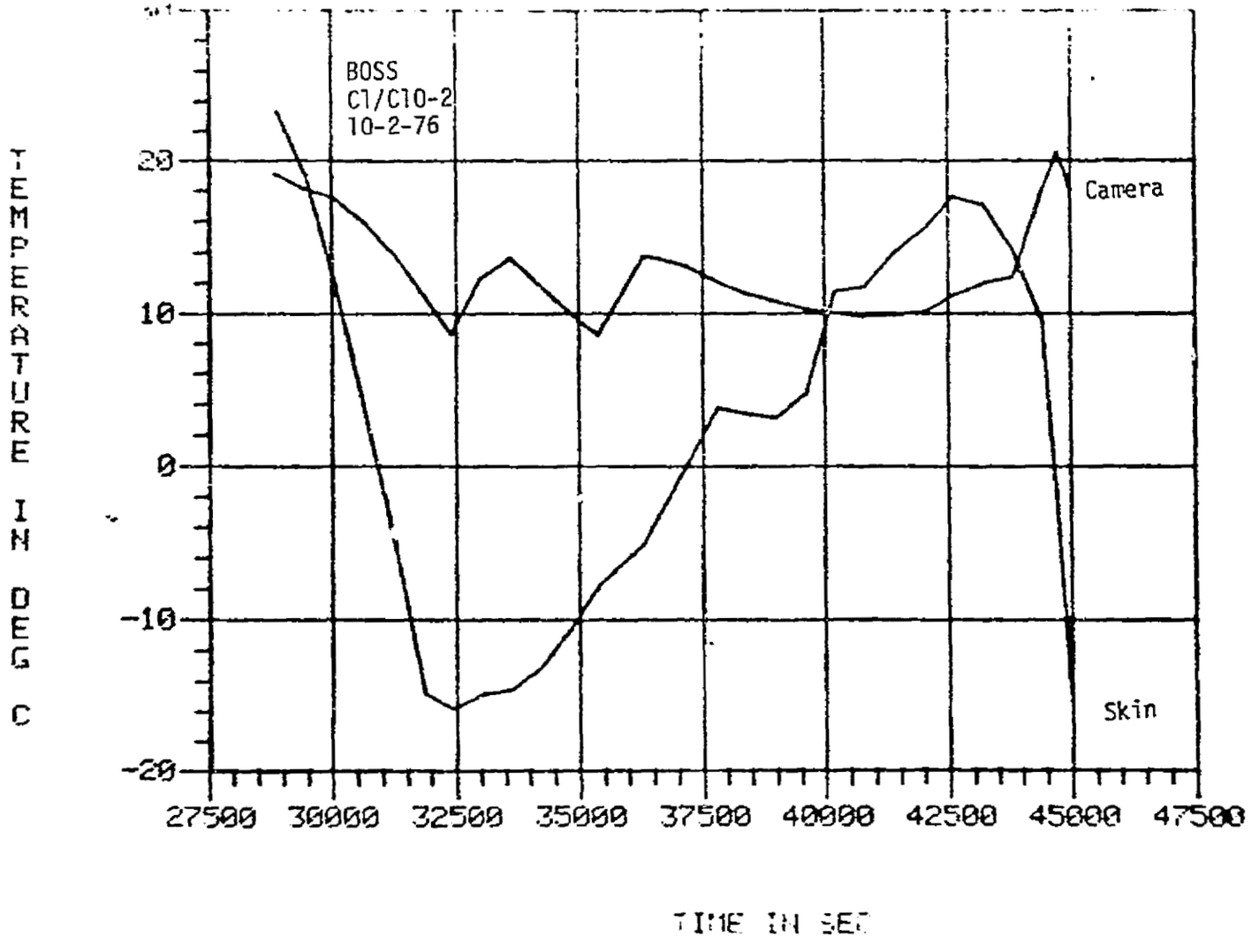

Figure 48. Thermal History of the Camera and Payload Skin During the Second Atomic Chlorine/Chlorine Oxide (Cl/ClO-2) Flight

5.4.3 POSTFLIGHT ACTIVITIES

The payload landed in the edge of the town of Calvert, Texas which is north of Bryan , Texas. Failure of the pod attachment structure occurred at the predicted points. One of the vertical support struts to the resonant fluorescence modules failed on impact but did not damage any of the other equipment and experiments. Recovery was completed and the equipment returned to NCAR on the afternoon of 2 October 1976. Postflight testing indicated that all components survived and were still in fully functional order.

5.4.4 DATA RESULTS

5.4.4.1 Resonance Fluorescence Experiment

The results of the resonance fluorescence measurements of atomic chlorine and chlorine oxide which were obtained on this flight are included in the scientific write-up which is attached to appendix E.

5.4.4.2 Ozone Data

Personnel from the Wallops Flight Center supported this flight by launching three radiosondes from Longview, Texas. The first radiosonde which was launched at 0856 CDT only produced data to approximately 20 km. The other two radiosondes launched at 1053 CDT and 1331 CDT, respectively, produced data up beyond 30 km. The concentration produced by the use of ozonesondes is shown in figure 49.

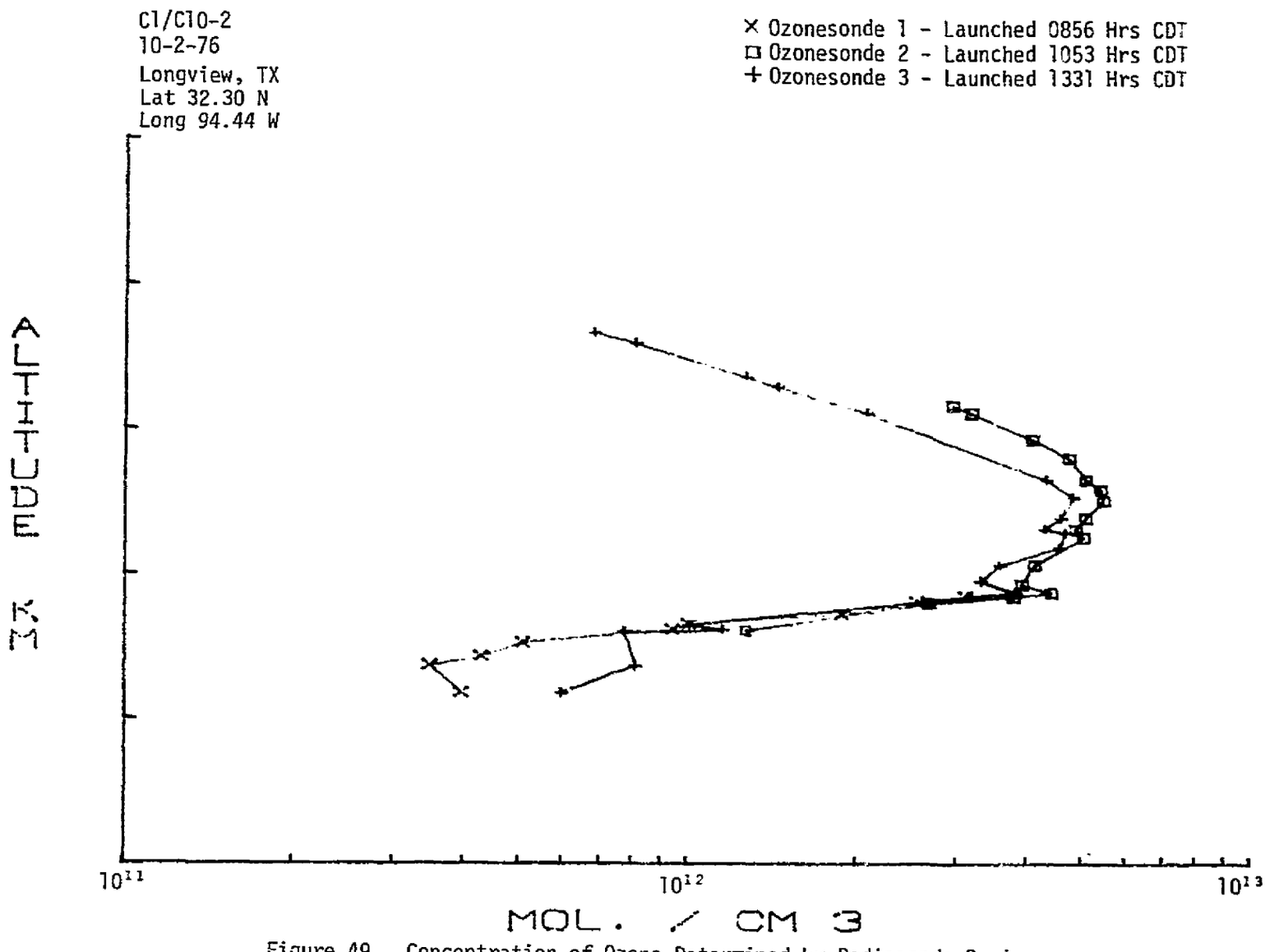

Figure 49. Concentration of Ozone Determined by Radiosonde During the first Atomic Chlorine/Chlorine Oxide (Cl/ClO-1) flight

The UV absorption ozone monitor was onboard this flight but because of noise in the system, did not produce what is considered a good concentration profile of ozone.

5.4.4.3 Total Air Temperature

A Rosemount Total Air Temperature (TAT) sensor was installed on this flight. The temperature measurement that this instrument recorded is shown in figure 50.

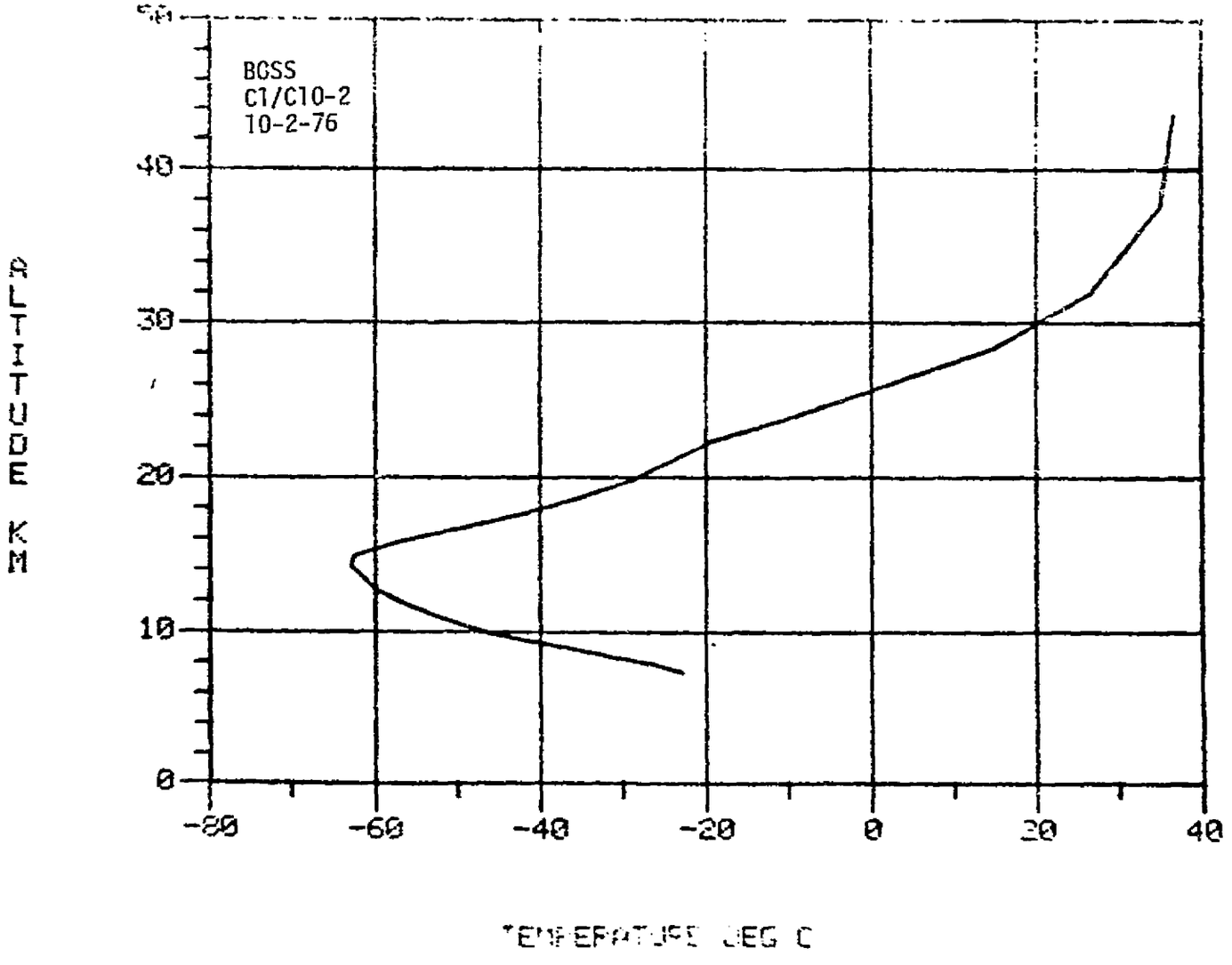

Figure 50. Air Temperature Profile Measured during the Second Atomic Chlorine/Chlorine Oxide (Cl/ClO-2) Flight

5.5 Third Atomic Chlorine/Chlorine Oxide (Cl/ClO-3), Ozone Measurement

5.5.1 Summary

This parachute flight was the tenth flight of laminar flow through/resonance fluorescence instrumentation (principal investigator: Dr. James Anderson, University of Michigan) and took place on 8 December 1976. The purpose of this flight was to measure the vertical concentration profiles of atomic chlorine (Cl), chlorine oxide (ClO), and ozone (O_3) in the stratosphere. A temperature measuring device was also included in addition to the concentration measurement instrumentation.

The flight was launched at 0853 CST from the National Science Balloon Facility at Palestine, Texas. The morning launch was again chosen to maximize the opportunity for low surface winds needed to launch the balloon and to drop around noon when the chlorine photochemistry has stabilized.

The two-pod configuration for the laminar flow through/resonance fluorescence measurements were utilized and again the ozone monitor was installed in the NCAR electronics box. The total payload weight was 720 lbs and a 14-meter diameter guide surface parachute was used for the drop on this flight. The payload was carried off by a 4.4×10^5 m^3 helium filled balloon. A sketch of the payload and a listing of support instrumentation is shown in figure 51. Figure 52 shows the payload just prior to launch. The payload reached full altitude at approximately 42 km at 1132 CST. The flight was released at 1200 CST and the parachute/payload landed approximately

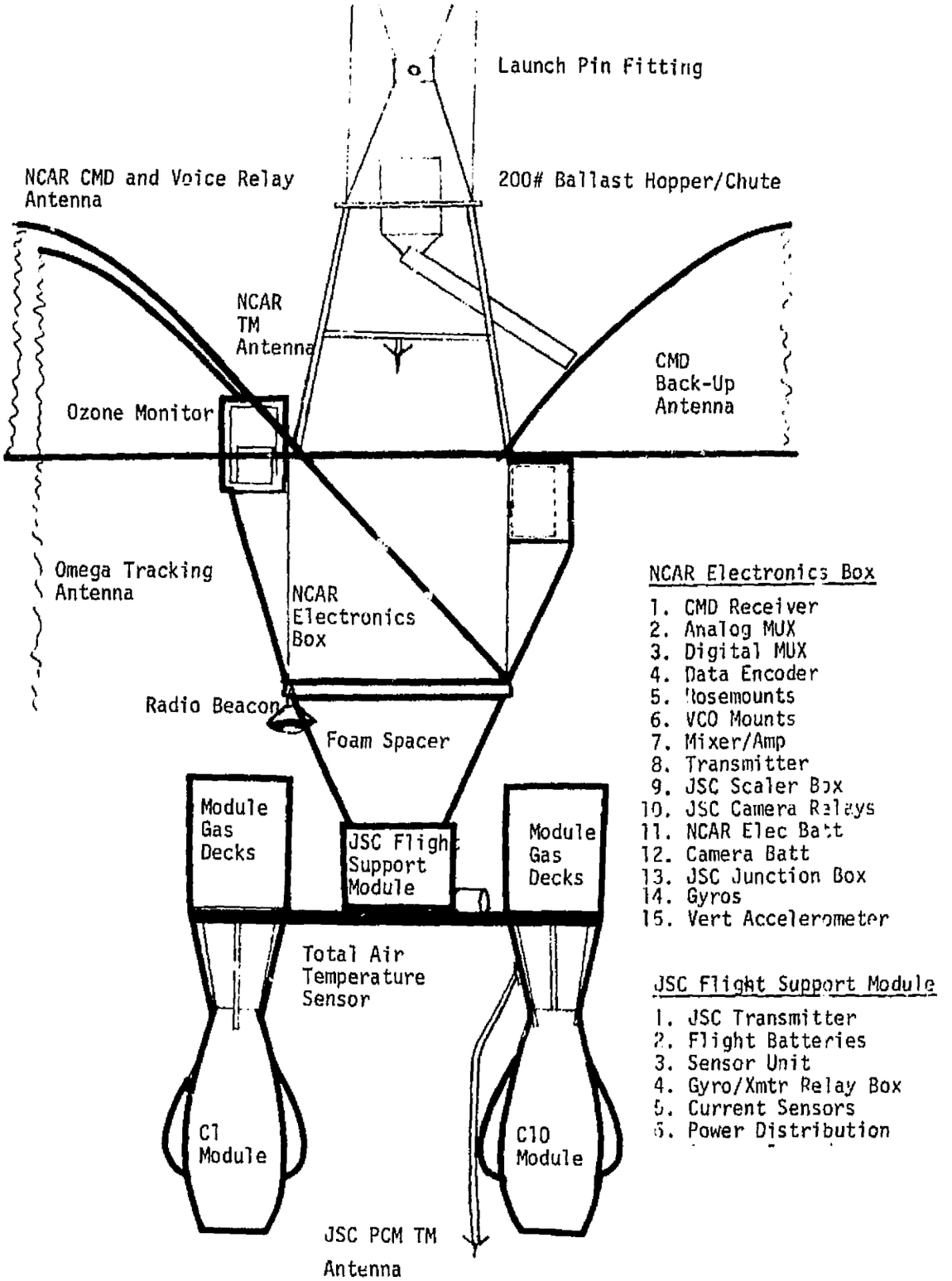

Figure 51. Sketch of Third Atomic Chlorine/Chlorine Oxide (Cl/ClO-3) Payload

NASA
S- 76- 33227

Figure 52. Third Atomic Chlorine/Chlorine Oxide (Cl/ClO-3) Payload Ready for Launch

10 nautical miles south of Jena, Louisiana. Due to the sandy, soft soil conditions, the pod attachment structure was bent but did not fracture. No unusual damage occured on landing.

5.5.2 Payload Operations

5.5.2.1 Ascent Phase

The flight profile for the third atomic chlorine/chlorine oxide (Cl/ClO-3) flight is illustrated in figure 53. Launch occurred at 0853 CST, 8 December 1976, and was accomplished using the dynamic launch technique. The 4.4×10^5 m^3 balloon and payload were launched from the NCAR launch pad with no visible interference, ground contact, or excessive swing of the payload. Payload obtained altitude at approximately 42 km at 1132 CST.

Operation of all systems during ascent was nominal. Figure 54 shows the pressures indicated by the three onboard pressure transducers during the ascent phase of our flight.

5.5.2.2 Descent Phase

The payload was released on command from the NCAR tower at 1200 CST. An onboard motion picture camera observed the parachute deployment, an accelerometer measured the vertical forces on parachute deployment, and two ve tical reference gyros monitored the descent attitude of the payload. The altitude profile during descent as averaged from the pressure transducers is shown in figure 55. The velocity as a

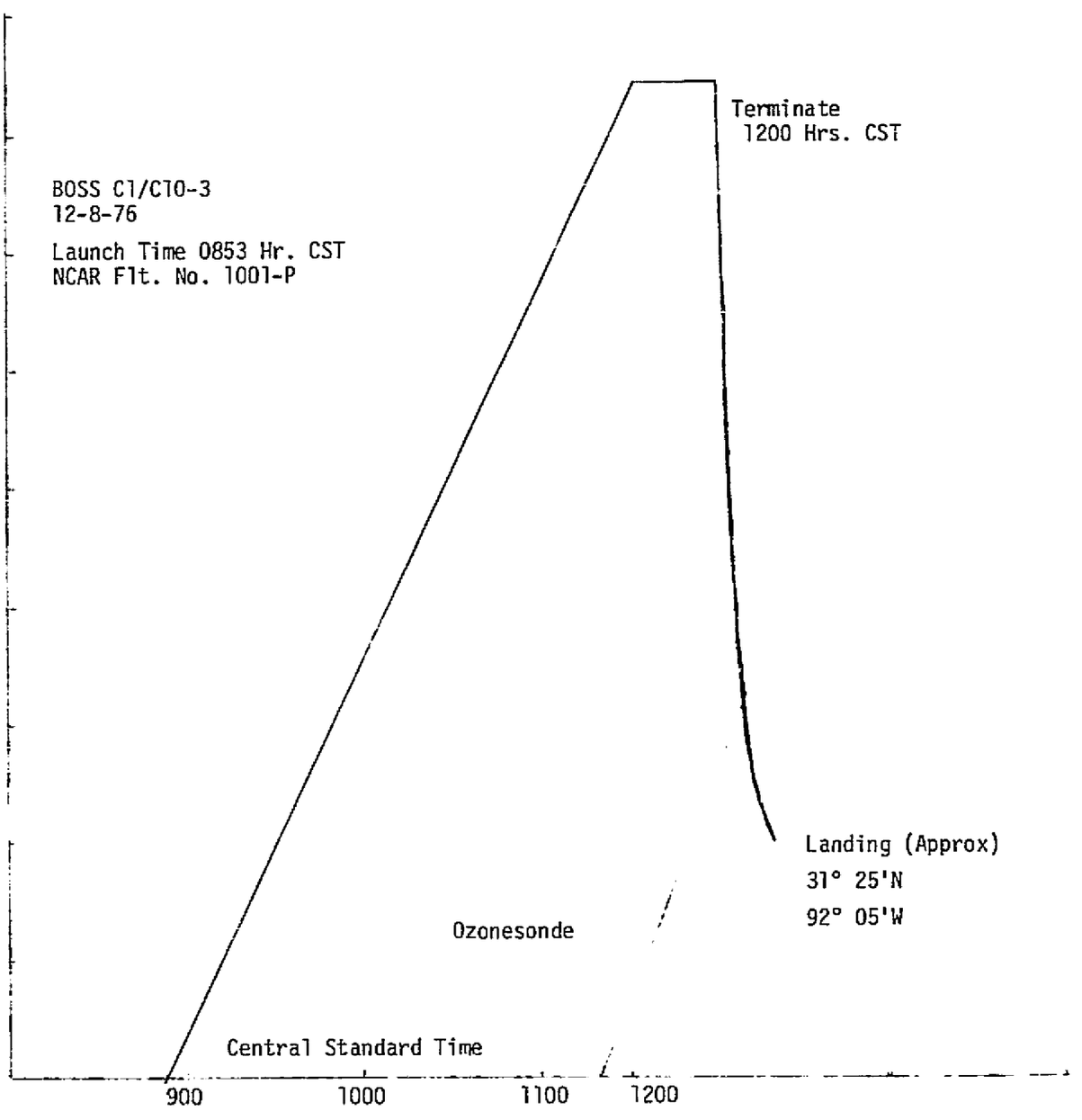

Figure 53. Flight Profile for the Third Atomic Chlorine/Chlorine Oxide (Cl/ClO-3) Flight

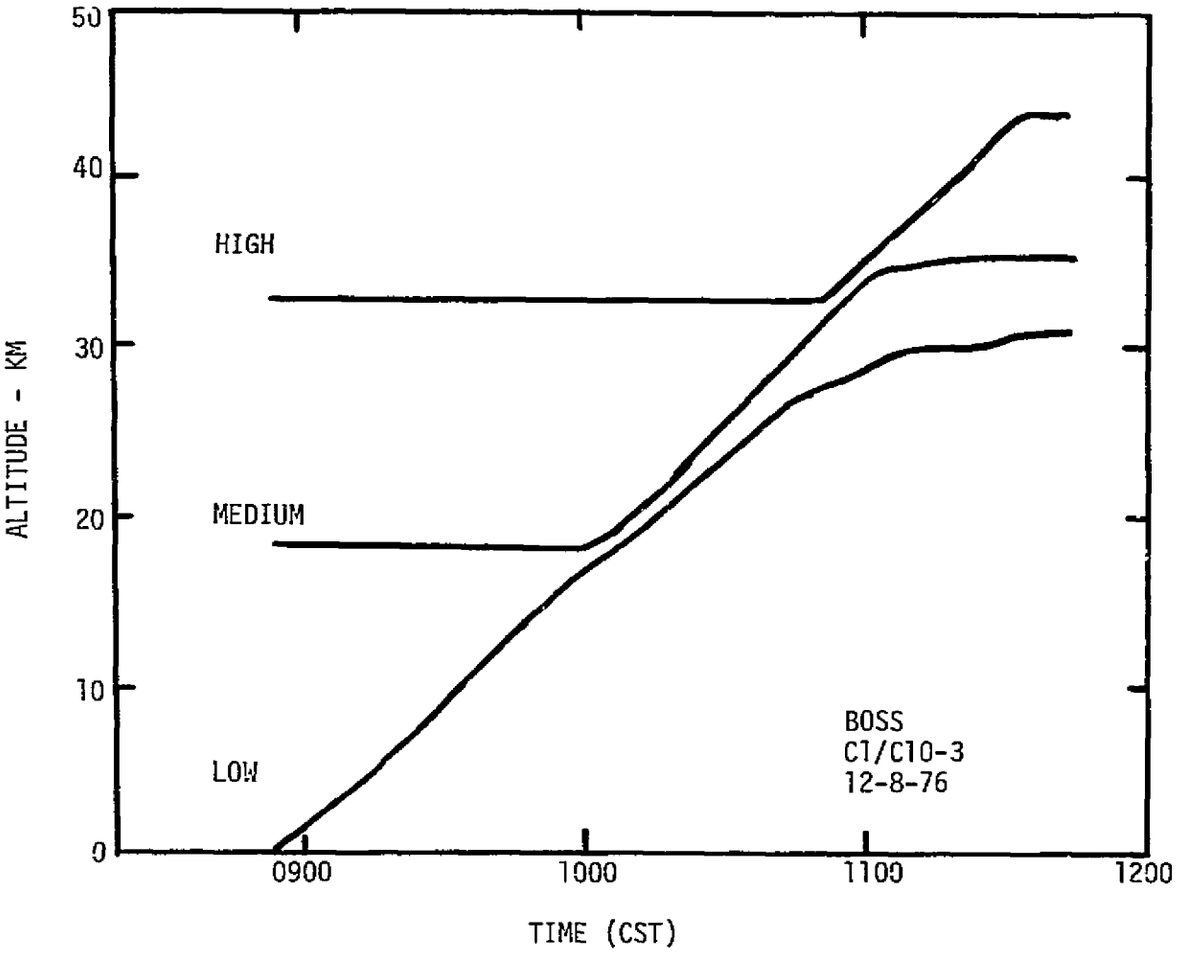

Figure 54. Altitude/time profiles for the ascending payload during the third Atomic Chlorine/Chlorine Oxide (Cl/ClO-3) flight as measured by three pressure transducers

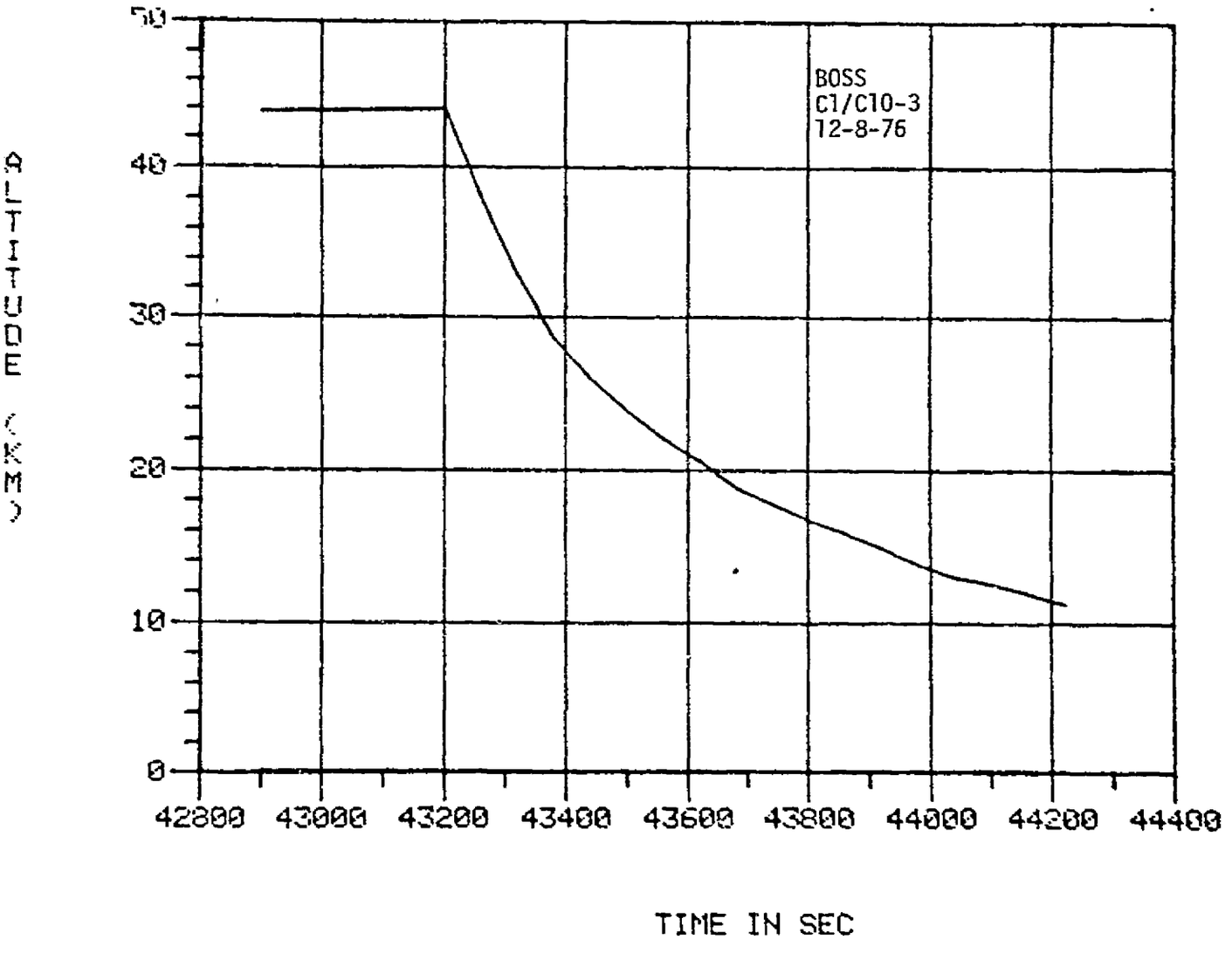

Figure 55. Altitude/Time Profile for the Descending Payload During the Third Atomic Chlorine/ChlorineOxide (Cl/ClO-3) Flight

function of altitude for the descending payload is shown in figure 56. Vertical forces which were experienced by the payload during release and deployment of the 14-meter diameter parachute are shown in figure 57. Figure 58 shows the stability of the payload during descent.

Upper altitude winds at this time of year are very high which carried the balloon approximately 165 nautical miles from NSBF. This situation recommended that the down-range telemetry station located at Tuscaloosa, Alabama, be activated. This station was in operation prior to the payload approximately 15 minutes before drop and was able to acquire data until about 15 minutes after release. Range from Tuscaloosa was approximately 300 nautical miles. Data reception at the station appeared to be good at this range.

5.5.2.3 Power and Temperature Profiles

Figure 59 shows the payload power consumption integrated as a function of time for the flight. Also shown in this figure are the separate power consumption profiles for the ozone electronics and ozone pump. Total power consumption was approximately 34 ampere-hours. Figure 60 shows the temperature of the transmitter, camera, and battery pack. Since the ozone monitor was being flight qualified on this flight, several data points were taken regarding temperature on that unit during flight. Figure 61 shows the temperatures which were measured at the sample chamber the ozone destroying filter and the UV lab inside the package. Figure 62 shows the temperature measured at the

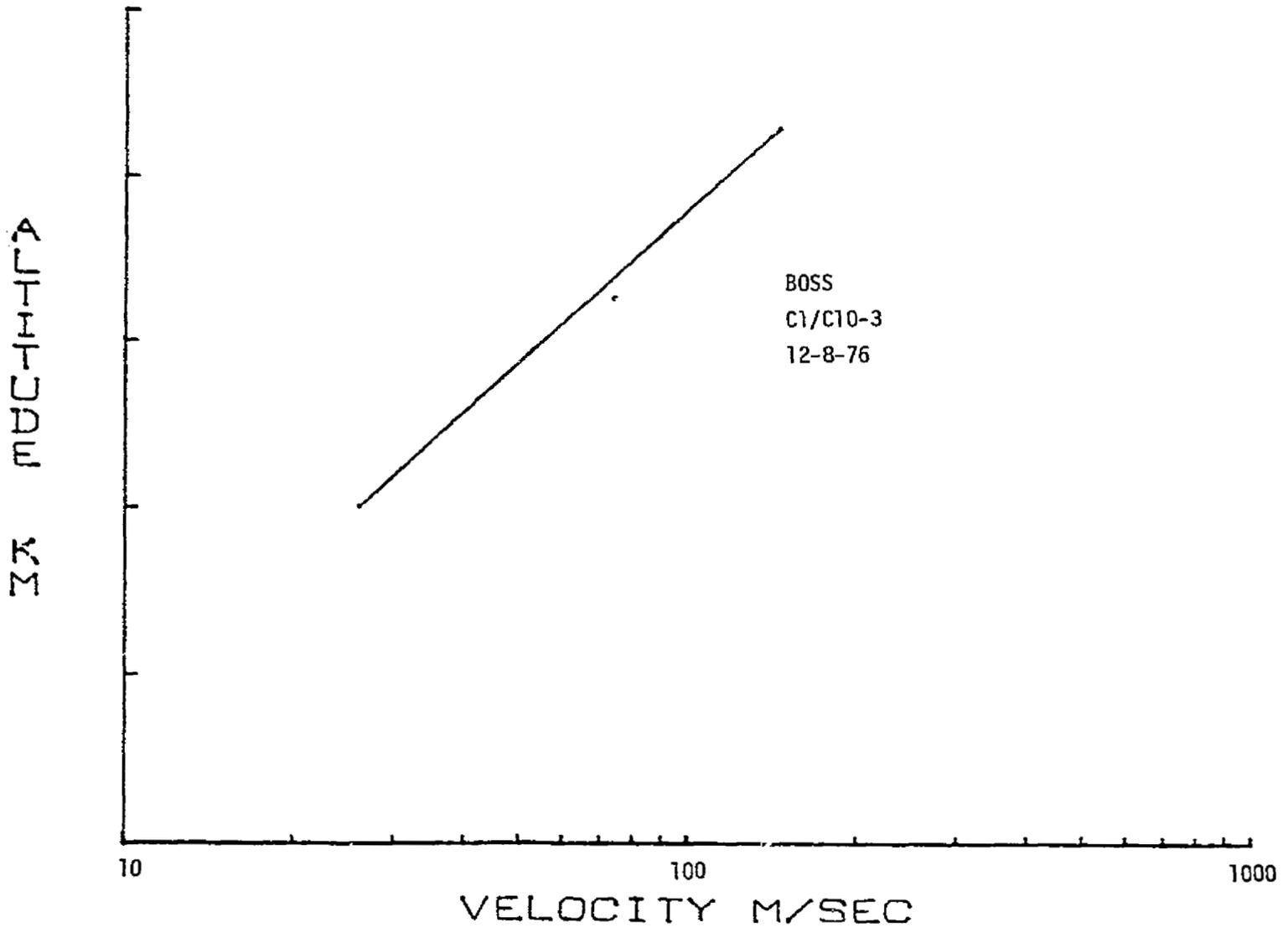

Figure 56. Velocity/Altitude Profile of the Descending Payload for the Third Atomic Chlorine/Chlorine Oxide (Cl/ClO-3) Flight

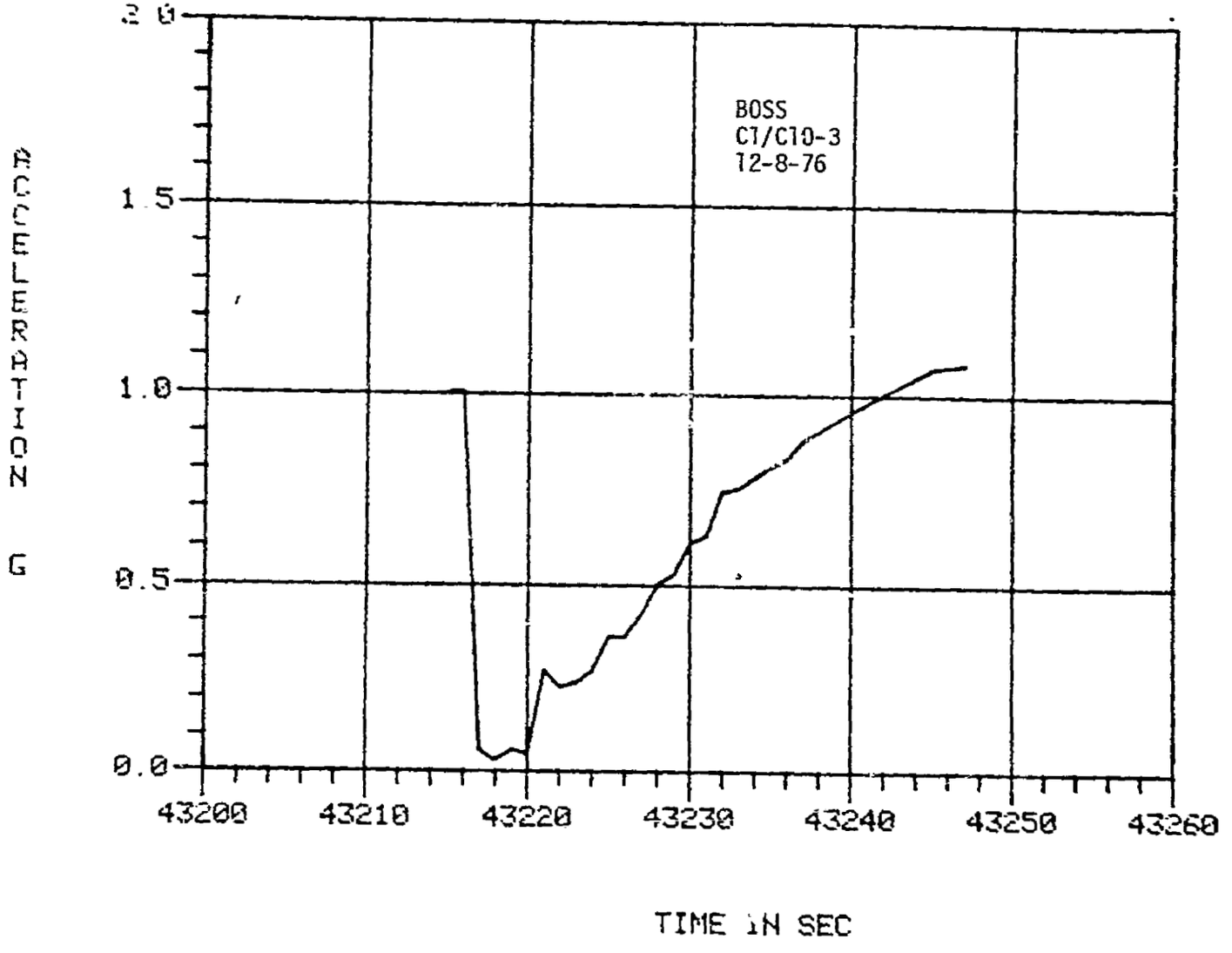

Figure 57. Vertical Force on Payload after Parachute Deployment for the Third Atomic Chlorine/Chlorine Oxide (Cl/ClO-3) Flight

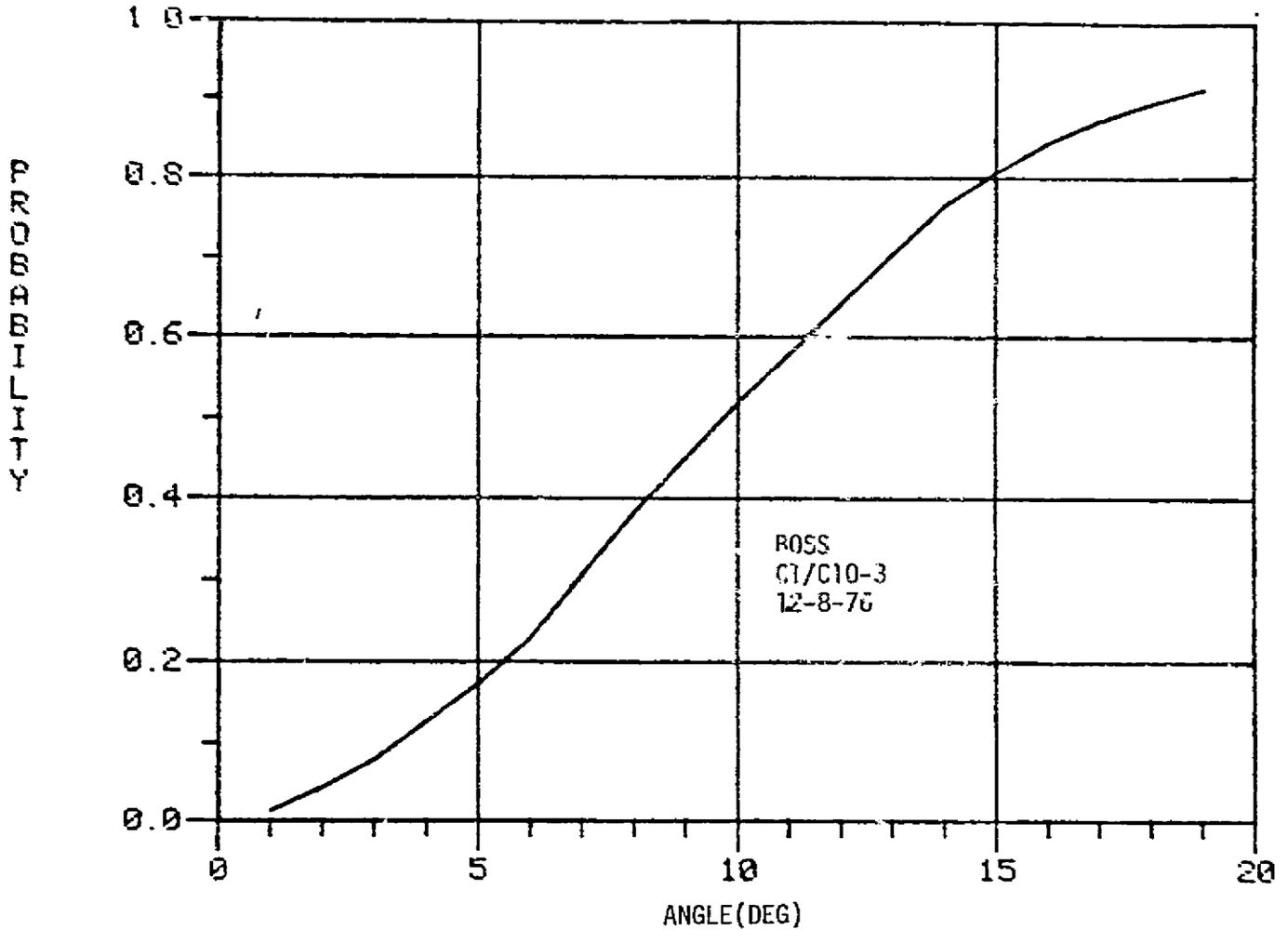

Figure 58. Probability that the Angular Deviation of the Payload from Vertical is less than a Given Angle as a Function of Angle on the Third Atomic Chlorine/Chlorine Oxide (Cl/ClO-3) Flight

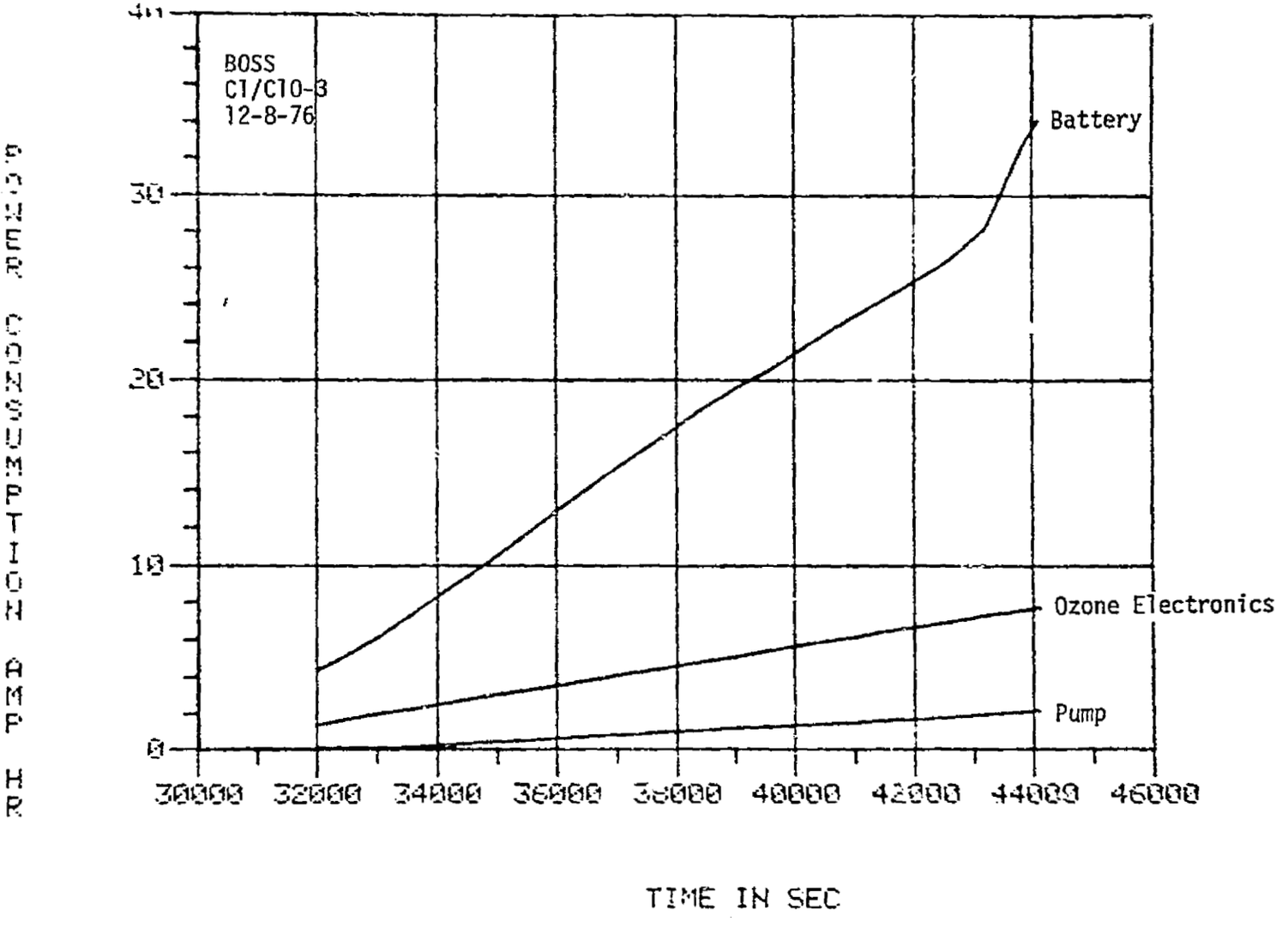

Figure 59. Payload Power Consumption for the Third Atomic Chlorine/Chlorine Oxide (Cl/ClO-3) Flight

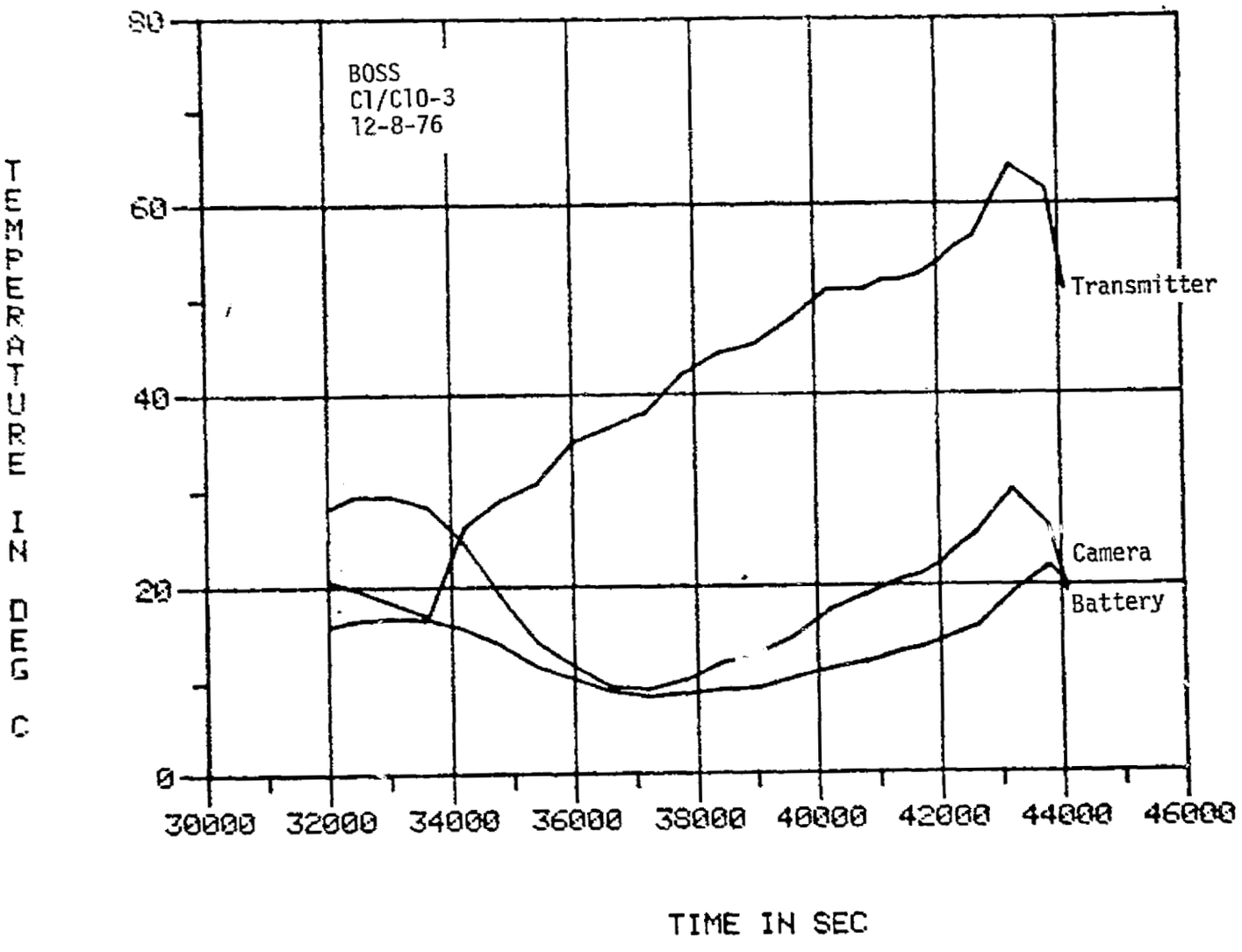

Figure 60. Thermal History of the Transmitter, Camera and Battery on the Third Atomic Chlorine/Chlorine Oxide (Cl/ClO-3) Flight

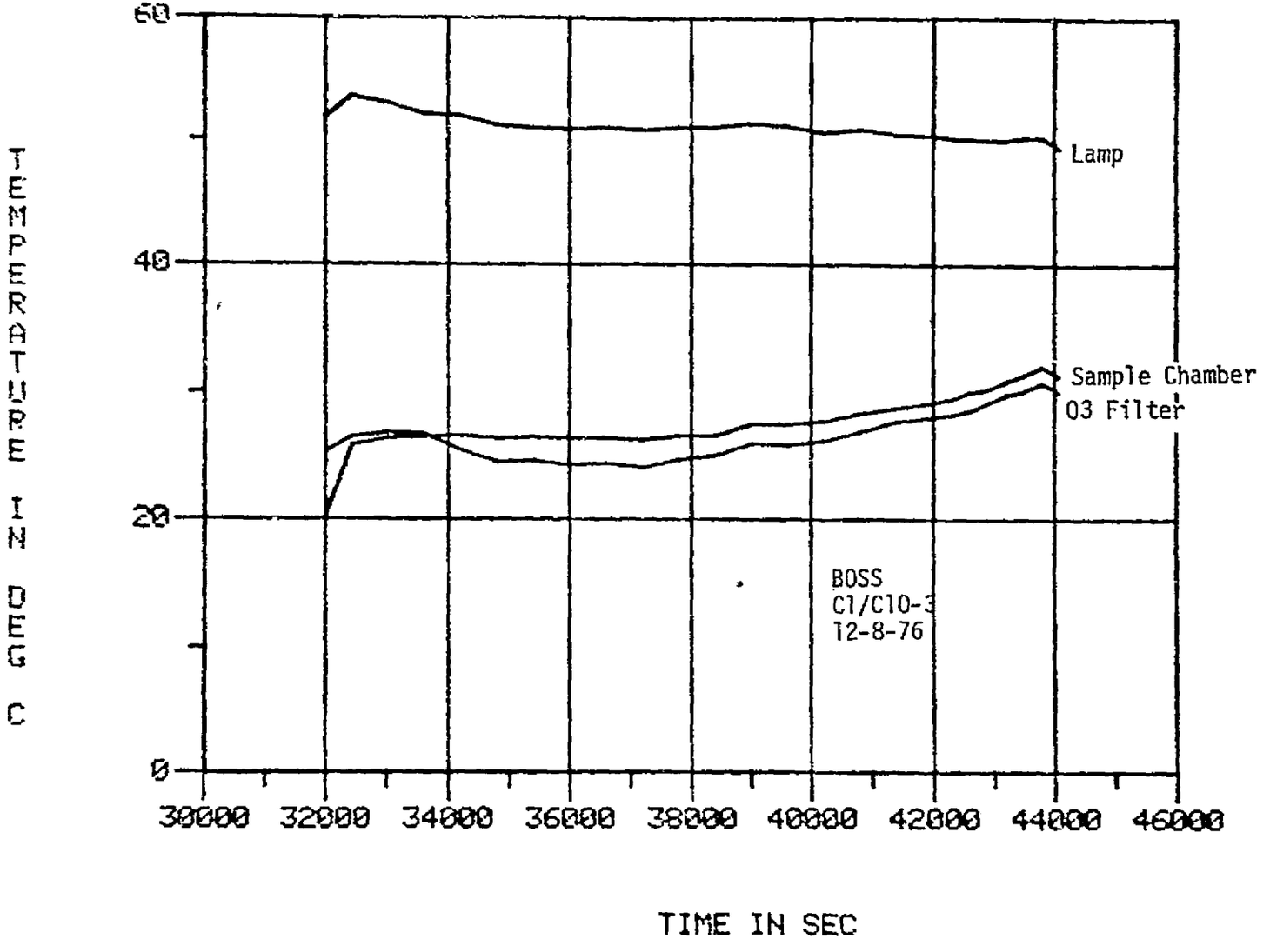

Figure 61.. Thermal History of the Lamp, Sample Chamber, and O_3 Filter on the Third Atomic Chlorine/Chlorine Oxide (Cl/Cl)-3) Flight

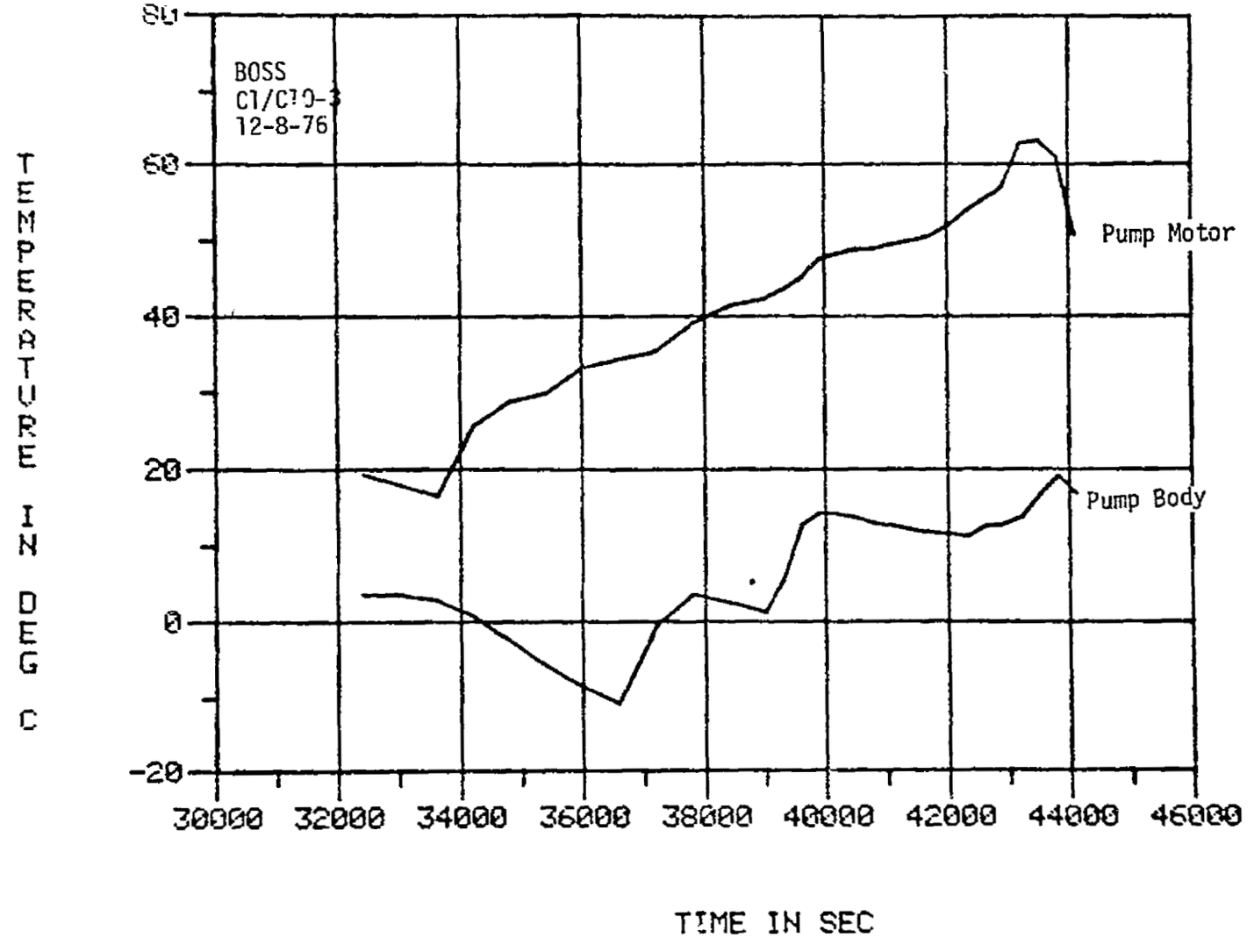

Figure 62. Thermal History of the Pump Motor and Pump Body on the Third Atomic Chlorine/Chlorine Oxide (Cl/Cl)-3) Flight

data pump body and the air pump motor. All these temperature are well within operational limits for the ozone monitor.

5.5.3 POSTFLIGHT ACTIVITIES

The payload landed in sandy soil bottom land approximately 10 nautical miles south of Jena, Louisiana. This very soft ground provided a good landing spot and very little structural damage was incurred in the payload. The supporting struts bent at high stress points but did not fail structurally. Some damage was incurred to the University of Michigan wiring points during the recovery process which may necessitate repair or replace, but overall payload faired very well. Recovery was completed the afternoon of the drop and returned to NSBF on the afternoon of the following day. All items of equipment functioned well with no damage indicated.

5.5.4 DATA RESULTS

5.5.4.1 Resonance Fluorescence Experiment

Concentration measurements collected during this flight are described in appendix E.

5.5.4.2 Ozone Data

Results on ozone concentration profiles measured with the ozone monitor are described in Environmental Effects Office Internal Report JFC-12524. Figure 63 shows the concentration of ozone measured by this

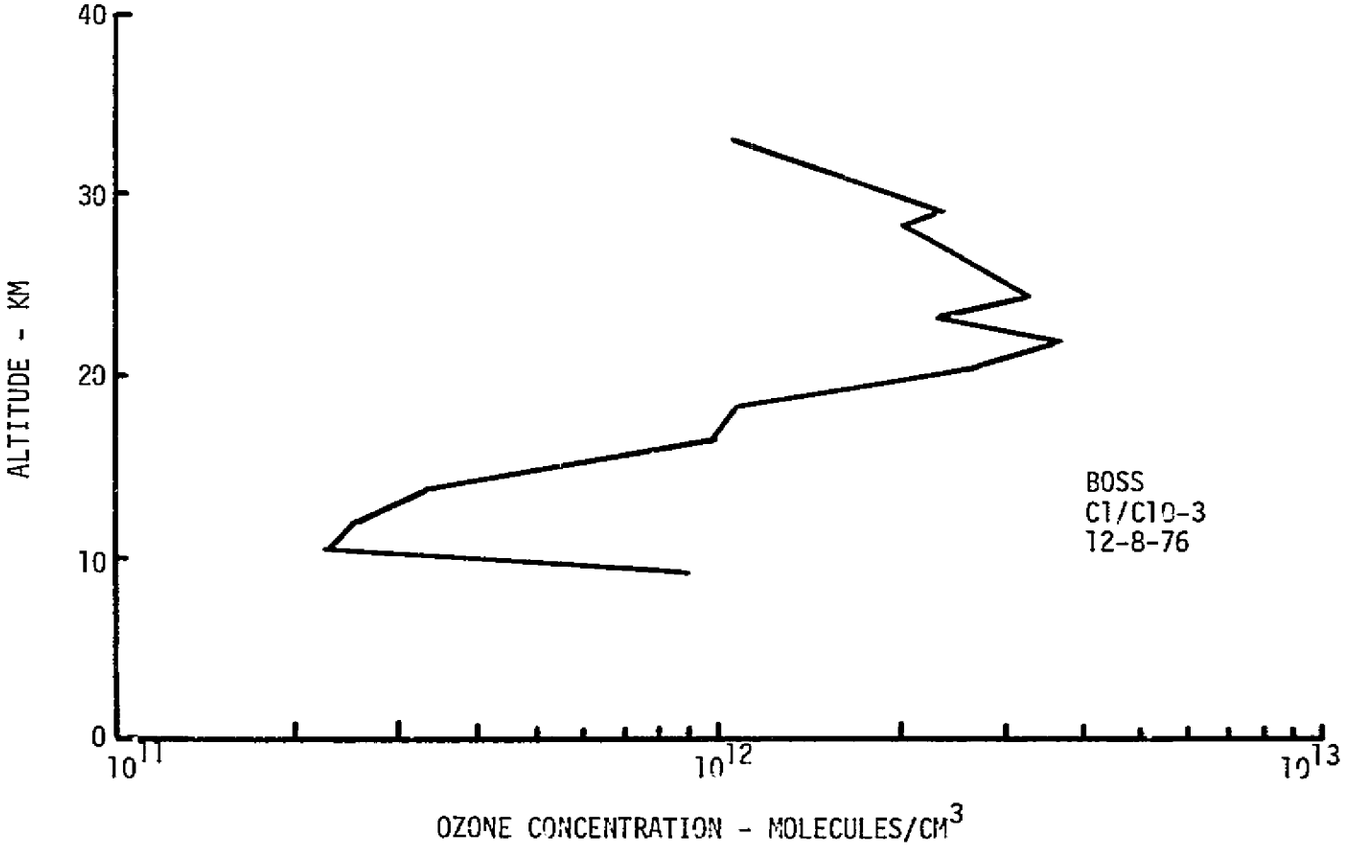

Figure 63. Concentration of Ozone Determined by Ozonesonde During the third Atomic Chlorine/Chlorine Oxide (Cl/ClO-3) flight

instrument compared with data from an ozonesonde launched from Palestine by Nation Air Service personnel from Wallops Flight Center which supported this flight.

5.5.4.3 Total Air Temperature Measurements

Figure 64 shows the total air temperature which was measured during this flight. The low density air in the stratosphere combined with the high thermal inertia of the total air temperature sensor and its protective mounting produce significant errors in this measurement above about 24 km. Methods are being investigated to improve the accuracy of this measurement at high altitudes.

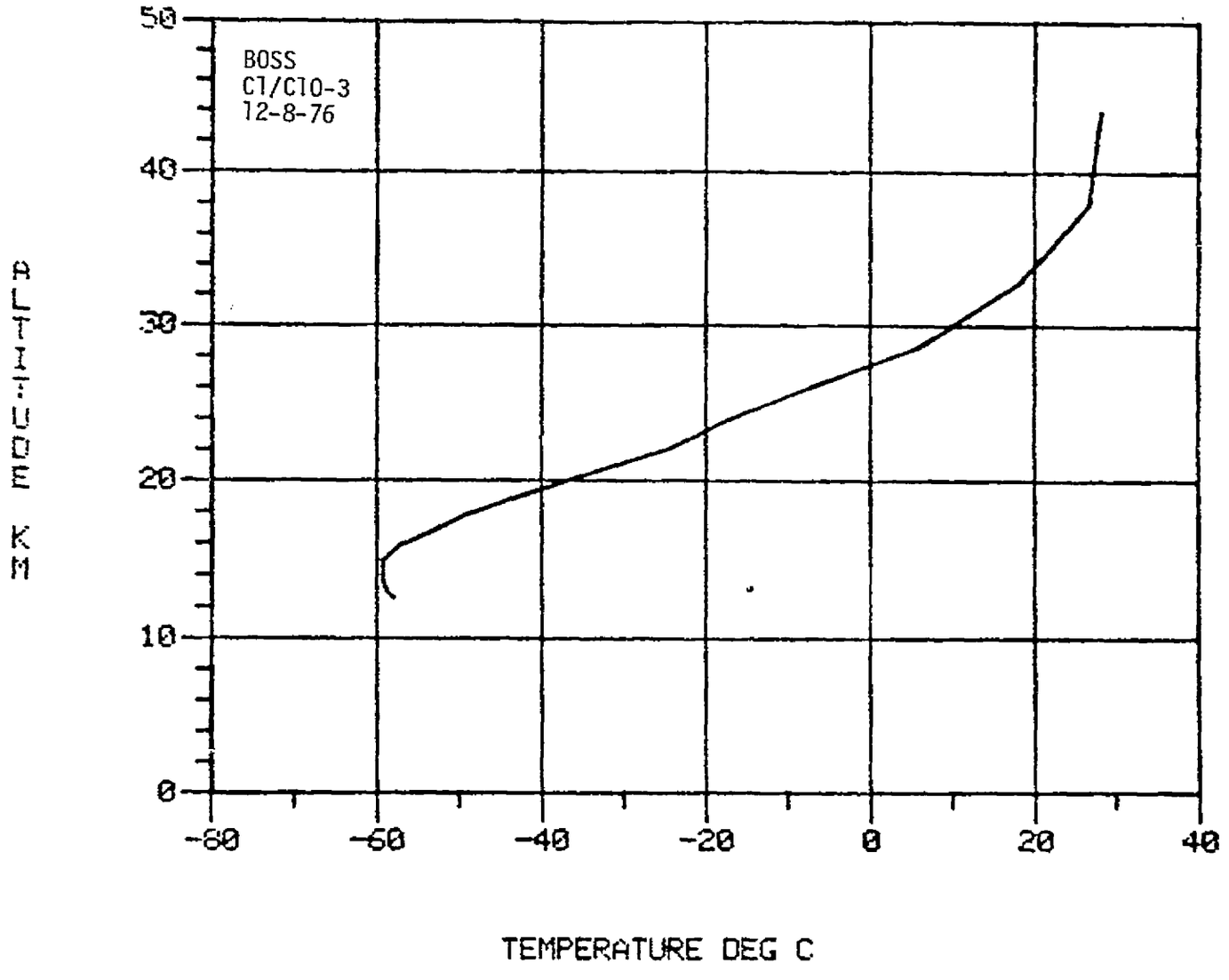

Figure 64. Total Air Temperature Measured on the Third Atomic Chlorine/Chlorine Oxide (Cl/ClO-3) Flight

APPENDIX A

DETAILED INSTRUMENTATION LISTINGS

APPENDIX A

ITEMIZATION OF SUPPORT INSTRUMENTATION FOR BALLOON STRATOSPHERIC RESEARCH FLIGHTS CONDUCTED FROM 4 APRIL 1976 TO 8 DECEMBER 1976 (NCAR FLIGHT NUMBERS 954-P, 965-P, 977-P, 990-P, AND 1001-P)

INSTRUMENT	MEASUREMENT FUNCTION	MANUFACTURER	MODEL NUMBER	SERIAL NUMBER
Pressure Transducers	Payload altitude	Rosemount	830A13 (0 to 15 PSIA) 830A5 (0 to 1 PSIA) 830A15 (0 to .1 PSIA)	
Vertical Reference Gyros	Payload attitude	Humphrey	VG24-0822-1	HG1 & HG2
3-axis Magnetometer	Payload attitude	Schönstedt	RAM-3	1290 1291 1285
Accelerometers	z-axis loading force during parachute deployment	Systron-Donner	Z - 4310	
Motion Picture Cameras	Monitor parachute deployment			

APPENDIX B

PERTINENT DRAWING LISTS

February 1, 1977

APPENDIX B

JSC-LEC EEPO MASTER DRAWING LIST

Size	Dwg. No.	Config.	Title
Pre-Scaler			
C	SDE39112446	A	Box
B	SDE39112447	A	Cover
Scaler			
D	SDE39112448	A	Box
C	SDE39112449	A	Cover
C	SDE39112450	A	Gasket
B	SDE39112451	A	Stand-off
Goddard Ozone Platform			
C	SEE39112452	A	Platform Ass'y
B	SDE39112453	A	Angle, Lifting
B	SDE39112454	A	Spacer
B	SDE39112455	A	Spacer
B	SDE39112456	A	Plate, Front Pump
B	SEE39112457	A	Pump Enclosure
B	SDE39112458	A	Bracket, Pump
B	SDE39112459	A	Nut
B	SEE39112460	A	Bracket Ass'y Inverter
B	SDE39112461	A	Plate, Ozone Detector
Shutter/Lamp			
C	SEE39112462	A	Shutter Ass'y
B	SDE39112463	A	Body
B	SDE39112464	A	Bracket
B	SEE39112465	A	Holder Ass'y-Motor
B	SDE39112466	A	Gear Mod
B	SDE39112467	A	Lever
B	SDE39112468	A	Shutter
B	SDE39112469	A	Cover
B	SDE39112470	A	Foot
Cables, Etc.			
[illegible]	SHE39112471	A	GSE Power Cable
A	SHE39112472	A	GSE Power Cable/Connector Saver
A	SIE39112473	A	Flight Plug Wiring
C	SIE39112474	A	GSE OH-OZ Command Simulator
C	SHE39112475	A	Flight Cable 'A'
D	SIE39112476	A	Interface Cabling OH-Ozone
C	SDE39112477	A	Bracket-Flight Plug
D	SHE39112478	A	Flight Cable 'B'
C	SHE39112479	A	Flight Cable 'C'

Size	Dwg. No.	Config.	Title
Cables, Etc. (Continued)			
D	SHE39112480	A	Flight Cable 'D'
	SHE39112481	Res	Flight Cable 'E'
	SHE39112482	Res	Rosemont Flight Cable
E	SIE39112483	B	Wiring Diagram JSC Flight Module
D	SIE39112484	A	Logic Diagram, Scaler (2 shts)
D	SIE39112485	A	Placement, Scaler (2 shts)
D	SIE39112486	A	Logic Diagram Prescaler
C	SIE39112487	A	PC Board Prescaler
D	SIE39112488	A	Schematic, Sensor Box
D	SHE39112489	A	Cable, Scaler/Prescaler
Gyro Relay Box and Frame			
C	SIE39112490	A	Schematic-Mechanical Dimensions, Gyro Relay Box
C	SDE39112491-001	New	Plate, Center
C	SDE39112491-002	New	Plate, End
C	SDE39112491-003	New	Plate, Fwd
C	SDE39112491-004	New	Plate, Rear
D	SDE39112491-005	New	Plate, Top
D	SIE39112499	New	Payload Status Indicator System
JSC Ozone Instrument			
D	SIE39112500	New	Main Logic Board
C	SIE39112501	New	Command & Telemetry Interface (Deleted, Replaced by SIE39112514)
C	SIE39112502	New	Temperature Sensor & Output Dr.
D	SIE39112503	New	Interconnection Diag.
D	SIE39112504	New	GSE Timing Diag., Memory Control
D	SIE39112505	New	GSE Print Sequence Timing Diag.
D	SIE39112506	New	GSE System
D	SIE39112507	New	GSE Printer Interface Circuit
D	SIE39112508	New	GSE Display Cell Circuits
E	SIE39112514	New	Command & Telemetry Interface
D	SIE39112536	New	Printed Circuit Wiring Ass'y, Sensor Card
D	SIE39112538	New	Magnetic Shield Ass'y
D	SDE39112539	New	Shell & Base
D	SDE39112540	New	Spacer Block
D	SDE39112541	New	Spacer Sheet, Base
D	SDE39112542	New	Spacer Sheet, Side
D	SDE39112543	New	Nut
D	SDZ36114917-1	New	Detail Parts
D	SDZ36114917-2	New	Detail Parts
D	SDZ36114917-3	New	Detail Parts
D	SDZ36114917-4	New	Detail Parts
D	SDZ36114917-5	New	Detail Parts
E	SEE36115200	New	Housing Ass'y
D	SDE36115201	New	Front Cover
D	SDZ36115217	New	End Closure (Deleted)
E	SEE36115238-1	New	Ozone Instrument Ass'y
E	SEE36115238-2	New	Ozone Instrument Ass'y
D	SDZ36115510-1	New	Detail Parts (Deleted)
D	SDZ36115510-2	New	Detail Parts (Deleted)

Size	Dwg. No.	Config.	Title
JSC Ozone Instrument (Continued)			
D	SDZ36115548-1	New	Detail Parts
D	SDZ36115548-2	New	Detail Parts
D	SDZ36115548-3	New	Detail Parts
JSC Integrated Telemetry System			
B	SDE39112509	Res	Camera Bracket
D	SEE39112510	Pre	Mech. Ass'y (2 shts)
D	SIE39112512	Pre	Sensor Box; Multi-module
C	SIE39112516	Pre	PIP Power Distribution System
C	SIE39112517	Pre	PIP Connections & Interface Cabling
C	SIE39112518	Pre	PIP Wiring Schematic
Power Controller			
D	SIE39112519	Pre	Switch Status Memory
D	SIE39112520	Pre	Auto Off & Power Cond.
D	SIE39112521	Pre	Auto Off & Power Cond. Printed Wiring Layout
Command Decoder			
D	SIE39112522	Pre	Data Bus Drive & Printed Wiring Ass'y
D	SIE39112523	Pre	Address Buss Driver Printed Wiring Ass'y
D	SIE39112524	Pre	Command Bus Driver
D	SIE39112525	Pre	Address Bus Driver
Command Status Encoder			
D	SIE39112526	New	Interconnection Diagram
E	SIE39112527	New	Board #1
E	SIE39112528	New	Board #2
E	SIE39112529	New	Board #3
Data Buffers			
D	SIE39112532	A	Frame Sync Connector & Bin/BCD Converter
D	SIE39112533	A	Subframe Sync Connector
D	SIE39112534	A	Drivers
D	SIE39112535	A	Placement
NASA-Langley-U/Pitt Experiment			
D	SIE39112694	New	Telemetry Interface Electronics
A	SIE39112693	New	Interface Cable
GSFC Parachute Test Drop			
A	SIE39112692	New	Bottom Battery Box & Cell Placement
A	SIE39112691	New	Top Battery Box Wiring & Cell Placement
A	SIE39112690	A	Electronic Ass'y #2
A	SIE39112689	A	Connections from Ass'y #2 & Interface Cabling
A	SIE39112688	A	Electronic Ass'y #1
A	SIE39112687	A	Connections from Electronic Ass'y #1
A	SIE39112686	New	Squib Fire Circuit
A	SIE39112685	New	External Electrical Plug
A	SIE39112684	New	FM/FM Ground Station Block Diag.
A	SIE39112683	New	Payload Block Diagram
A	SEE39112682	New	Cross, Interface Support

Size	Dwg. No.	Config.	Title
Field Programmable Logic Array (Analog Display Panel)			
C	SIE38106206	A	Program Chart - Prom #1
D	SIE38106207	A	Connectors
D	SIE38106208	A	Decode Logic
D	SIE38106209	A	Control Logic
D	SIE38106210	A	Bar Drivers
E	SIE38106211	A	IC Placement
D	SIE39112537	New	Programming Chart, Multi-module Payload
Miscellaneous			
E	SEZ39111941	New	Antenna Support (Boss Proj. Radar Tracking)
D	SEE39112511	Pre	Total Air Temperature Ass'y (TAT)
Large Scale Integration (11/1023A)			
D	SIE38106212	New	Interface Logic
D	SIE38106213	New	Printed Wiring Ass'y

APPENDIX C

TELEMETRY AND DATA SYSTEM USED DURING BALLOON OBSERVATION OF STRATOSPHERIC SPECIES FLIGHTS MADE DURING 1976

CONTENTS:

STRATOSPHERIC MEASUREMENTS PROGRAM

MULTI-SPECIES ANALOG MEASUREMENT LIST/DISPLAY ARRANGEMENT

SINGLE MODULE TELEMETRY ON C10-1(4-4-76) and C10-2 (5-15-76) FLIGHTS

DAC	WORD/FRAME	PRIME RATE	
1	9	A1 GAS 1 FUDUCIAL	
24	10	A2 GAS 2 FUDUCIAL	
	11	A3 REACTION ZONE PRESSURE	
	13	A4 ROSEMOUNT PRESS LOW #1	
	14	A5 ROSEMOUNT PRESS MID #2	
4	15	A6 GYRO 1 PITCH	DISPLAY
5	16	A7 GYRO 1 ROLL	GROUP A
	25	A8 ROSEMOUNT PRESS HI #3	
7	26	A9 OZONE CONTROL ELECTROMETER (GSB MONITOR)	
8	27	A10 MONITOR AUX CMD	
		SUBCOM	
9	12/1	A11 VM1A (VISIBLE MONITOR, MODULE 1, LAMP A)	
10	12/2	A12 VM1B	
	12/3	A13 VM1C*	
	12/4	A14 VM1D*	
	12/5	A15 VM2A*	
	12/6	A16 VM2B*	DISPLAY
	12/7	A17 VM2C*	GROUP-B
	12/8	A18 VM2D*	
11	12/9	A19 VM3A (MAGNETRON CURRENT)	
12	12/10	A20 VM3B (MAGNETRON VOLTAGE)	
	12/11	A21 VM3C*	
	12/12	A22 VD3D*	
	12/13	A23 VM4A*	
	12/14	A24 VM4B*	
	12/15	A25 VM4C*	
	12/16	A26 VM4D*	
13	12/17	A27 PMT #1 HV (C10 DATA)	
14	12/18	A26 PMT #2 HV (C10 UV MON.)	
	12/19	A29 PMT #3 HV	
	12/20	A30 PMT #4 HV (LANGLEY ELECTROMETER)+	
	12/21	A31 PMT #5 HV (LANGLEY LED DECOUPLER)+	
	12/22	A32 PMT #6 HV (LANGLEY HV MONITOR)+	
	12/23	A33 PMT #7 HV*	DISPLAY GROUP-C
	12/24	A34 PMT #8 HV*	
15	12/25	A35 GAS PRESSURE (TANK A) LOW	
23	12/26	A36 GAS PRESSURE (TANK A) HIGH	

*Designates Parameters not required for C10-1 Flight

+Not used on C10-2 Flight

Group C
Continued

16	12/27	A37 FRAME TEMP L (LAMP MODULE)	
17	12/28	A38 FRAME TEMP 2 (DETECTOR)	
18	12/29	A39 FRAME TEMP 3	
19	12/30	A40 GYRO 2 PITCH	
20	12/31	A41 GYRO 2 ROLL	
21	28/1	A42 FT1A (FURNACE TEMP, MODULE 1, LAMP A)	
31	28/2	A43 FT1B (TANK TEMP.)	
32	28/3	A44 FT1C (MAGNETRON TUBE TEMP.)	Display Group-D
	28/4	A45 FT1D*	
	28/5	A46 FT2A*	
	28/6	A47 FT2B*	
	28/7	A48 FT2C*	
	28/8	A49 FT2D*	
	28/9	A50 FT3A*	
	28/10	A51 FT3B*	
	28/11	A52 FT3C*	
	28/12	A53 FT3D*	
2	28/13	A54 FT4A* (GAS PRESSURE B LOW)	
3	28/14	A55 FT4B* (GAS PRESSURE B HIGH)	
6	28/15	A56 FT4C* (LAMP BODY TEMP 1A)	
22	28/16	A57 FT4D* (LAMP BODY TEMP 1B)	
	28/17	A58 0V CAL	
	28/18	A59 2.5 V CAL	
	28/19	A60 5 V CAL	
25	28/20	A61 TEMP. 1-BATTERY TEMP.	
	28/21	A62 TEMP. 2-OZONE MONITOR TEMP.	
	28/22	A63 TEMP 3-OZONE PUMP TEMP.	Display Group-E
	28/23	A64 TEMP 4	CAMERA TEMP
	28/24	A65 TEMP 5-SCIENCE TEMP.	XMITTER TEMP
	28/25	A66 BATTERY HEATER MON.	
26	28/26	A67 BATTERY VOLTAGE	
	28/27	A68 OZONE MONITOR CURRENT	
	28/28	A69 OZONE PUMP CURRENT (G.S.B. EXP. I)	
27	28/29	A70 OH EXPERIMENT CURRENT	
28	28/30	A71 BATTERY CURRENT	
29	28/31	A72 Z-AXIS ACCELEROMETER	

STRATOSPHERIC MEASUREMENTS PROGRAM

MULTI-SPECIES ANALOG MEASUREMENT LIST/DISPLAY ARRANGEMENT

DUAL MODULE TELEMETRY ON Cl/ClO-1 (7-28-76) FLIGHT

DAC	WORD/FRAME	PRIME RATE	
1	9	A1 Gas FUDUCIAL (Ethane-C_2H_6)	
24	10	A2 GAS 2 FUDUCIAL	
	11	A3 REACTION ZONE PRESSURE*	
	13	A4 ROSEMOUNT PRESS LOW #1	
	14	A5 ROSEMOUNT PRESS MID #2	
4	15	A6 GYRO 1 PITCH	DISPLAY
5	16	A7 GYRO 1 ROLL	GROUP A
	25	A8 ROSEMOUNT PRESS HI #3	
7	26	A9 OZONE CONTROL ELECTROMETER*(AUX CMD MON)	
8	27	A10	
		SUBCOM	
9	12/1	A11 VM1 (VISIBLE MONITOR, 1)	
10	12/2	A12 VM2 (VISIBLE MONITOR, 2)	
	12/3	A13 VM1C*	
	12/4	A14 VM1D*	
	12/5	A15 VM2A*	DISPLAY
	12/6	A16 VM2B*	GROUP-B
	12/7	A17 VM2C*	
	12/8	A18 VM2D*	
11	12/9	A19 VM3A (MAGNETRON MONITOR 1-Cl)	
12	12/10	A20 VM3B (MAGNETRON MONITOR 2-ClO)	
	12/11	A21 VM3C* Cl DATA	
	12/12	A22 VM3D* Cl UV MON	
	12/13	A23 VM4A* ClO DATA	
	12/14	A24 VM4B* ClO UV MON	
	12/15	A25 VM4C*	
	12/16	A26 VM4D*	
13	12/17	A27 PMT #1 HV (FURN TEMP 1)	
14	12/18	A28 PMT #2 HV (FURN TEMP 2)	
	12/19	A29 PMT #3 HV	
	12/20	A30 PMT #4 HV	
	12/21	A31 PMT #5 HV	
	12/22	A32 PMT #6 HV (TAT SIGNALS)	
	12/23	A33 PMT #7 HV*	DISPLAY GROUP-C
	12/24	A34 PMT #8 HV*	
15	12/25	A35 GAS 1 PRESSURE A (TANK-Ethane)	
23	12/26	A36 GAS 1 PRESSURE B (TANK-Ethane)	

*Designates Parameters not required for Cl/ClO-1 Flight

16	12/27	A37 GAS PRES 2A	
17	12/28	A38 GAS PRES 2B	
18	12/29	A39 FRAME TEMP 3 (O_2 PRES 1)	
19	12/30	A40 GYRO 2 PITCH	
20	12/31	A41 GYRO 2 ROLL	
21	28/1	A42 FT1A (CAV TEMP 1)	
31	28/2	A43 (CAV Temp 2)	
32	28/3	A44 FT1C (MAG TEMP 1)	DISPLAY GROUP-D
	28/4	A45 FT1D*	
	28/5	A46 FT2A*	
	28/6	A47 FT2B*	
	28/7	A48 FT2C*	
	28/8	A49 FT2D*	
	28/9	A50 FT3A*	
	28/10	A51 FT3B*	
	28/11	A52 FT3C*	
	28/12	A53 FT3D*	
2	28/13	A54 MAG TEMP 2	
3	28/14	A55 FT4B* GAS TEMP 1	
6	28/15	A56 GAS TEMP 2	
22	28/16	A57 FT4D O_2 PRES 2	
	28/17	A58 0V CAL	
	28/18	A59 2.5 V CAL	
	28/19	A60 5V CAL	
25	28/20	A61 TEMP. 1-BATTERY TEMP.	
	28/21	A62 TEMP. 2-TEMP. 0→ 1 PSI ROSEMOUNT	
	28/22	A63 TEMP 3-TEMP. 0→ 15 PSI ROSEMOUNT	
			DISPLAY GROUP-E
	28/23	A64 TEMP 4-OZONE INVERTER TEMP. CAMERA TEMP.	
	28/24	A65 TEMP 5-SCIENCE TEMP. XMITTER TEMP.	
	28/25	A66 BATTERY HEATER MON.	
26	28/26	A67 BATTERY VOLTAGE	
	28/27	A68 OZONE MONITOR CURRENT	
	28/28	A69 OZONE PUMP CURRENT	
27	28/29	A70 OH EXPERIMENT CURRENT	
28	28/30	A71 BATTERY CURRENT	
29	28/31	A72 Z-AXIS ACCELEROMETER	

STRATOSPHERIC MEASUREMENTS PROGRAM

MULTI-SPECIES ANALOG MEASUREMENT LIST/DISPLAY ARRANGEMENT

DUAL MODULE TELEMETRY ON C1/C10-2 (10-2-76) FLIGHT

DAC	WORD/FRAME	PRIME RATE	
1	9	A1 Gas 1 FUDUCIAL (Ethane-C_2H_6)	
24	10	A2 GAS 2 FUDUCIAL (NO)	
	11	A3 REACTION ZONE PRESSURE*	
	13	A4 ROSEMOUNT PRESS LOW #1	
	14	A5 ROSEMOUNT PRESS MID #2	
4	15	A6 GYRO 1 PITCH	DISPLAY
5	16	A7 GYRO 1 ROLL	GROUP-A
	25	A8 ROSEMOUNT PRESS HI #3	
7	26	A9 OZONE CONTROL ELECTROMETER*	
8	27	A10 TOTAL AIR TEMP.	
		SUBCOM	
9	12/1	A11 VM1 (VISIBLE MONITOR, 1)	
10	12/2	A12 VM2 (VISIBLE MONITOR, 2)	
	12/3	A13 VM1C*	
	12/4	A14 (OZ LAMP TEMP)	
	12/5	A15 (OZ CONV TEMP)	
	12/6	A16 (OZ PUMP TEMP)	DISPLAY
	12/7	A17 (OZ CURR MON)	GROUP-B
	12/8	A18 VM2D*	
11	12/9	A19 VM3A (MAGNETRON MONITOR 1-C1)	
12	12/10	A20 VM3B (MAGNETRON MONITOR 2-C10)	
	12/11	A21 VM3C* C1 DATA	
	12/12	A22 VM3D* C1 UV MON	
	12/13	A23 VM4A* C10 DATA	
	12/14	A23 VM4B* C10 UV MON	
	12/15	A25 VM4C*	
	12/16	A26 VM4D*	
13	12/17	A27 (FURN TEMP 1)	
14	12/18	A28 (FURN TEMP 2)	
	12/19	A29 PMT #3 HV	
	12/20	A30 PMT #4 HV	
	12/21	A31 PMT #5 HV	
	12/22	A32 (OZ DIFF PRESS.)	
	12/23	A33 PMT #7 HV*	DISPLAY GROUP-C
	12/24	A34 PMT #8 HV*	
15	12/25	A35 GAS 1 PRESSURE A (TANK-Ethane)	
23	12/26	A36 GAS 1 PRESSURE B (TANK-Ethane)	

*Designates Parameters not required for Cl/ClO-2 Flight

Group C continued

16	12/27	A37 NO PRES A	
17	12/28	A38 NO PRES B	
18	12/29	A39 FRAME TEMP 3 (O_2 PRES 1)	
19	12/30	A40 GYRO 2 PITCH	
20	12/31	A41 GYRO 2 ROLL	
21	28/1	A43 FT1A (CAV TEMP 1)	
31	28/2	A43 (CAV TEMP 2)	
32	28/3	A44 FT1C (MAG TEMP 1)	DISPLAY GROUP-D
	28/4	A45 FT1D*	
	28/5	A46 FT2A*	
	28/6	A47 FT2B*	
	28/7	A48 FT2C*	
	28/8	A49 FT2D*	
	28/9	A50 FT3A*	
	28/10	A51 FT3B*	
	28/11	A52 FT3C*	
	28/12	A53 FT3D*	
2	28/13	A54 MAG TEMP 2	
3	28/14	A55 FT4B* GAS TEMP 1	
6	28/15	A56 GAS TEMP 2	
22	28/16	A57 FT4D O_2 PRES 2	
	28/17	A58 OV CAL	
	28/18	A59 2.5 V CAL	
	28/19	A60 5 V CAL	
25	28/20	A61 TEMP. 1-BATTERY TEMP.	
	28/21	A62 TEMP. 2-OZONE PUMP TEMP.	
	28/22	A63 TEMP 3- FSIN SKIN TEMP.	DISPLAY GROUP-E
	28/23	A64 TEMP 4-OZONE INVERTER TEMP.	(CAMERA TEMP)
	28/24	A65 TEMP 5-SCIENCE TEMP. XMITTER TEMP	
	28/25	A66 BATTERY HEATER MON.	
26	28/26	A67 BATTERY VOLTAGE	
	28/27	A68 OZONE OZ PUMP I	
	28/28	A69 MAG 2 I	
27	28/29	A70 OH EXPERIMENT CURRENT	
28	28/30	A71 BATTERY CURRENT	
29	28/31	A72 Z-AXIS ACCELEROMETER	

STRATOSPHERIC MEASUREMENTS PROGRAM

MULTI-SPECIES ANALOG MEASUREMENT LIST/DISPLAY ARRANGEMENT

DUAL MODULE TELEMETRY ON C1/C1O-3 (12-8-76) FLIGHT

DAC	WORD/FRAME	PRIME RATE	
1	9	A1 GAS 1 FUDUCIAL (Ethane C_2H_6)	
24	10	A2 GAS 2 FUDUCIAL (NO)	
	11	A3 REACTION ZONE PRESSURE*	
	13	A4 ROSEMOUNT PRESS LOW #1	
	14	A5 ROSEMOUNT PRESS MID #2	
4	15	A6 GYRO 1 PITCH	DISPLAY
5	16	A7 GYRO 1 ROLL	GROUP A
	25	A8 ROSEMOUNT PRESS HI #3	
7	26	A9	
8	27	A10 OZONE DIFFERENTIAL PRESS	
		SUBCOM	
9	12/1	A11 VM1 (VISIBLE MONITOR, 1)	
10	12/2	A12 VM2 (VISIBLE MONITOR, 2)	
	12/3	A13 VM1C*	
	12/4	A14 VM1D (OZ. LAMP TEMP)	
	12/5	A15 VM2A (OZ. CONV.TEMP)	DISPLAY
	12/6	A16 VM2B (OZ. PUMP TEMP)	GROUP-B
	12/7	A17 VM2C (OZ. CURRENT MON)	
	12/8	A18 VM2D	
11	12/9	A19 VM3A (MAGNETRON MONITOR 1-C1)	
12	12/10	A20 VM3B (MAGNETRON MONITOR 2-C1O)	
	12/11	A21 VM3C (C1 DATA PMT)	
	12/12	A22 VM3D (C1 UV PMT)	
	12/13	A23 VM4A (C1O DATA PMT)	
	12/14	A24 VM4B (C1O UV PMT)	
	12/15	A25 VM4C*	
	12/16	A26 VM4D*	
13	12/17	A27 PMT #1 HV FT1	
14	12/18	A28 PMT #2 HV FT2	
	12/19	A29 PMT #3 HV	
	12/20	A30 PMT #4 HV (OZ. CONT. ELEC.)	
	12/21	A31 PMT #5 HV (OZ. SAMPLE ELEC.)	
	12/22	A32 PMT #6 HV (TAT)	
	12/23	A33 PMT #7 HV*	DISPLAY GROUP-C
	12/24	A34 PMT #8 HV*	
15	12/25	A35 GAS 1 PRESSURE A (TANK-Ethane)	
23	12/26	A36 GAS 1 PRESSURE B (TANK-Ethane)	

*Designates Parameters not required for C1/C1O Flight

Group C continued

16	12/27	A37 (NO PRESS A)
17	12/28	A38 (NO PRESS B)
18	12/29	A39 (O_2 PRESS 1)
19	12/30	A40 GYRO 2 PITCH
20	12/31	A41 GYRO 2 ROLL
21	28/1	A42 FT1A (CAV TEMP 1)
31	28/2	A43 GAS 2 PRESS "B" (CAV TEMP 2)
32	28/3	A44 FT1C GAS #1 TEMP (MAG TEMP 1) DISPLAY GROUP-D
	28/4	A45 FT1D*
	28/5	A46 FT2A*
	28/6	A47 FT2B*
	28/7	A48 FT2C*
	28/8	A49 FT2D*
	28/9	A50 FT3A*
	28/10	A51 FT3B*
	28/11	A52 FT3C*
	28/12	A53 FT3D*
2	28/13	A54 (MAG TEMP 2)
3	28/14	A55 FT4B* (GAS TEMP 1)
6	28/15	A56 (GAS TEMP 2)
22	28/16	A57 FT4D (O_2 PRESS 2)
	28/17	A58 0V CAL
	28/18	A59 2.5 V CAL
	28/19	A60 5 V CAL
25	28/20	A61 TEMP. 1-BATTERY TEMP.
	28/21	A62 TEMP. 2 O_3 PUMP BODY TEMP.
	28/22	A63 TEMP 3 O_3 PUMP MOTOR TEMP DISPLAY GROUP-E
	28/23	A64 TEMP 4 (CAMERA TEMP)
	28/24	A65 TEMP 5-SCIENCE TEMP. (XMTR TEMP)
	28/25	A66 BATTERY HEATER MON.
26	28/26	A67 BATTERY VOLTAGE
	28/27	A68 OZONE MONITOR CURRENT
	28/28	A69 MAG 2 CURRENT
27	28/29	A70 OH EXPERIMENT CURRENT
28	28/30	A71 BATTERY CURRENT
29	28/31	A72 Z-AXIS ACCELEROMETER

APPENDIX C - DATA REDUCTION PROGRAMS FOR BALLOON FLIGHT DATA

There are four programs for reduction of flight data. These programs are set up on a disc pack for use on the Environmental Effects Office DEC PDP-11/45 computer. The equipment required to use these programs are: (1) 9-track tape drive, (2) line printer, (3) CRT terminal, and (4) card reader. Each of the programs uses the CRT terminal for interactive loading of titles, telemetry locations, conversion factors, and time periods for data readout. The 9-track tape drive is used for the flight data tapes. (The original tapes are 7-track and must be converted to 9-track for use on the system.) The reduced data appears on the line printer. The card reader can be used to input data conversion tables, but this can also be done from the CRT terminal.

The simplest program is NCARRD. It prints out the raw data from the flight tapes. It produces a print-out of all of the data in each frame in an octal format or as counts. This program is useful for locating data in a frame and for determining what data is on a given tape.

NCAR30 is a general purpose program for printing out up to eight parameters as a function of time. The parameters can be converted to engineering units by a simple linear conversion or through the use of a data table using Lagrange interpolation. The time resolution time interval of interest can be inputed from the CRT terminal. The program averages the data over the time resolution value and then converts to engineering units for print-out.

NCAR10 is for producing profiles of altitude, attitude, and z-axis acceleration as a function of time with a 1 sec resolution. The altitudes are determined by using a Lagrange interpolation on pressure sensor data. The attitude is determined from the pitch and roll reading of a vertical reference gyro. The z-axis acceleration is obtained from an accelerometer. At the end of the print-out of the profile, an attitude distribution is presented. This distribution gives an indication of the parachute stability during descent.

NCAR20 provides a profile of current and power consumption for each flight. The currents are determined from various current sensors on the payload. They are averaged over the time resolution requested and printed out, along with the power consumption in amp-hrs. This program is valuable in ascertaining how much of the battery power was actually used during a flight.

The subroutines listed after the programs are used by all four of the progrmas. NTRAN reads the data from the tape into memory. CONVER converts the data from the format on the data tape into the 16-bit words required by the processor. HRMNIT converts the time in hrs, min, and sec into a running integer time for processing. ITHRMN performs the reverse process, so that the times on the print-out are in hrs, min, and sec. YLGINT performs the Lagrange interpolation to convert data into engineering units using a telemetry table. ORDER is used to set up the telemetry tables in the proper order for use with YLGINT.

NCARRD PRINTS ENTIRE 30x32 MATRIX

```
      DIMENSION IBUFF(732),IDATA(960),INPUT(30,32),IGND(16)
      EQUIVALENCE (IDATA(1),INPUT(1,1))
      INTEGER*4 ITIM,ITIM1,ITIM2
      TYPE 1
    1 FORMAT(1H0,'THIS PROGRAM PRODUCES PRINT-OUT OF DATA FROM NCAR DIGI
     1TAL TAPES'//4X,'ENTER PRINT-OUT OPTIONS :  '/8X,'1 - RECORD NUMBER
     2 AND GROUND FRAME DATA ONLY'/8X,'2 - OCTAL DUMP OF RECORD PLUS TEL
     3EMETRY DATA IN COUNTS'/8X,'3 - TELEMETRY DATA IN COUNTS')
      TYPE 2
    2 FORMAT(1HS,'     PRINT-OUT OPTION = ')
      ACCEPT 3,IOPT
    3 FORMAT(I1)
      TYPE 4
    4 FORMAT(1H0,'     ENTER START TIME (HR:MN:SC) = ',$)
      ACCEPT 5,IHR,IMN,ISC
    5 FORMAT(3(I2,1X))
      CALL HRMNIT(IHR,IMN,ISC,0,0,ITIM1)
      TYPE 6
    6 FORMAT(1H0,'     ENTER STOP TIME (HR:MN:SC) = ',$)
      ACCEPT 5,IHR,IMN,ISC
      CALL HRMNIT(IHR,IMN,ISC,0,0,ITIM2)
      N=0
    7 N=N+1
      CALL MTRAN(7,0,IBUFF,732,ISTAT,IBYTE,1)
    8 IF(ISTAT) 9,8,12
    9 IF(ISTAT.EQ.-10)WRITE(6,10) N
   10 FORMAT(1X,'END OF FILE ENCOUNTERED AT RECORD ',I6)
      IF(ISTAT.EQ.-10) GO TO 100
      WRITE(6,11) ISTAT
   11 FORMAT(1X,'ERROR ON READ, CODE = ',O8)
   12 CALL CONVER(IBUFF,IDATA,IGND)
      CALL HRMNIT(IGND(4),IGND(5),IGND(6),IGND(7),IGND(8),ITIM)
      IF(ITIM.LT.ITIM1) GO TO 7
   13 N=N+1
      CALL MTRAN(7,0,IBUFF,732,ISTAT,IBYTE,1
   14 IF(ISTAT) 15,14,16
   15 IF(ISTAT.EQ.-10)WRITE(6,10) N
      IF(ISTAT.EQ.-10) GO TO 100
   16 CALL CONVER(IBUFF,IDATA,IGND)
      CALL HRMNIT(IGND(4),IGND(5),IGND(6),IGND(7),IGND(8),ITIM)
      IF(ITIM.GT.ITIM2) GO TO 100
      IF(IOPT.EQ.2) GO TO 17
      IF(IOPT.EQ.3) GO TO 20
      GO TO 22
   17 WRITE(6,18) N
   18 FORMAT(1H1,'RECORD = ',I6//)
      WRITE(6,19) (IBUFF(I),I=1,732)
   19 FORMAT(16O8)
   20 WRITE(6,21)
   21 FORMAT(1H1)
   22 WRITE(6,23) N,(IGND(I),I=1,16)
   23 FORMAT(1X,'RECORD = ',I6,10X,16I5//)
      IF(IOPT.EQ.1) GO TO 13
      DO 24 I=1,32
   24 WRITE(6,25) I,(INPUT(J,I),J=1,30)
   25 FORMAT(1X,I2,'=',4X,30I4)
      GO TO 13
  100 CALL EXIT
      END
```

C11

```
NCAR30 PRODUCES PROFILES UP TO 8 PARAMETERS AS A FUNCTION OF TIME.
      DIMENSION ITITLE(40),ITIT1(8,7),ITIT2(8,7),IBUFF(732),IDATA(960),
     1          IGND(16),IWD(8),IFR(8),OFF(8),CON(8),INPUT(30,32),
     2          IGDwwD(30),IGDw(30),X(8),L(8),Y(8),NPTS(8),
     3          TM(8,25),PAR(8,25),ITIM4(32),TM1(25),PAR1(25)
      INTEGER*4 ITIM1,ITIM2,ITIM3,ITIM4,ITIM5,ITIM6,IDELT,NREC,L
      EQUIVALENCE (IDATA(1),INPUT(1,1))
      TYPE 1
    1 FORMAT(1H0,'THIS PROGRAM PRODUCES PROFILES OF UP TO EIGHT PARAMETE
     1RS'/1X,'AS A FUNCTION OF TIME'//1X,'ENTER TITLE FOR TABLES (UP TO
     2 280 CHARACTERS AND SPACES) =')
      ACCEPT 2,(ITITLE(I),I=1,40)
    2 FORMAT(40A2)
      TYPE 3
    3 FORMAT(1H0)
      TYPE 4
    4 FORMAT(1HS,'ENTER NUMBER OF PARAMETERS TO BE PROCESSED = ')
      ACCEPT 5,NCOL
    5 FORMAT(I1)
      TYPE 6
    6 FORMAT(1HS,'ENTER START TIME (HR:MN:SC) = ')
      ACCEPT 7, IHR,IMN,ISC
    7 FORMAT(3(I2,1X))
      CALL HRMNIT(IHR,IMN,ISC,0,0,ITIM1)
      TYPE 8
    8 FORMAT(1HS,'ENTER STOP TIME (HR:MN:SC) = ')
      ACCEPT 7,IHR,IMN,ISC
      CALL HRMNIT(IHR,IMN,ISC,0,0,ITIM2)
      TYPE 9
    9 FORMAT(1HS,'ENTER TELEMETRY BIT RATE IN KHZ = ')
      ACCEPT 10,A
   10 FORMAT(F10.4)
      DELT=3200./A
      TYPE 11
   11 FORMAT(1HS,'ENTER TIME RESOLUTION IN SECONDS = ')
      ACCEPT 10,B
      IDELT=10000.*B
      TYPE 12
   12 FORMAT(1H0,'ENTER TELEMETRY WORDS WITH KNOWN VALUES FOR USE AS INT
     1ERNAL SYNC WORDS.'/1X,'WHEN ALL SYNC WORDS HAVE BEEN ENTERED, KEY
     2RETURN WITHOUT ENTERING WORD.'//1X,'WORD DATA')
      NGDw=0
   13 NGDw=NGDw+1
      ACCEPT 14,IGDwwD(NGDw),IGDw(NGDw)
   14 FORMAT(I2,3X,I4)
      IF(IGDwwD(NGDw).LE.0) GO TO 15
      GO TO 13
   15 NGDw=NGDw-1
      NCOL1=0
   16 NCOL1=NCOL1+1
      TYPE 3
      TYPE 17,NCOL1
   17 FORMAT(1H ,'ENTER MAIN TITLE FOR COLUMN NUMBER ',I1,' (UP TO 10 CH
     1ARACTERS AND SPACES) = ')
      ACCEPT 18,(ITIT1(NCOL1,I),I=1,5)
   18 FORMAT(5A2)
      TYPE 19,NCOL1
   19 FORMAT(1H ,'ENTER SUB-TITLE FOR COLUMN NUMBER ',I1,' (UP TO 10 CHA
     1RACTERS AND SPACES) = ')
      ACCEPT 18,(ITIT2(NCOL1,I),I=1,5)
      TYPE 20
   20 FORMAT(1HS,'ENTER TELEMETRY LOCATION (WD/FR) = ')
      ACCEPT 21,IWD(NCOL1),IFR(NCOL1)
   21 FORMAT(I2,1X,I2)
      TYPE 22
```

```
 22 FORMAT(1HS,'ENTER OFFSET = ')
    ACCEPT 10, OFF(NCOL1)
    TYPE 23
 23 FORMAT(1HS,'ENTER CONVERSION FACTOR = ')
    ACCEPT 10,COR(NCOL1)
    TYPE 24
 24 FORMAT(1HO,'ENTER INTERPOLATION TABLE FOR PARAMETER,'/1X,'IF NO IN
   1TERPOLATION IS REQUIRED, ENTER -1 FOR TM VALUE AND KEY RETURN.'/
   21X,'WHEN ALL DATA POINTS HAVE BEEN ENTERED, ENTER -1 FOR TM VALUE
   3AND KEY RETURN,'//1X,'TM         PAR')
    NPTS(NCOL1)=0
 25 NPTS(NCOL1)=NPTS(NCOL1)+1
    IF(NPTS(NCOL1).EQ.26) GO TO 27
    I=NPTS(NCOL1)
    ACCEPT 26,TM(NCOL1,I),PAR(NCOL1,I)
 26 FORMAT(2F10.3)
    IF(TM(NCOL1,I).EQ.-2.) GO TO 34
    IF(TM(NCOL1,I).EQ.-1.) GO TO 27
    GO TO 25
 33 NPTS(NCOL1)=NPTS(NCOL1)+1
 34 IF(NPTS(NCOL1).EQ.26) GO TO 27
    I=NPTS(NCOL1)
    READ(8,26) TM(NCOL1,I),PAR(NCOL1,I)
    WRITE(6,26) TM(NCOL1,I),PAR(NCOL1,I)
    IF(TM(NCOL1,I).EQ.-1.) GO TO 27
    GO TO 33
 27 NPTS(NCOL1)=NPTS(NCOL1)-1
    IF(NPTS(NCOL1).EQ.0) GO TO 31
    J=NPTS(NCOL1)
    DO 30 I=1,J
    TM1(I)=TM(NCOL1,I)
 30 PAR1(I)=PAR(NCOL1,I)
    CALL ORDER(TM1,PAR1,J)
    DO 32 I=1,J
    TM(NCOL1,I)=TM1(I)
 32 PAR(NCOL1,I)=PAR1(I)
 31 IF(NCOL1.GE.NCOL.OR.NCOL1.GE.8) GO TO 28
    GO TO 16
 28 DO 29 I=1,NCOL1
    X(I)=0.
    L(I)=0
 29 Y(I)=0.
    NREC=0
    ITIM3=ITIM1+IDELT
    NLOOP5=0
100 NREC=NREC+1
    CALL STRAN(7,0,IBUFF,732,ISTAT,IHYTE,1)
101 IF(ISTAT) 102,101,105
102 IF(ISTAT.EQ.-10) WRITE(6,103) NREC
103 FORMAT(1X,'END OF FILE ENCOUNTERED AT RECORD ',I6)
    IF(ISTAT.EQ.-10) GO TO 300
    WRITE(6,104) ISTAT
104 FORMAT(1X,'ERROR ON READ, CODE = ',O8)
105 CALL CONVER(IBUFF,IDATA,IGND)
    IF(IGND(4).GT.23.OR.IGND(4).LT.0) GO TO 113
    IF(IGND(5).GT.59.OR.IGND(5).LT.0) GO TO 113
    IF(IGND(6).GT.59.OR.IGND(6).LT.0) GO TO 113
    GO TO 115
113 TYPE 114,IGND(4),IGND(5),IGND(6),IGND(7),IGND(8),NREC
114 FORMAT(1H ,'ERROR IN GROUND FRAME TIME.',1X,5I10/
   11X,'RECORD NUMBER',I10,' DISREGARDED')
    GO TO 100
115 CONTINUE
    CALL HRMNIT(IGND(4),IGND(5),IGND(6),IGND(7),IGND(8),ITIM3)
    IF(ITIM3.LT.ITIM1) GO TO 100
    IF(ITIM3.GT.ITIM2) GO TO 300
```

```
      DO 106 I=1,32
      IDELT1=DELT*(I-1)
  106 ITIM4(I)=ITIM3+IDELT1
      DO 112 I=1,32
  107 IF(ITIM4(I).GT.ITIM5) GO TO 200
      IF(NGDW.EQ.0) GO TO 109
      DO 108 J=1,NGDW
      K=IGDWWD(J)
  108 IF(INPUT(K,I).NE.IGDW(J)) GO TO 112
  109 DO 111 J=1,NCOL1
      IF(IFR(J).EQ.0) GO TO 110
      IF(IFR(J).NE.1) GO TO 111
  110 K=JWD(J)
      X(J)=X(J)+INPUT(K,I)
      L(J)=L(J)+1
  111 CONTINUE
  112 CONTINUE
      GO TO 100
  200 DO 202 J=1,NCOL1
      IF(L(J).GT.0) GO TO 201
      Y(J)=99999.
      GO TO 202
  201 Y(J)=CON(J)*((X(J)/L(J))-OFF(J))
  202 CONTINUE
      DO 204 J=1,NCOL1
      IF(Y(J).GT.99998.9.OR.NPTS(J).EQ.0) GO TO 204
      K=NPTS(J)
      DO 203 M=1,K
      TM1(M)=TM(J,M)
  203 PAR1(M)=PAR(J,M)
      XBAR=Y(J)
      Y(J)=YLGINT(TM1,PAR1,K,XBAR,3)
  204 CONTINUE
      ITIM6=ITIM5-IDELT
      CALL ITHRMN(IHR,IMN,SEC,ITIM6)
      IF(NLINES.GT.0) GO TO 208
      WRITE(6,205)(ITITLE(J),J=1,40)
  205 FORMAT(1H1,40A2)
      WRITE(6,206)((ITIT1(N,K),K=1,5),N=1,NCOL1)
  206 FORMAT(1H0,'CLOCK TIME',4X,8(2X,5A2))
      WRITE(6,207)((ITIT2(N,K),K=1,5),N=1,NCOL1)
  207 FORMAT(1H ,'(HR:MN:SC)',4X,8(2X,5A2))
      WRITE(6,3)
  208 WRITE(6,209) IHR,IMN,SEC,(Y(J),J=1,NCOL1)
  209 FORMAT(1H ,1X,I2,':',I2,':',F5.2,8(2X,F10.4))
      NLINES=NLINES+1
      IF(NLINES.EQ.30) NLINES=0
      DO 210 J=1,NCOL1
      X(J)=0.
  210 L(J)=0
      ITIM5=ITIM5+IDELT
      GO TO 107
  300 CALL EXIT
      END
```

```
NCAR10 PRODUCE DESCENT PROFILE
      DIMENSION JBUFF(737),IDATA(960),INPUT(30,32),IGND(16),IGYRO(21),
     1          ITIM3(32),ALHAR(25),TMHAR(25),ALMAR(25),TMMAR(25),
     2          ALLAR(25),TMLAR(25),IGDWWD(30),IGDW(30),ITITLE(40)
      EQUIVALENCE (IDATA(1),INPUT(1,1))
      INTEGER*4 ITIM,ITIM1,ITIM2,ITIM3,ITIM4,ITIM5,ITIM6,IGYRO,ITIM7,
     1          ITIM8,ITIM9
      TYPE 1
    1 FORMAT(1HO,'THIS PROGRAM PRODUCES PROFILES OF ALTITUDE,ATTITUDE, A
     1ND ACCELERATION'/1X,'AS A FUNCTION OF TIME, WITH A 1 SECOND RESOLU
     2TION. IT ALSO DETERMINES'/1X,'THE ATTITUDE DISTRIBUTION IN A GIVEN
     3 TIME INTERVAL'//)
      TYPE 37
   37 FORMAT(1HO,'ENTER TITLE FOR TABLES (UP TO 80 CHARACTERS AND SPACES
     1) = ')
      ACCEPT 38,(ITITLE(I),I=1,40)
   38 FORMAT(40A2)
      TYPE 2
    2 FORMAT(1HS,'     ENTER START TIME (HR:MN:SC) = ')
      ACCEPT 3,IHR,IMN,ISC
    3 FORMAT(3(I2,1X))
      CALL HRMNIT(IHR,IMN,ISC,0,0,ITIM1)
      TYPE 4
    4 FORMAT(1HS,'     ENTER STOP TIME (HR:MN:SC) = ')
      ACCEPT 3,IHR,IMN,ISC
      CALL HRMNIT(IHR,IMN,ISC,0,0,ITIM2)
      TYPE 5
    5 FORMAT(1HS,'     ENTER START TIME FOR ATTITUDE DISTRIBUTION (HR:MN:
     1SC) = ')
      ACCEPT 3,IHR,IMN,ISC
      CALL HRMNIT(IHR,IMN,ISC,0,0,ITIM4)
      TYPE 6
    6 FORMAT(1HS,'     ENTER STOP TIME FOR ATTITUDE DISTRIBUTION (HR:MN:S
     1C) = ')
      ACCEPT 3,IHR,IMN,ISC
      CALL HRMNIT(IHR,IMN,ISC,0,0,ITIM5)
      TYPE 39
   39 FORMAT(1HS,'     ENTER CUT-DOWN TIME (HR:MN:SC) = ')
      ACCEPT 3,IHR,IMN,ISC
      CALL HRMNIT(IHR,IMN,ISC,0,0,ITIM7)
      TYPE 7
    7 FORMAT(1HS,'     ENTER TELEMETRY BIT RATE IN KHZ = ')
      ACCEPT 8,A
    8 FORMAT(F10.4)
      DELT=3200./A
      TYPE 9
    9 FORMAT(1HO,'ENTER TELEMETRY WORDS WITH KNOWN VALUES FOR USE AS INT
     1ERNAL SYNC WORDS.'/1X,'WHEN ALL SYNC WORDS HAVE BEEN ENTERED, KEY
     2RETURN WITOUT ENTERING WORD.'//1X,'WORD DATA')
      NGDW=0
   10 NGDW=NGDW+1
      ACCEPT 11,IGDWWD(NGDW),IGDW(NGDW)
   11 FORMAT(I2,1X,I4)
      IF(IGDWWD(NGDW).LE.0) GO TO 12
      GO TO 10
   12 NGDW=NGDW-1
      TYPE 13
   13 FORMAT(1HO)
      TYPE 14
   14 FORMAT(1HS,'ENTER TELEMETRY LOCATION OF HIGH ALTITUDE ROSEMOUNT (W
     1D/FR) = ')
      ACCEPT 15,IHARWD,IHARFR
   15 FORMAT(I2,1X,I2)
      TYPE 16
   16 FORMAT(1H ,'ENTER DATA TABLE FOR HIGH ALTITUDE ROSEMOUNT.'/1X,'ENT
```

```
     1ER =1 FOR TM VALUE WHEN ALL DATA POINTS HAVE BEEN ENTERED.'//1X,'T
     2M       ALT')
      NHAR=0
   17 NHAR=NHAR+1
      IF(NHAR.EQ.26) GO TO 19
      ACCEPT 18,TMHAR(NHAR),ALHAR(NHAR)
   18 FORMAT(2F8.3)
      IF(TMHAR(NHAR).EQ.-1.) GO TO 19
      IF(TMHAR(NHAR).EQ.-2.) GO TO 66
      GO TO 17
   65 NHAR = NHAR + 1
   66 IF(NHAR.EQ.26) GO TO 19
      READ(8,67) TMHAR(NHAR),ALHAR(NHAR)
   67 FORMAT(2F10.3)
      IF(TMHAR(NHAR).EQ.-1.) GO TO 19
      GO TO 65
   19 NHAR=NHAR-1
      CALL ORDER(TMHAR,ALHAR,NHAR)
      TYPE 13
      TYPE 20
   20 FORMAT(1HS,'ENTER TELEMETRY LOCATION OF MEDIUM ALTITUDE ROSEMOUNT
     1(0/FR) = ')
      ACCEPT 15,IMARAD,IMARFR
      TYPE 21
   21 FORMAT(1H ,'ENTER DATA TABLE FOR MEDIUM ALTITUDE ROSEMOUNT.'/1X,'E
     1TER -1 FOR TM VALUE WHEN ALL DATA POINTS HAVE BEEN ENTERED.'//1X,
     2'TM       ALT')
      NMAR=0
   22 NMAR=NMAR+1
      IF(NMAR.EQ.26) GO TO 23
      ACCEPT 18,TMMAR(NMAR),ALMAR(NMAR)
      IF(TMMAR(NMAR).EQ.-1.) GO TO 23
      IF(TMMAR(NMAR).EQ.-2.) GO TO 77
      GO TO 22
   76 NMAR=NMAR+1
   77 IF(NMAR.EQ.26) GO TO 23
      READ(8,67) TMMAR(NMAR),ALMAR(NMAR)
      IF(TMMAR(NMAR).EQ.-1.) GO TO 23
      GO TO 76
   23 NMAR=NMAR-1
      CALL ORDER(TMMAR,ALMAR,NMAR)
      TYPE 13
      TYPE 24
   24 FORMAT(1HS,'ENTER TELEMETRY LOCATION OF LOW ALTITUDE ROSEMOUNT (WO
     1/FR) = ')
      ACCEPT 15,ILARWD,ILARFR
      TYPE 25
   25 FORMAT(1H ,'ENTER DATA TABLE FOR LOW ALTITUDE ROSEMOUNT.'/1X,'ENTE
     1R -1 FOR TM VALUE WHEN ALL DATA POINTS HAVE BEEN ENTERED.'//1X,'TM
     2       ALT')
      NLAR=0
   26 NLAR=NLAR+1
      IF(NLAR.EQ.26) GO TO 27
      ACCEPT 18,TMLAR(NLAR),ALLAR(NLAR)
      IF(TMLAR(NLAR).EQ.-1.) GO TO 27
      IF(TMLAR(NLAR).EQ.-2.) GO TO 87
      GO TO 26
   86 NLAR=NLAR+1
   87 IF(NLAR.EQ.26) GO TO 27
      READ(8,67) TMLAR(NLAR),ALLAR(NLAR)
      IF(TMLAR(NLAR).EQ.-1.) GO TO 27
      GO TO 86
   27 NLAR=NLAR-1
      CALL ORDER(TMLAR,ALLAR,NLAR)
      TYPE 13
      TYPE 28
```

```
   28 FORMAT(1HS,'ENTER TELEMETRY LOCATION OF GYRO PITCH (WD/FR) = ')
      ACCEPT 15,IGPTWD,IGPTFR
      TYPE 29
   29 FORMAT(1H ,'ENTER OFFSET AND CONVERSION FACTOR FOR GYRO PITCH.')
      TYPE 30
   30 FORMAT(1HS,'OFFSET = ')
      ACCEPT 31,GPTOFF
   31 FORMAT(F10.3)
      TYPE 32
   32 FORMAT(1HS,'CONVERSION FACTOR = ')
      ACCEPT 31,GPTCON
      TYPE 13
      TYPE 33
   33 FORMAT(1HS,'ENTER TELEMETRY LOCATION OF GYRO ROLL (WD/FR) = ')
      ACCEPT 15,IGRLWD,IGRLFR
      TYPE 41
   41 FORMAT(1H ,'ENTER OFFSET AND CONVERSION FACTOR FOR GYRO ROLL.')
      TYPE 30
      ACCEPT 31,GRLOFF
      TYPE 32
      ACCEPT 31,GRLCON
      TYPE 13
      TYPE 35
   35 FORMAT(1HS,'ENTER TELEMETRY LOCATION OF Z-AXIS ACCELEROMETER (WD/F
     1R) = ')
      ACCEPT 15,IZACWD,IZACFR
      TYPE 36
   36 FORMAT(1H ,'ENTER OFFSET AND CONVERSION FACTOR FOR Z-AXIS ACCELERO
     1METER.')
      TYPE 30
      ACCEPT 31,ZACOFF
      TYPE 32
      ACCEPT 31,ZACCON
      NREC=0
      ITIM6=ITIM1+10000
      LHAR=0
      LMAR=0
      LLAR=0
      LGPT=0
      LGRL=0
      LZAC=0
      IR=0
      IP=0
      XHARTM=0.
      XMARTM=0.
      XLARTM=0.
      XGPTTM=0.
      XGRLTM=0.
      XZACTM=0.
      XGPTTM=0.
      XGRLTM=0.
      XZACTM=0.
      DO 40 I=1,21
   40 IGYRO(I)=0
  100 NREC=NREC+1
      CALL NTRAN(7,0,IBUFF,732,ISTAT,IBYTE,1)
  101 IF(ISTAT) 102,101,105
  102 IF(ISTAT.EQ.-10) WRITE(6,103) NREC
  103 FORMAT(1X,'END OF FILE ENCOUNTERED AT RECORD ',I6)
      IF(ISTAT.EQ.-10) GO TO 300
      WRITE(6,104)ISTAT
  104 FORMAT(1X,'ERROR ON READ, CODE = ',O8)
  105 CALL CONVER(IBUFF,IDATA,IGND)
      CALL HRMNIT(IGND(4),IGND(5),IGND(6),IGND(7),IGND(8),ITIM)
      IF(ITIM.LT.ITIM1) GO TO 100
      IF(ITIM.GT.ITIM2) GO TO 300
```

```
      DO 106 I=1,32
      IDELT=DELT*(I-1)
  106 ITIM3(I)=ITIM+IDELT
      DO 122 I=1,32
  107 IF(ITIM3(I).GT.ITIM6) GO TO 200
      IF(NGDW.EQ.0) GO TO 109
      DO 108 J=1,NGDW
      K=IGDWWD(J)
  108 IF(INPUT(K,I).NE.IGDW(J)) GO TO 122
  109 IF(IHARFR.EQ.0) GO TO 110
      IF(IHARFR.NE.I) GO TO 111
  110 XHARTM=XHARTM+INPUT(IHARWD,I)
      LHAR=LHAR+1
  111 IF(IMARFR.EQ.0) GO TO 112
      IF(IMARFR.NE.I) GO TO 113
  112 XMARTM=XMARTM+INPUT(IMARWD,I)
      LMAR=LMAR+1
  113 IF(ILARFR.EQ.0) GO TO 114
      IF(ILARFR.NE.I) GO TO 115
  114 XLARTM=XLARTM+INPUT(ILARWD,I)
      LLAR=LLAR+1
  115 IF(IGPTFR.EQ.0) GO TO 116
      IF(IGPTFR.NE.I) GO TO 117
  116 XGPITM=XGPITM+INPUT(IGRTWD,I)
      LGPT=LGPT+1
      PITCH=INPUT(IGPTWD,I)
      IP=1
  117 IF(IGRLFR.EQ.0) GO TO 118
      IF(IGRLFR.NE.I) GO TO 119
  118 XGRLTM=XGRLTM+INPUT(IGRLWD,I)
      LGRL=LGRL+1
      ROLL=INPUT(IGRLWD,I)
      IR=1
  119 IF(IP.EQ.0.OR.IR.EQ.0) GO TO 120
      CALL GYRO(PITCH,ROLL,GPTOFF,GPTCON,GRLOFF,GRLCON,THETA,PHI)
      IP=0
      IR=0
      IF(ITIM3(I).LT.ITIM4.OR.ITIM3(I).GT.ITIM5) GO TO 120
      K=PHI+1
      IF(K.GT.20) K=20
      IGYRO(K)=IGYRO(K)+1
      IGYRO(21)=IGYRO(21)+1
  120 IF(IZACFR.EQ.0) GO TO 121
      IF(IZACFR.NE.I) GO TO 122
  121 XZACTM=XZACTM+INPUT(IZACWD,I)
      LZAC=LZAC+1
  122 CONTINUE
      GO TO 100
  200 IF(LHAR.GT.0) GO TO 201
      YHAR=99.99
      GO TO 202
  201 XHAR=XHARTM/LHAR
      YHAR=YLGINT(TMHAR,ALHAR,NHAR,XHAR,3)
  202 IF(LMAR.GT.0) GO TO 203
      YMAR=99.99
      GO TO 204
  203 XMAR=XMARTM/LMAR
      YMAR=YLGINT(TMMAR,ALMAR,NMAR,XMAR,3)
  204 IF(LLAR.GT.0) GO TO 205
      YLAR=99.99
      GO TO 206
  205 XLAR=XLARTM/LLAR
      YLAR=YLGINT(TMLAR,ALLAR,NLAR,XLAR,3)
  206 IF(LGPT.GT.0.AND.LGRL.GT.0) GO TO 207
      YGYRO=99.99
      GO TO 208
```

```
  207 XGPT=XGPTTM/LGPT
      XGRL=XGRLTM/LGRL
      CALL GYRO(XGPT,XGRL,GPTOFF,GPTCON,GRLOFF,GRLCON,THETA,YGYRO)
  208 IF(LZAC.GT.0) GO TO 209
      YZAC=99.99
      GO TO 210
  209 YZAC=ZACCON*((XZACTM/LZAC)-ZACOFF)
  210 ITIM9=-10000
      ITIM9=ITIM9+ITIM6
      CALL ITHRMN(IHR,IMN,SEC,ITIM9)
      ITIM8=ITIM9-ITIM7
      A=ITIM8
      ETIM=A/10000
      IF(NLINES.GT.0) GO TO 212
      WRITE(6,211)(ITITLE(J),J=1,40)
  211 FORMAT(1H1,40A2//'   CLOCK         ELAPSED       ALTITUDE           A
     1TTITUDE       ACCELERATION'/'   TIME            TIME     HIGH  MED   L
     2ON.  (DEG. OFF VERT.)      (G)'/' (HR:MN:SC)       (SEC)   (KM)  (K
     3M)   (KM)'/)
  212 WRITE(6,213)IHR,IMN,SEC,ETIM,YHAR,YMAR,YLAR,YGYRO,YZAC
  213 FORMAT(2X,I2,':',I2,':',F5.2,F10.2,3(1X,F5.2),7X,F6.2,9X,F6.2)
      NLINES=NLINES+1
      IF(NLINES.EQ.30) NLINES=0
      LHAR=0
      LMAR=0
      LLAR=0
      LGPT=0
      LGRL=0
      LZAC=0
      XHARTM=0.
      XMARTM=0.
      XLARTM=0.
      XGPTTM=0.
      XGRLTM=0.
      XZACTM=0.
      ITIM6=ITIM6+10000
      GO TO 107
  300 IF(IGYRO(21).LE.0) GO TO 400
      WRITE(6,301)(ITITLE(I),I=1,40)
  301 FORMAT(1H1,40A2//1X,'ATTITUDE DISTRIBUTION')
      CALL ITHRMN(IHR,IMN,SEC,ITIM4)
      WRITE(6,302)IHR,IMN,SEC
  302 FORMAT(1H ,'START TIME = ',I2,':',I2,':',F5.2)
      CALL ITHRMN(IHR,IMN,SEC,ITIM5)
      WRITE(6,303)IHR,IMN,SEC
  303 FORMAT(1H ,'STOP TIME  = ',I2,':',I2,':',F5.2)
      WRITE(6,304)IGYRO(21)
  304 FORMAT(1H ,'TOTAL NUMBER OF POINTS EQUALS =',I7)
      WRITE(6,305)
  305 FORMAT(1H0,'ANGLE      DISTRIBUTION'//)
      DO 306 I=1,20
      X=IGYRO(I)
      Y=X/IGYRO(21)
      J=I-1
  306 WRITE(6,307)J,Y
  307 FORMAT(1H ,2X,I2,12X,F6.4)
  400 CALL EXIT
      END
```

```
      NCAR20 PRODUCES CURRENT AND POWER
      DIMENSION ITITLE(40),ITIT(5,7),ITIM4(32),IWD(5),OFF(5),
     1          CON(5),AMPHR(5),ITIT1(5,7),IBUFF(732),IDATA(960),
     2          INPUT(30,32),IGDWWD(30),IGDW(30),XCUR(5),LCUR(5),
     3          AMPHR1(5),YCUR(5),ITIT2(7),IGND(16),IFR(5)
      EQUIVALENCE (IDATA(1),INPUT(1,1))
      INTEGER*4 ITIM1,ITIM2,ITIM3,ITIM4,ITIM5,ITIM6,IDELT,LCUR,NREC
      DATA ITIT2/2H A,2HMP,2HS.,2H  ,2HAM,2HP-,2HHR/
      DO 26 I=1,5
      DO 26 J=1,7
   26 ITIT1(I,J)=ITIT2(J)
      TYPE 1
    1 FORMAT(1H0,'THIS PROGRAM PRODUCES PROFILES OF CURRENT AND POWER'/
     11X,'AS A FUNCTION OF TIME'//1X,'ENTER TITLE FOR TABLES (UP TO 80 C
     2HARACTERS AND SPACES) = ')
      ACCEPT 2,(ITITLE(I),I=1,40)
    2 FORMAT(40A2)
      TYPE 3
    3 FORMAT(1H0)
      TYPE 4
    4 FORMAT(1HS,'NUMBER OF CURRENTS TO BE CALCULATED = ')
      ACCEPT 5,NCOL
    5 FORMAT(I1)
      TYPE 6
    6 FORMAT(1HS,'ENTER START TIME (HR:MN:SC) = ')
      ACCEPT 7,IHR,IMN,ISC
    7 FORMAT(3(I2,1X))
      CALL HRMNIT(IHR,IMN,ISC,0,0,ITIM1)
      TYPE 8
    8 FORMAT(1HS,'ENTER STOP TIME (HR:MN:SC) = ')
      ACCEPT 7,IHR,IMN,ISC
      CALL HRMNIT(IHR,IMN,ISC,0,0,ITIM2)
      TYPE 9
    9 FORMAT(1HS,'ENTER TELEMETRY BIT RATE IN KHZ = ')
      ACCEPT 10,A
   10 FORMAT(F10.4)
      DELT=3200./A
      TYPE 11
   11 FORMAT(1HS,'ENTER TIME RESOLUTION IN SECONDS = ')
      ACCEPT 10,B
      IDELT=10000.*B
      TYPE 12
   12 FORMAT(1H0,'ENTER TELEMETRY WORDS WITH KNOWN VALUES FOR USE AS INT
     1ERNAL SYNC WORDS.'/1X,'WHEN ALL SYNC WORDS HAVE BEEN ENTERED, KEY
     2RETURN WITHOUT ENTERING WORD.'//1X,'WORD DATA')
      NGDW=0
   13 NGDW=NGDW+1
      ACCEPT 14,IGDWWD(NGDW),IGDW(NGDW)
   14 FORMAT(I2,3X,I4)
      IF(IGDWWD(NGDW).LE.0) GO TO 15
      GO TO 13
   15 NGDW=NGDW-1
      NCOL1=0
   16 NCOL1=NCOL1+1
      TYPE 3
      TYPE 17,NCOL1
   17 FORMAT(1H ,'ENTER TITLE FOR COLUMN NUMBER ',I1,' (UP TO 14 CHARACT
     1ERS) =')
      ACCEPT 18,(ITIT(NCOL1,I),I=1,7)
   18 FORMAT(7A2)
      TYPE 19
   19 FORMAT(1HS,'ENTER TELEMETRY LOCATION (WD/FR) =')
      ACCEPT 20,IWD(NCOL1),IFR(NCOL1)
   20 FORMAT(I2,1X,I2)
      TYPE 21
```

```
   21 FORMAT(1HS,'ENTER OFFSET =')
      ACCEPT 10,OFF(NCOL1)
      TYPE 22
   22 FORMAT(1HS,'ENTER CONVERSION FACTOR =')
      ACCEPT 10,CON(NCOL1)
      TYPE 21
   23 FORMAT(1HS,'ENTER POWER CONSUMPTION UP TO START TIME IN AMP-HRS ='
     1)
      ACCEPT 10,AMPHR(NCOL1)
      IF(NCOL1.EQ.NCOL.OR.NCOL1.EQ.5) GO TO 24
      GO TO 16
   24 NREC=0
      ITIM5=ITIM1+IDELT
      DO 25 I=1,NCOL1
      XCUR(I)=0.
      YCUR(I)=0.
      LCUR(I)=0
   25 AMPHR1(I)=AMPHR(I)
      NLINES=0
  100 NREC=NREC+1
      CALL MTRAN(7,0,IBUFF,732,ISTAT,IBYTE,1)
  101 IF(ISTAT) 102,101,105
  102 IF(ISTAT.EQ.-10) WRITE(6,103) NREC
  103 FORMAT(1X,'END OF FILE ENCOUNTERED AT RECORD ',I6)
      IF(ISTAT.EQ.-10) GO TO 300
      WRITE(6,104)ISTAT
  104 FORMAT(1X,'ERROR ON READ, CODE = ',O8)
  105 CALL CONVER(IBUFF,IDATA,IGND)
      CALL HRMNIT(IGND(4),IGND(5),IGND(6),IGND(7),IGND(8),ITIM3)
      IF(ITIM3.LT.ITIM1) GO TO 100
      IF(ITIM3.GT.ITIM2) GO TO 300
      DO 106 I=1,32
      IDELT1=DELT*(I-1)
  106 ITIM4(I)=ITIM3+IDELT1
      DO 112 I=1,32
  107 IF(ITIM4(I).GT.ITIM5) GO TO 200
      IF(NGDW.EQ.0) GO TO 109
      DO 108 J=1,NGDW
      K=IGDWD(J)
  108 IF(INPUT(K,I).NE.IGDW(J)) GO TO 112
  109 DO 111 J=1,NCOL1
      IF(IFR(J).EQ.0) GO TO 110
      IF(IFR(J).NE.1) GO TO 111
  110 K=IWD(J)
      XCUR(J)=XCUR(J)+INPUT(K,I)
      LCUR(J)=LCUR(J)+1
  111 CONTINUE
  112 CONTINUE
      GO TO 100
  200 DO 201 J=1,NCOL1
      IF(LCUR(J).EQ.0) GO TO 201
      YCUR(J)=CON(J)*((XCUR(J)/LCUR(J))-OFF(J))
  201 CONTINUE
      DO 202 J=1,NCOL1
  202 AMPHR1(J)=AMPHR1(J)+(YCUR(J)*R)/3600.
      ITIM6=ITIM5-IDELT
      CALL ITHRMN(IHR,IMN,SEC,ITIM6)
      IF(NLINES.GT.0) GO TO 206
      WRITE(6,203) (ITITLE(J),J=1,40)
  203 FORMAT(1H1,40A2)
      WRITE(6,204)((ITIT(N,K),K=1,7),N=1,NCOL1)
  204 FORMAT(1HO,'CLOCK TIME',4X,5(3X,7A2))
      WRITE(6,205)((ITIT1(N,K),K=1,7),N=1,NCOL1)
  205 FORMAT(1H ,'(HR:MN:SC)',3X,5(3X,7A2))
      WRITE(6,3)
  206 WRITE(6,207)IHR,IMN,SEC,(YCUR(J),AMPHR1(J),J=1,NCOL1)
```

```
207 FORMAT(1H ,1X,I2,':',I2,':',F5.2,5(3X,2F7.2))
    NLINES=NLINES+1
    IF(NLINES.EQ.30) NLINES=0
    DO 208 J=1,NCOL1
    XCUR(J)=0.
208 LCUR(J)=0.
    ITIM5=ITIM5+IDELT
    GO TO 107
300 CALL EXIT
    END
```

SUBROUTINES USED BY ALL 3 MAIN PROGRAMS

```
SUBROUTINE HRMSIT(IHR,IMN,ISC,ISC1,ISC2,ITIM)
INTEGER*4 ITIM,IHR1,IMN1,ISC1,ISC11,ISC21
IHR1=IHR
IMN1=IMN
ISC1=ISC
ISC11=ISC1
ISC21=ISC2
ITIM=IHR1*36000000+IMN1*600000+ISC1*10000+ISC11*100+ISC21
RETURN
END
```

```
      SUBROUTINE ORDER(X,Y,N)
      DIMENSION X(1),Y(1)
      M=N-1
      DO 1 J=1,N
      L=N-J
      DO 1 I=1,L
      IF(X(I).LT.X(I+1)) GO TO 1
      A=X(I)
      X(I)=X(I+1)
      X(I+1)=A
      A=Y(I)
      Y(I)=Y(I+1)
      Y(I+1)=A
    1 CONTINUE
      RETURN
      END
```

```
      SUBROUTINE CONVER(IBUFF,IDATA,IGND)
C
C     THIS SUBROUTINE CONVERTS DATA FROM THE NCAR PDP-11 FORMAT TO
C     A FORMAT USING 16-BIT WORDS.
C
C     IBUFF = INPUT ARRAY USING NCAR FORMAT
C     IDATA = OUTPUT ARRAY CONTAINING TELEMETRY DATA
C     IGND  = OUTPUT ARRAY CONTAINING GROUND FRAME INFORMATION
C
C     THE DATA IS HANDLED IN 16 WORD CHUNCKS.
C
      DIMENSION IBUFF(732),IDATA(960),IGND(16)
      K=0
      DO 1 I=1,718,3
      K=K+1
      IDATA(K)=IAND(ISHFT(IBUFF(I),-4),1023)
      K=K+1
      M=IAND(ISHFT(IBUFF(I),8),1023)
      N=ISHFT(IBUFF(I+1),-8)
      IDATA(K)=IOR(M,N)
      K=K+1
      M=IAND(ISHFT(IBUFF(I+1),4),1023)
      N=ISHFT(IBUFF(I+2),-12)
      IDATA(K)=IOR(M,N)
      K=K+1
      IDATA(K)=IAND(IBUFF(I+2),1023)
    1 CONTINUE
      K=0
      DO 2 I=721,730,3
      K=K+1
      M=ISHFT(IBUFF(I),-10)-48
      N=IAND(ISHFT(IBUFF(I),-4),63)-48
      IGND(K)=10*M+N
      K=K+1
      J=IAND(ISHFT(IBUFF(I),2),63)
      M=IOR(ISHFT(IBUFF(I+1),-14),J)-48
      N=IAND(ISHFT(IBUFF(I+1),-8),63)-48
      IGND(K)=10*M+N
      K=K+1
      M=IAND(ISHFT(IBUFF(I+1),-2),63)-48
      J=IAND(ISHFT(IBUFF(I+1),4 ,63)
      N=IOR(ISHFT(IBUFF(I+2),-12),J)-48
      IGND(K)=10*M+N
      K=K+1
      M=IAND(ISHFT(IBUFF(I+2),-6),63)-48
      N=IAND(IBUFF(I+2),63)-48
      IGND(K)=10*M+N
    2 CONTINUE
      RETURN
      END
```

```
      FUNCTION YLGINT(X,Y,N,XBAR,NPTS)
C
C     LAGRANGE INTERPOLATION SUBROUTINE.
C     X = INDEPENDENT VARIABLE
C     Y = DEPENDENT VARIABLE
C     N = NUMBER OF POINTS IN TABLE
C     XBAR = INTERPOLATION POINT
C     NPTS = NUMBER OF POINTS USED IN INTERPOLATION
C
      DIMENSION X(1),Y(1)
      IF(NPTS.GT.1.AND.NPTS.LT.N) GO TO 2
      NPTS = N
    1 JL=1
      JH=NPTS
      GO TO 9
    2 DO 3 JH=1,N
      IF(XBAR-X(JH)) 5,12,3
    3 CONTINUE
    4 JH=N
      JL=N-NPTS+1
      GO TO 9
    5 JL=JH
      D2=X(JH)-XBAR
    6 JL=JL-1
      IF(JL.LE.1) GO TO 1
      D1=D2+XBAR-X(JL)
      IF(JL+1.EQ.NPTS) GO TO 8
      IF(XBAR-X(JL-1).LE.D2) GO TO 6
      JH=JH+1
      IF(JH.GT.N) GO TO 4
      D2=X(JH)-XBAR
      GO TO 7
    8 INDCT=0
      IF(JL.GT.1.AND.XBAR-X(JL-1).LT.D2) INDCT=-1
      IF(JH.LT.N.AND.X(JH+1)-XBAR.LT.D1) INDCT=1
      JL=JL+INDCT
      JH=JH+INDCT
    9 YLGINT=0.
      DO 11 K=JL,JH
      PROD=1.
      DO 10 J=JL,JH
      IF(K.EQ.J) GO TO 10
      PROD=PROD*(XBAR-X(J))/(X(K)-X(J))
   10 CONTINUE
      YLGINT=YLGINT+Y(K)*PROD
   11 CONTINUE
      RETURN
   12 YLGINT=Y(JH)
      RETURN
      END
```

```
      SUBROUTINE ITHRMN(IHR,IMN,SEC,ITIM)
      INTEGER*4 ITIM,ITIM1
      IHR=ITIM/36000000
      ITIM1=ITIM-IHR*36000000
      IMN=ITIM1/600000
      ITIM1=ITIM1-IMN*600000
      SEC=ITIM1/10000.
      RETURN
      END
```

Flight	NCAR Flight # Launch Date	Type of Equipment	Manufacturer's Tape Number	Phase	Time Interval
7	954-P 4-4-76	1st Chlorine Oxide (ClO-1) Measurement (ClO-Aerosol-1)	62353461124 62353450123 62353443302 62353443010 62353443323	Ascent " " " Descent	Tape 1 " 2 " 3 " 4 " 5
8	961-P 5-2-76	Parachute test flight (14 m diameter guide surface and 16.75m diameter cross parachute	1100881077 1100881081 1100885090 110881083 25E-3200FC1-9TR-A5	Ascent " " " Descent	Tape 1 " 2 " 3 " 4 " 5
9	965-P 5-5-76	2nd Chlorine Oxide (ClO-2) Measurement (ClO/grab sample-2)	114766102 114772117 7607221 114766104	Ascent " " Descent	Tape 1 " 2 " 3 " 4
10	977-P 7-28-76	1st Atomic Chlorine/Chlorine Oxide (Cl/ClO-1) Measurement (Cl/ClO-1)	114772094 7607215 114772103 114771120	Ascent " " Descent	9:34-10:47 10:48-12:00 12:01-12:39 12:40-
11	990-P 10-2-76	2nd Atomic Chlorine/Chlorine Oxide (Cl/ClO-2) Measurement ($Cl/ClO/O_3$)	7607626 7607256 114773076 7299340	Ascent " " Descent	7:45-8:59 8:59-10:15 10:17-11:34 11:35-12:40
12	12	3rd Atomic Chlorine/Chlorine Oxide (Cl/ClO-3) Ozone O_3 total air temp. (TAT)	117565011 7780411 117592058 117592062	Ascent " " Descent	8:11-9:25 9:25-10:38 10:38-11:45 11:45-12:17

* All digital tapes are 7 track odd purity with 800 BPI density.

DIGITAL TAPES (PCM TELEMETRY DATA) FOR BALLOON STRATOSPHERIC RESEARCH FLIGHTS CONDUCTED FROM APRIL, 1976 TO DECEMBER, 1976

APPENDIX D

PHOTOGRAPHIC COVERAGE

APPENDIX D

PHOTOGRAPHIC DOCUMENTATION FOR BALLOON OBSERVATION OF STRATOSPHERIC SPECIES APRIL 1976 THROUGH DEC 1976

FLIGHT	NCAR FLIGHT NUMBER AND LAUNCH DATE	TYPE OF MEASUREMENTS	STILL FRAME NUMBERS	NASA-JSC MOTION PICTURE FILE ROLL NUMBERS
7	954-P 4-4-76	First Chlorine Oxide (ClO-1)	S76-24266 thru S7624306	S76-037*
8	961-P 5-2-76	Parachute Test Flight	S76-24855 thru S76-24872	S76-044 S76-045
9	965-P 5-15-76	Second Chlorine Oxide (ClO-2)	S76-25175 thru S76-25181	S76-046
10	977-P 7-28-76	First Atomic Chlorine/ Chlorine Oxide(Cl/ClO-1)	S76-27804 thru S76-27816	S76-058
11	990-P 10-2-76	Second Atomic Chlorine/ Chlorine Oxide (Cl/ClO-2)	S76-29705 thru S76-29725	S76-077 S76-078
12	1001-P 12-8-76	Third Atomic Chlorine/ Chlorine Oxide (Cl/ClO-3)	S76-33224 thru S76-33237	S76-087

*Pad abort (4-1-76) Movie coverage on 576-036

APPENDIX E

FREE CHLORINE IN THE STRATOSPHERE: AN IN SITU STUDY OF Cl AND ClO

J. G. Anderson

J. J. Margitan

D. H. Stedman

Space Physics Research Laboratory

Department of Atmospheric and Oceanic Science

University of Michigan

February 19, 1977

A. Introduction

An appreciation for the importance of chlorine containing compounds in the earth's stratosphere is a relatively new development following an evolution of upper atmospheric oxygen-hydrogen-nitrogen photochemical theory extending over several decades (1, 2, 3, 4, 5, 6). During this period the importance of ozone as the sole atmospheric constituent capable of screening the earth's surface from harmful near ultraviolet solar radiation and the vulnerability of the ozone shield to photochemical perturbations resulting from man's activities became clearly understood. In 1974, a number of research groups identified chlorine as a potentially important stratospheric photochemical constituent (7, 8, 9, 10) and discussed the effect of various chlorine sources upon the global ozone budget.

The greatest potential threat to ozone now appears to be that suggested by Molina and Rowland (8) who first related the ubiquitous presence of chlorofluoromethanes in the troposphere, reported by Lovelock (11), to gas phase catalytic destruction of ozone in the stratosphere following the photolytic release of free chlorine from the parent molecules, principally $CFCl_3$ and CF_2Cl_2, in the middle and upper stratosphere resulting from exposure to solar ultraviolet radiation. The most probable fate of the chlorine atom thus formed is reaction with ozone

$$Cl + O_3 \xrightarrow{k_1} ClO + O_2 \qquad [1]$$

forming the chlorine monoxide radical which then reacts principally either with atomic oxygen

$$ClO + O \xrightarrow{k_2} Cl + O_2 \qquad [2]$$

or with nitric oxide

$$ClO + NO \xrightarrow{k_3} Cl + O_2 \qquad [3]$$

to reform atomic chlorine. Reactions [1] - [3] are rapid bimolecular reactions which have been studied extensively in the laboratory (12, 13, 14) and are now well understood. The first two constitute a catalytic chain which recombines an oxygen atom and an ozone molecule, hereafter collectively termed "odd oxygen," into molecular oxygen thereby enhancing the rate of ozone destruction.

In evaluating the quantitative importance of chlorine upon the global ozone budget, it is of interest to determine the concentration of both species as a function of altitude throughout the region in which atmospheric ozone is controlled by local photochemistry (25-45 kilometers). We report here the results of three in situ experiments which determined simultaneously the concentrations of Cl and ClO in the stratosphere over the altitude range of interest. A discussion of the resonance fluorescence detection technique used for this study, which has been employed previously to determine the stratospheric concentrations of atomic oxygen and hydroxyl, appears elsewhere (15, 16) so that only a brief overview of the experimental method is given, dealing primarily with those aspects of the technique unique to chlorine.

B. Experimental

In general, atoms and diatomic molecules possess allowed transitions between bound electronic states separated in energy by 3-15 eV corresponding to the vacuum and near ultraviolet spectral regions. Their resonance absorption and subsequent spontaneous isotropic reemission of photons provides a signature indicating their presence in the gas phase at concentrations extending down to a part per trillion. In order to detect the atom or molecule, a beam of photons, resonant in energy with a selected transition of that species, is passed through

the sample gas and photons, resonantly scattered from the beam, are counted by a photomultiplier tube - pulse detection system. The number of photons resonantly scattered from the beam per unit time, in the absence of reabsorption, is proportional to the concentration of scattering centers within the beam.

For the in situ sampling of atoms and free radicals in the stratosphere, the photon source beam, formed by collimating the output from a low pressure (~2 torr) plasma discharge lamp, and the observation direction of the fluorescent photon detector are arranged such that they are mutually perpendicular to a high velocity (~100 m/sec) flow of stratospheric air. The air sample flow, which passes through the interior of a hollow, aerodynamically shaped pod or nacelle shown in Figure 1, is created by lowering the device through the atmosphere on a stabilized parachute dropped from a balloon near the stratopause. The instrument shape and dimensions (length 100 cm, o.d. 35 cm, i.d. 15 cm) were selected to (a) contain the flow so that chemical conversion can be effected within the sample by the addition of a reactant gas at the instrument throat; (b) optically isolate the photon detectors from background atmospheric radiation; (c) maintain laminar flow through the instrument and (d) eliminate wall removal of the atoms or radicals within the "measurement volume," defined by the intersection of the beam and the field of view of the detector, at the axis of the flow.

B1. Atomic Chlorine

The vacuum ultraviolet spectrum of atomic chlorine is dominated by three major multiplets involving the ^2P ground state which are represented by the energy level diagram shown in Figure 2. Figure 3 presents a high resolution spectrum of the photon source, or "lamp," used to induce Cl atom fluorescence,

showing each of the resonance lines from 1189Å to 1396Å. Because molecular oxygen absorbs strongly at the wavelengths of all Cl atomic transitions except the $^2D_{5/2} - {}^2P_{3/2}$ line at 1189Å, a cell containing O_2 is placed between the lamp and the measurement volume so that only those photons resonant in energy with the $^2D_{5/2} - {}^2P_{3/2}$ transition of Cl, as shown in Figure 4, traverse the atmospheric sample. Thus atmospheric attenuation within the sample is eliminated and scattered light within the instrument, which contributes to the background count rate (determined in the absence of Cl atom fluorescence), is reduced by nearly an order of magnitude as are any secondary emission processes. The residual photon count rate resulting from sources other than chlorine atom fluorescence is periodically checked during the flight by adding ethane (C_2H_6) (which reacts rapidly with chlorine atoms) to the entrance throat of the instrument in order to eliminate them from the atmospheric sample. The gas addition sequence is a continuously cycled 4 step series; (1) a fixed C_2H_6 flow of 5 scc/sec is maintained for 1.5 seconds, (2) gas flow is terminated for 1.5 seconds, (3) a C_2H_6 flow of 20 scc/sec is maintained for 1.5 seconds and (4) the gas flow is terminated for 1.5 seconds. Thus the atomic chlorine flight data consist of differences in the photon count rate in the absence and presence of chlorine atoms in the stratospheric sample. The data are checked for contributions to the count rate resulting from the presence of ethane by analyzing the dependence of the background count rate on ethane concentration.

B2. Chlorine Monoxide

The spectroscopy of ClO has been the subject of considerable study in recent years (17, 18) and although the molecule possesses an allowed transition from the $X^2\Pi$ ground state to the $A^2\Pi$ excited state in a convenient spectral region (2700-3000Å), the A state predissociates, eliminating direct molecular

resonance fluorescence as a useful stratospheric measurement technique. However, the rapid bimolecular reaction between NO and ClO, reaction [3] above, provides a convenient means for converting chlorine monoxide to atomic chlorine by adding nitric oxide to the instrument throat and detecting the product Cl atom by resonance fluorescence at 1189Å. A gas addition system similar to that used to add ethane in the Cl atom experiment is programmed as follows: (1) a fixed NO flow of 8 scc/sec is added for 2.0 seconds, (2) gas is terminated for 0.5 seconds, (3) a fixed NO flow of 48 scc/sec is added for 2.0 seconds and (4) the gas flow is terminated for 1.5 seconds. As in the case of C_2H_6, the gas addition cycle is initiated when the instrument package is dropped from the balloon and repeated continuously during descent. Flow rates are selected such that at the low flow rate the conversion from ClO to Cl is complete within the time required for the sample to traverse the distance between the gas loop injector and the optical axis so that any difference in the observed fluorescence signal between the two NO injection rates must result from the presence of NO alone.

Although, in principle, a single instrument could be used to detect both Cl and ClO by alternately adding C_2H_6 and NO, in practice, two separate detection nacelles are used, mounted approximately a meter apart on a common support frame suspended below the parachute as shown in Figure 5. For the ClO experiment, the amount of NO is insufficient to affect the ambient Cl concentration so that even if the ratio of [Cl] to [ClO] were appreciable, which it is not, the ClO concentration would still be simply proportional to the difference in the photon count rates in the absence and presence of NO.

B3. Calibration

The absolute calibration is identical for both instruments.

The photon count rate, S, recorded by the detector for a given chlorine atom concentration, [Cl], can be expressed in simplified form as

$$S = [Cl]\ F\ \sigma_o \left\{\varepsilon T \eta\right\} V \qquad [4]$$

where F is the resonant photon flux at 1189Å, including transmission losses in the lamp optical system, σ_o is the $^2D_{5/2} - {}^2P_{3/2}$ resonance absorption cross section of atomic chlorine, ε is the collection efficiency of the detector, T is the transmission of the detection optics, η is the phototube quantum efficiency and V is the volume of the measurement region defined by the intersection of the lamp beam and the field of view of the detector. For a given chlorine atom concentration, [Cl], and the photon flux, F, all quantities on the right hand side of Equation [4] are constants so that the relationship between S and [Cl] can be expressed as a proportionality factor C(F) which, for a given instrumental geometry, is a function only of the lamp flux and temperature and can be written

$$C(F) = F\ \sigma_o \left\{\varepsilon T \eta\right\} V.$$

The flight instrument is calibrated by determining C(F) as a function of F in the laboratory, using a fast flow reactor (15, 16) capable of providing a known concentration of chlorine atoms in the appropriate pressure regime.

A known Cl atom concentration is established in the laboratory by using O_3 to convert Cl, formed in the microwave discharge of a Cl_2/He mixture, to ClO via reaction [1]. The O_3 is premixed with Cl before the discharged mixture is introduced into the main reaction zone, upstream of the instrument throat in the fast flow calibration facility, in order to insure that the Cl to ClO conversion is complete. Typically, after reaction, $[ClO] \sim 1 \times 10^{13}$ cm^{-3} and $[O_3] \sim 1 \times 10^{12}$ cm^{-3}.

Nitric oxide is then added ~10 cm upstream of the optical detection axis of the instrument in concentrations ranging from $10^{10} - 10^{11}$ cm^{-3} so that, by Reaction [3], one Cl atom is formed for each added NO molecule. The one to one correspondence between the NO added and the Cl formed is strictly true only in the limit of diminishingly small $[O_3]$ because the Cl formed in Reaction [3] reacts with the residual O_3 from reaction [1]. Under conditions appropriate to this calibration the atomic chlorine concentration is related to the added nitric oxide concentration $[NO]_o$ by the expression

$$[Cl] = [NO]_o \frac{k_3[ClO]}{k_1[O_3]-k_3[ClO]} \left\{\exp(-k_3[ClO]t) - \exp(-k_1[O_3]t)\right\}$$

which shows that $[Cl] \simeq 0.8\ [NO]_o$ for t = 10 msec. The growth of Cl in the formation step, Reaction [3], and its subsequent decay, by Reaction [1], in the instrument throat is directly verified during the calibration step by adding NO to the flow at varying positions by means of a sliding injector.

A major simplification is achieved by calibrating the instrument in the identical configuration used during the atmospheric measurement so that all geometric quantities contained in C(F) remain invariant between calibration

and flight. During setup and test of the instruments in the laboratory fast flow facility, the dependence of C(F) upon (a) total gas sample pressure, (b) resonance lamp temperature, chlorine content and photon flux, F, and (c) the kinetics of Cl atom formation used in the calibration, is studied. In addition, the response of the instruments to ethane and nitric oxide in the absence of Cl and ClO is examined. While the amount of ethane required to eliminate Cl atoms from the atmospheric sample does not affect the detector count rate, care must be taken in the case of nitric oxide addition. An Ascarite trapping system, included as an integral part of the gas addition system of the ClO instrument, is used to eliminate the higher oxides of nitrogen, which enhance fluorescence longward of 1400Å in the presence of 1189Å radiation, from the NO injected into the instrument throat.

A second precaution in the ClO experiment is the use of an interference filter in series with the photomultiplier tube which limits the detector response to the wavelength region between 1150 and 1400Å, thus suppressing any measurable contribution to the count rate in the presence of NO and the absence of ClO (19).

C. Results and Discussion

Three simultaneous observations of Cl and ClO have been performed; the first on 28 July 1976 at 12:00N CDT (local solar zenith angle $\chi = 16°$), the second on 2 October 1976 at 12:15 PM CDT ($\chi = 30°$), and the third on 8 December 1976 at 12:00N CST ($\chi = 55°$). In all cases a $1.5 \times 10^7 ft^3$ helium balloon, launched at dawn from Palestine, Texas, 32°N latitude, bore the experimental package to an altitude of ~141,000 ft (43 km). After activation and stabilization of the instruments, the measurement phase commenced upon severence from the balloon of the stabilized parachute which controlled both the velocity and the angle of attack of the experimental package during descent.

Figure 6 displays a segment of the 2 October ClO data with 0.08 second time resolution synchronized with the 4 step gas addition sequence which was used on all flights reported here. Typically, the detector count rate is independent of [NO] as shown in Figure 6 after the probe has accelerated to its terminal velocity and the NO addition lines have been cleared, which require a period of approximately 30 seconds during which the data are discarded. An exception occurred during the 28 July flight when a decrease in the O_2 absorption cell pressure, used to eliminate all lines in the chlorine atom spectrum except the $^2D_{5/2}$-$^2P_{3/2}$ transition, permitted the ^2P-^2P multiplet to enter the fluorescence chamber, inducing measurable fluorescence from injected NO. However, because the flow rates of NO were measured during descent and thus the ratio of the added NO concentrations was known, the contribution to the total count rate resulting from NO could be determined given the difference in the detector count rates. The correction amounted to 30% in the upper stratosphere decreasing to 10% at 22 km because of the rapid quenching of the NO fluorescence. For the

2 October flight above 35 km a difference in the detector count rate for the high and low NO flow rate, corresponding to a 10% correction in [ClO], was observed which could have resulted from residual NO emission. These factors were taken into account in calculating the experimental uncertainty for each experiment.

An important diagnostic afforded by the addition of NO at two significantly different flow rates involves the three body recombination step

$$Cl + NO + M \longrightarrow NOCl + M.$$

As the parachute-suspended probe descended, the atmospheric density, and thus [M], increased exponentially with decreasing altitude while the velocity, which is inversely proportional to the square root of the atmospheric density, decreased thereby increasing both the concentration of NO for a given flow rate and the reaction time after injection of the NO. Below 25 kilometers these factors sufficiently accentuated the above recombination step for the higher NO flow to measurably suppress the Cl atom concentration following its initial formation from ClO. For each flight the dependence of the detector count rate on added NO was checked by comparing the calculated Cl atom concentration ratios for the high and low flow rate cases with the observed ratios as a function of altitude. Good agreement was found in each case.

The concentrations of Cl and ClO measured on each flight are shown in Figure 7. For ClO the result of each data frame, (i.e. each 6 second gas addition sequence) is plotted whereas for Cl the data represent a 0.5 km average for the 28 July and 2 October results and a 4 kilometer average for the 8 December data. The decreased signal to noise ratio of the 8 December data results from (a) lower Cl densities and (b) a change in the oscillation mode

of the microwave cavity used to sustain the plasma discharge in the resonance lamp, reducing the 1189Å photon flux and thus the instrument's sensitivity.

Experimental uncertainties for each measurement are listed in Figure 7 and are based upon uncertainties in (a) laboratory absolute calibration (± 20%), (b) convolution of the lamp resonance line and the atomic absorption cross section, as a function of lamp body temperature (± 20%) and (c) absolute flux measurements during flight (± 10%). The instruments were calibrated before and after each flight and the hardware, interference filters and key optical components were identical for all flights. Continuing laboratory work will provide the background information necessary to reduce the quoted uncertainties.

Figure 8 presents the data of Figure 7 averaged over an altitude interval of 1 km. Although significant variability is present in the integrated data, the large fluctuations are decidedly reduced. Figure 9 displays the smoothed data of Figure 8 in terms of the Cl and ClO mixing ratio by volume. The peak observed Cl mixing ratios occur at the maximum altitude of the experiment (41 km) and were 1.9 and 2.6 x 10^{-11} respectively for the July and October flights. The maximum ClO mixing ratios occurred at 36 km for all three flights but the peak mixing ratios were significantly different for all three flights, 1.8, 2.9 and 5.6 x 10^{-9} for July, October and December respectively.

Figure 10 presents a comparison between the 1 km averaged data of Figure 8 and 4 theoretical predictions of Cl and ClO (20) calculated for conditions appropriate to summer midday conditions at 30°N latitude, corresponding to the maximum predicted Cl and ClO concentrations for the geographic position of the measurement. It is, of course, impossible to compare these experimental results with all the available

theoretical predictions; the above four models were selected because (a) they represent a cross section of the major theoretical efforts to quantitatively predict chlorine catalyzed ozone depletion and (b) they adequately encompass the range of theoretically predicted Cl and ClO concentrations. The chlorine mixing ratio, defined as the total number of chlorine atoms, bound and free, per unit volume divided by the total atmospheric number density, is indicated for each model and represents the considered opinion of the respective authors. Figure 11 presents a comparison between the measured and predicted [Cl]/[ClO] ratio as a function of altitude using the same models referred to in Figure 10.

Two conclusions can be drawn from an inspection of Figures 10 and 11:

(1) Observed Cl and ClO densities exceed the model predictions, particularly below 35 km for the July and October experiments but significantly less Cl and ClO were observed in the December flight.

(2) The observed [Cl] to [ClO] ratio is in rough agreement with prediction.

An interpretation of conclusion (2) is straightforward. Reactions [1]-[3] establish a photochemical steady state between Cl and ClO such that the ratio of their concentrations may be written

$$\frac{[Cl]}{[ClO]} = \frac{k_2[O]+k_3[NO]}{k_1[O_3]} = \left(\frac{k_2}{k_1}\right)\frac{[O]}{[O_3]} + \left(\frac{k_3}{k_1}\right)\frac{[NO]}{[O_3]} \qquad [5]$$

Moreover, atomic oxygen and ozone are in a mutual steady state controlled by ozone photolysis

$$O_3 + h\nu \xrightarrow{J_{O_3}} O + O_2$$

and oxygen atom recombination

$$O + O_2 + M \xrightarrow{k_4} O_3 + M$$

so that

$$\frac{[O]}{[O_3]} = \frac{J_{O_3}}{k_4[M][O_2]} \quad . \qquad [6]$$

Substitution of Expression [6], which has been empirically verified within the accuracy required here (14), into [5] yields

$$\frac{[Cl]}{[ClO]} = \left(\frac{k_2}{k_1}\right) \frac{J_{O_3}}{k_4[M][O_2]} + \left(\frac{k_3}{k_1}\right) \frac{[NO]}{[O_3]} \qquad [7]$$

Reaction rate constants, k_1, k_2, k_3 and k_4 are well known (12, 13, 14) and sufficient knowledge of [O], [NO] and $[O_3]$ exists to demonstrate that above 35 km, the term in Expression [7] involving NO is insignificant and thus

$$\frac{[Cl]}{[ClO]} = \left(\frac{k_2}{k_1}\right) \frac{J_{O_3}}{k_4[M][O_2]} \qquad [8]$$

in the altitude region where data on the [Cl]/[ClO] ratio exist. All quantities on the right hand side of [8] are well known and do not involve the intricacies of stratospheric photochemistry. Thus, Conclusion (2) represents rough experimental substantiation of a rather simple steady state relationship rather than a significant test of stratospheric photochemical theory. The difference among the various models on this point is somewhat surprising.

An interpretation of Conclusion (1) is not so straightforward. On the one hand, when the complexities inherent in a complete theoretical calculation are considered, an agreement between prediction and observation to within a factor of 2 is not unreasonable. It also must be stressed that three atmospheric experiments do not constitute a satisfactory statistical sampling of a fundamentally transient photochemical system.

On the other hand, the discrepancies apparent in Figure 2 may not be insignificant and can result from one or both of the following:

(a) An incorrect ClO_x (taken here to include both Cl and ClO) to total chlorine, Cl_x, (principally HCl and $ClONO_2$) ratio

(b) An underestimate of the total chlorine mixing ratio in the stratosphere.

Point (a) represents an area of significant uncertainty. The $[ClO_x]$ to $[Cl_x]$ ratio is believed (7, 8, 9, 10) to be controlled in the upper stratosphere primarily by the reaction between chlorine atoms and methane forming HCl

$$Cl + CH_4 \xrightarrow{k_5} HCl + CH_3$$

and the reaction between hydroxyl and HCl reforming free chlorine

$$OH + HCl \xrightarrow{k_6} H_2O + Cl \quad .$$

These reactions are sufficiently rapid to establish a steady state between Cl and HCl such that

$$\frac{[Cl]}{[HCl]} \simeq \frac{k_6[OH]}{k_5[CH_4]} \quad . \qquad [9]$$

With the aid of Expressions [7] and [9] we can then write

$$\frac{[ClO_x]}{[HCl]} = \frac{[Cl]}{[HCl]}\left\{1 + \frac{[ClO]}{[Cl]}\right\} = \frac{k_6[OH]}{k_5[CH_4]}\left\{1 + \frac{k_1[O_3]}{k_2[O]+k_3[NO]}\right\} .$$

The expression within the brackets, however, is a reasonably well defined quantity throughout the stratosphere as previously discussed. Both k_5 and k_6 have been studied extensively and, with the possible exception of minor uncertainties in the temperature dependence of k_5, are well known. Thus, within the context of current stratospheric photochemical theory, uncertainties in the concentrations of OH and CH_4 are a critical issue and represent a major point of divergence between the various theoretical predictions.

The hydroxyl radical has been measured in the stratosphere by three different methods, (15, 21, 22) but because the OH measurements were not done simultaneously with those of Cl and ClO, it is not possible to reliably determine the density vs. altitude profile of OH appropriate to the Cl-ClO flights. It has also been demonstrated that OH exhibits day to day variability, encompassing nearly an order of magnitude in its vertically integrated concentration between the tropopause and the mid mesosphere (22). It is thus tempting to assign a major fraction of the observed variability in ClO to OH but the evidence is thus far circumstantial.

Significantly more data exists on the vertical distribution of methane (23, 24) although limited information is available above 30 km and much of the information is integrated in either time or space. A direct correlation between ClO_x and HCl must await a simultaneous observation of OH, ClO, HCl and CH_4.

With respect to point (b), an appraisal of total stratospheric chlorine is accomplished by a detailed accounting of all chlorine containing molecules known

to exist at the tropopause, summing contributions from each assuming eventual liberation of all chlorine from the parent molecule by photolysis or chemical reacti n. Extensive research has taken place over the past three years (25, 26, 27, 28, 29) demonstrating both the existence of these chemical source terms in the stratosphere and, in many cases, their concentration gradient above the tropopause. It i generally assumed, based upon this accounting, that the total chlorine mixing ratio falls in the range 1.5 to 3.0 ppb as reflected in the choices adopted in the theoretical calculations displayed in Figure 10. However, ClO does not constitute the entire chlorine budget in the upper stratosphere. For example, at 36 km, where the ClO mixing ratio peaks, total chlorine is believed to be shared primarily between ClO and HCl so that

$$[Cl_x] = [ClO] + [HCl] = [ClO] \left\{1 + \frac{[HCl]}{[ClO]}\right\}.$$

However, for typical concentrations of [OH] and $[CH_4]$ and appropriate values for k_5 and k_6 one finds, using Expression [10], that

$$\frac{[HCl]}{[ClO]} \approx 1 \qquad \text{at 36 kilometers.}$$

Thus, for example, the peak mixing ratio ob: rved in the 2 October flight is a factor of two to four higher than the total chlorine mixing ratios of 3.0 and 1.5 ppb respectively would imply. Of course by assuming (1) the OH concentration at the time of the 2 October flight was as high as the maximum observed by Burnett and (2) a total chlorine mixing ratio approximately 30% higher than the maximum now accepted, reasonable agreement is achieved.

Another important consideration with respect to the question of total chlorine is the correlation between observed HCl mixing ratios at 26-28 km of 1 to 2 ppb (30, 31, 32, 33) and the peak observed ClO mixing ratio at 36 km. At 26 km chlorine nitrate and HCl are believed to dominate the total chlorine budget so that

$$[Cl_x] = [HCl] + [ClONO_2] = [HCl]\left\{1 + \frac{[ClONO_2]}{[HCl]}\right\}$$

Theoretical predictions (34) show that if an acceptable pressure dependence is used for $ClONO_2$ formation

$$ClO + NO_2 + M \longrightarrow ClONO_2 + M$$

the concentrations of HCl and $ClONO_2$ are roughly equivalent at this altitude, thus implying total chlorine mixing ratios of 2-4 ppb. In any event the total chlorine mixing ratio cannot be equated with the HCl mixing ratio in the region between 25 and 30 km until an adequate data base exists on the $[ClONO_2]/[HCl]$ ratio in that region. Simultaneous $ClONO_2$-HCl measurements, perhaps by long path IR absorption techniques, are needed to settle the issue.

Figure Captions

Figure 1 A schematic of the instrument detection pod along the flow axis showing the optical and mechanical configuration of the probe.

Figure 2 The vacuum ultraviolet spectrum of atomic chlorine showing the $^2P-^2P$, $^2P-^2D$ and $^2P-^4P$ multiplets.

Figure 3 The emission spectrum of the microwave plasma discharge lamp between 1150 and 1700Å showing the resonance lines corresponding to the energy level diagram of Figure 2.

Figure 4 The emission spectrum of the resonance lamp - O_2 cell combination demonstrates the removal of each resonance line except the 1189Å transition.

Figure 5 The double pod instrument configuration with supporting hardware and descent parachute.

Figure 6 Raw flight data from the 2 October experiment showing the gas addition sequence used in the ClO experiment.

Figure 7 Atomic chlorine and ClO density profiles for the 28 July, 2 October and 8 December flights. Data for each gas addition sequence are shown for ClO, the Cl data represent a 0.5 km integration interval.

Figure 8 Data for the three flights smoothed over a 1 km interval.

Figure 9 Atomic chlorine and ClO plotted in terms of mixing ratios for each flight.

Figure 10 A comparison between the Cl and ClO observation shown in Figure 8 and theoretical calculation of the noon time (30°N latitude) Cl and ClO densities.

Figure 11 A comparison between observed and calculated [Cl]/[ClO] ratios.

BIBLIOGRAPHY

1. S. Chapman, *Phil. Mag.*, 10, 369 (1930).

2. D. R. Bates and M. Nicolet, *J. Geophys. Res.*, 55, 301 (1950).

3. B. G. Hunt, *J. Geophys. Res.*, 71, 1385 (1966).

4. P. J. Crutzen, *Quart. J. Roy. Meteorol. Soc.*, 96, 320 (1970).

5. H. S. Johnston, *Science*, 173, 517 (1971).

6. J. C. McConnel and M. B. McElroy, *J. Atmos. Sci.*, 30, 1465 (1973).

7. R. S. Stolarski and R. J. Cicerone, *Can J. Chem.*, 52, 1582 (1974).

8. M. J. Molina and F. S. Rowland, *Nature*, 249, 810 (1974).

9. S. C. Wofsy and M. B. McElroy, *Can. J. Chem.*, 52, 1582 (1974).

10. P. J. Crutzen, *Can. J. Chem.*, 52, 1569 (1974).

11. J. E. Lovelock, R. J. Maggs and R. J. Wade, *Nature*, 241, 194 (1973).

12. Reaction [1] has been studied over the temperature range 205-630°K: See for example M. A. A. Clyne and W. S. Nip, *J. Chem. Soc. Far. Trans. II*, 72, 838 (1976); R. T. Watson, E. Machado, S. Fischer and D. D. Davis, *J. Chem. Phys.* in press, 1976; M. S. Zahniser, F. Kaufman and J. G. Anderson, *Chem. Phys. Lett.*, 37, 226 (1976); M. J. Kurylo and W. Braun, *Chem. Phys. Lett.*, 37, 232 (1976).

13. Reaction [2] has been studied over the temperature range 220-425°K: M. A. A. Clyne and W. Nip, *Typescript*, Queen Mary College, London, 1976; M. S. Zahniser and F. Kaufman, *Private Communication*, 14 June 1976; P. P. Bemand, M. A. A. Clyne and R. T. Watson, *J. Chem. Soc. Far. Trans. I*, 69, 1356 (1973).

14. Reaction [2] has been studied over the temperature range 230-295°K: M. S. Zahniser and F. Kaufman, *Private Communication*, 14 June 1976; P. P. Bemand, M. A. A. Clyne and R. T. Watson, *J. Chem. Soc. Far. Trans. I*, 70, 2250 (1974).

15. J. G. Anderson, *Geophys. Res. Lett.*, 2, 231 (1975).

16. J. G. Anderson, *Geophys. Res. Lett.*, 3, 165 (1976).

17. N. Basco and R. D. Morse, *J. Mol. Spectrosc.*, 45, 34 (1973).

18. J. A. Coxon and D. A. Ramsay, *Can. J. Phys.*, 54, 1074(1976).

19. The problem of interference resulting from the fluorescence of NO or any contaminant within the injected NO, was studied extensively after an experiment done on 15 May 1976, which looked only at ClO with a single instrument package, showed concentrations of ClO exceeding 10^9 cm^{-3}. It was determined that unpurified NO, which contains the higher oxides of nitrogen, will fluoresce longward of 1400Å when illuminated with 1189Å radiation, although not with sufficient yield to explain the ClO data of 15 May. These data also showed the detector count rate to be independent of the injected NO concentration which would not be expected if NO or any impurity were responsible for the fluorescence. Nevertheless, such a contribution of a contaminant to the count rate of the detector weakens the experiment and the data have not been published. An Ascarite trap to eliminate impurities from the added NO and the inclusion of an interference filter to restrict the detector's sensitivity to the region shortward 1400Å was added on subsequent flights.

20. The theoretical results shown in Figure 10 were communicated privately and represent the most recent work by each of the groups represented: S. C. Liu, R. J. Cicerone and T. M. Donahue: S. C. Wofsy and M. B. McElroy; P. J. Crutzen and M. McAfee; J. Chang and D. J. Wuebbles.

21. J. G. Anderson, *J. Geophys. Res.*, 76, 7820 (1971).

22. C. R. Burnett, *Geophys. Res. Lett.*, 3, 319 (1976).

23. D. H. Ehhalt, L. E. Heidt, R. H. Lueb and E. A. Martell, *J. Atmos. Sci.*, 32, 163 (1975).

24. D. H. Ehhalt, L. E. Heidt, R. H. Lueb and W. Pollack, *Pure Appl. Geophys.*, 113, 389 (1975).

25. R. A. Rasmussan, E. Robinson, D. J. Pierotti, D. R. Cronn, J. Krasnec and D. Harsch, Proceedings of the Symposium on Non-Urban Tropospheric Composition, Miami Beach, Nov. 10-12, 1976, *J. Geophys. Res.* in press.

26. A. L. Schmeltekopf, P. D. Goldan, W. R. Henderson, W. J. Harrop, T. L. Thompson, F. C. Fehsenfeld, H. I. Schiff, P. J. Crutzen, I. S. A. Isaksen and E. E. Ferguson, *Geophys. Res. Lett.*, 2, 393 (1975).

27. L. E. Heidt, R. Lueb, W. Pollock and D. H. Ehhalt, *Geophys. Res. Lett.*, 2, 445 (1975).

28. W. J. Williams, J. J. Kosters, A. Goldman and D. G. Murcray, *Geophys. Res. Lett.*, 3, 379 (1976).

29. A detailed analysis of chlorine sources appears in *"HALOCARBONS: EFFECTS ON STRATOSPHERIC OZONE" (H. S. GUTOWSKY, CHAIRMAN) NATIONAL ACADEMY OF SCIENCES*, Sept., 1976.

BIBLIOGRAPHY (Cont.)

30. W. I. Williams, J. J. Kosters, A. Goldman and D. G. Murcray, *Geophys. Res. Lett.*, 3, 383 (1976).

31. C. B. Farmer, O. F. Rader and R. H. Norton, *Geophys. Res. Lett.*, 3, 13 (1976).

32. M. Ackerman, D. Frimout, A. Girard, M. Gottignies and C. Mueller, *Geophys. Res. Lett.*, 3, 81 (1976).

33. A. L. Lazrus, B. W. Gandrud, R. N. Woodard and W. A. Sedlacek, *Geophys. Res. Lett.*, 2, 439 (1975).

34. R. J. Cicerone and S. C. Liu, *Private Communication*, Feb., 1977.

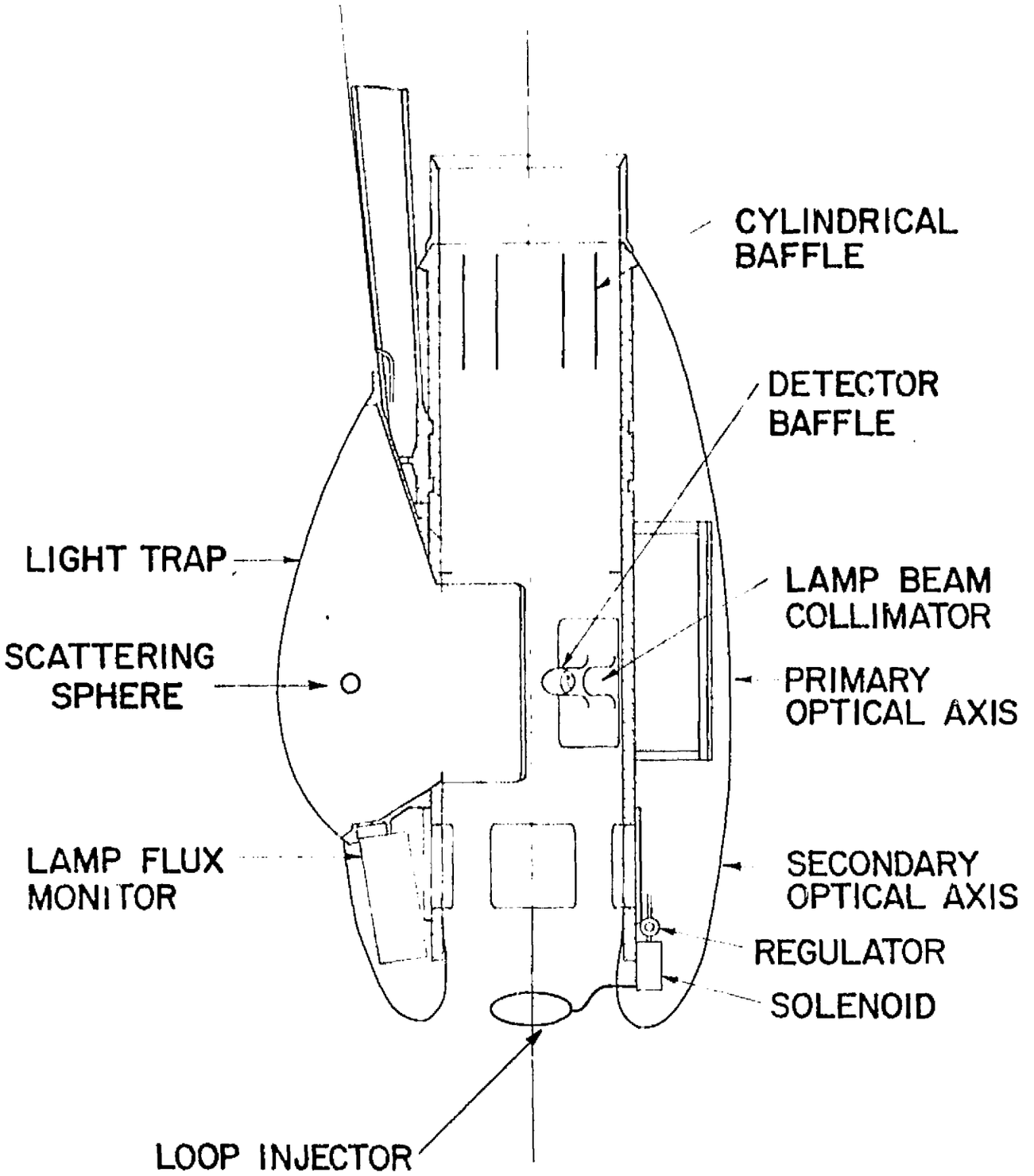
CYLINDRICAL BAFFLE
DETECTOR BAFFLE
LIGHT TRAP
LAMP BEAM COLLIMATOR
SCATTERING SPHERE
PRIMARY OPTICAL AXIS
LAMP FLUX MONITOR
SECONDARY OPTICAL AXIS
REGULATOR
SOLENOID
LOOP INJECTOR

E22

Figure 1

ATOMIC CHLORINE
ENERGY LEVEL DIAGRAM

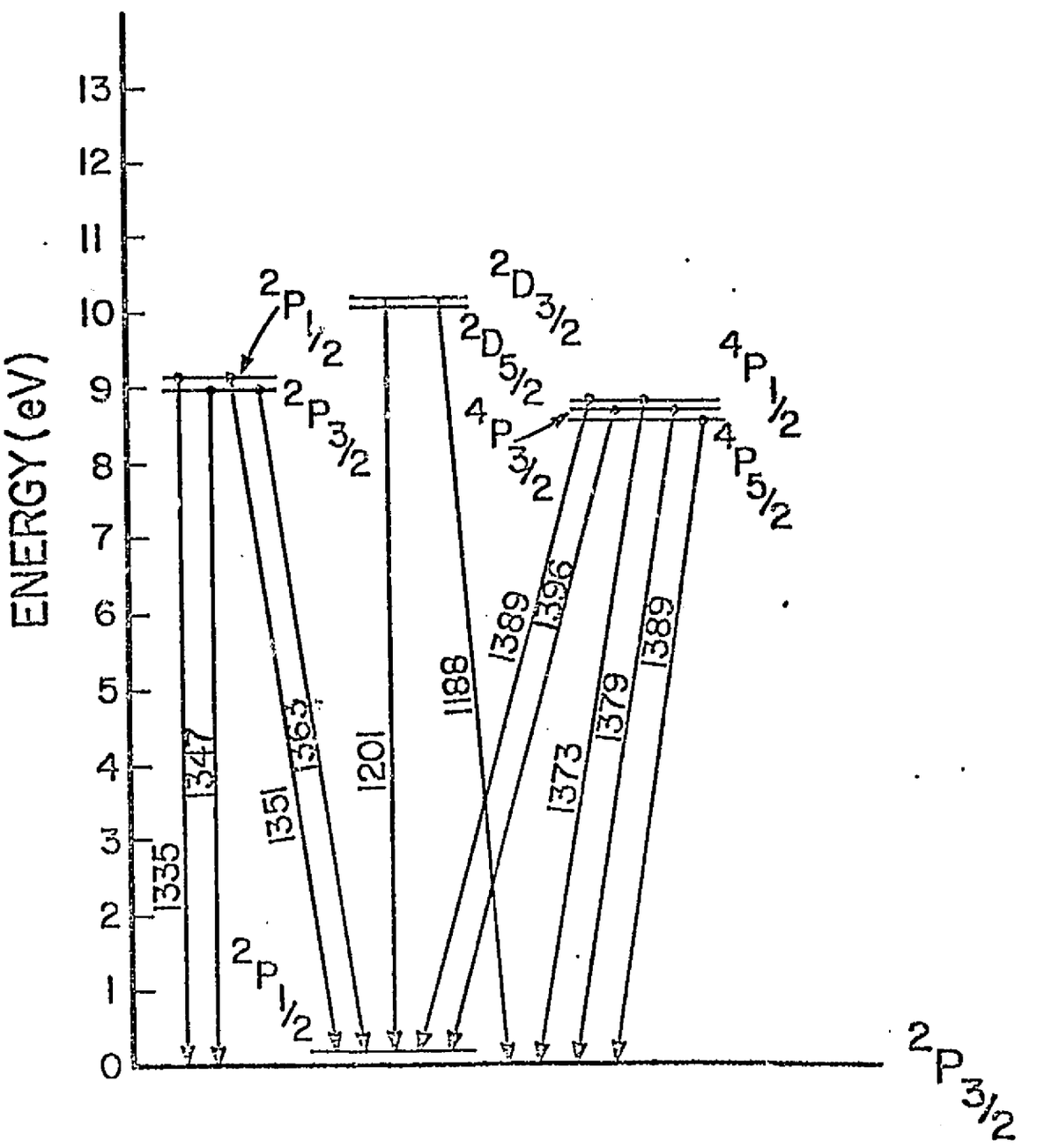

Figure 2

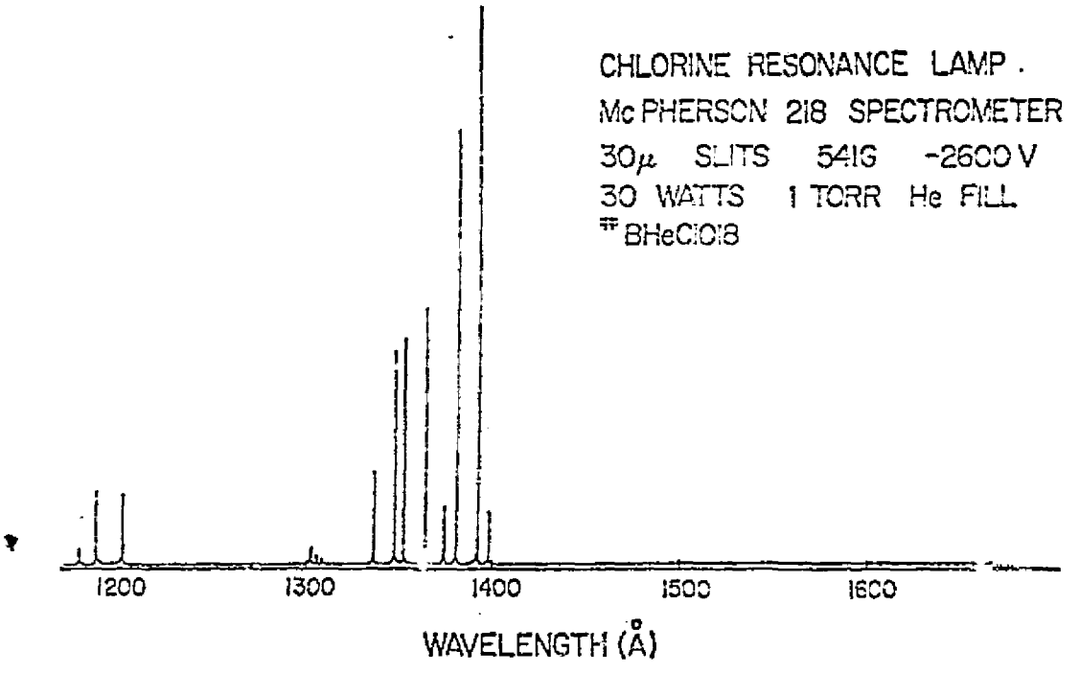
CHLORINE RESONANCE LAMP.
Mc PHERSON 218 SPECTROMETER
30μ SLITS 541G -2600 V
30 WATTS 1 TORR He FILL
∓ BHeClO18
1200
1300
1400
1500
1600
WAVELENGTH (Å)

Figure 3

FLIGHT LAMP + 0.5cm O_2 AT 750 TORR
McPHERSON 218 30μ SLITS
100Å/IN 3×10^{-8} AMPS FULL SCALE
EMR 541G -2500 VOLTS

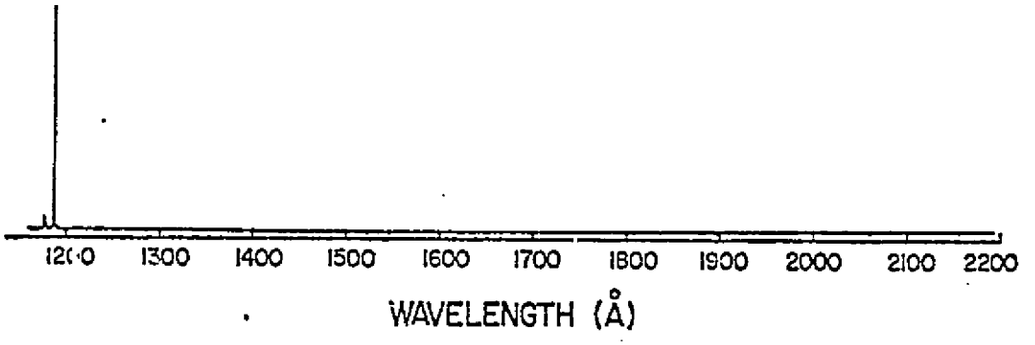

Figure 4

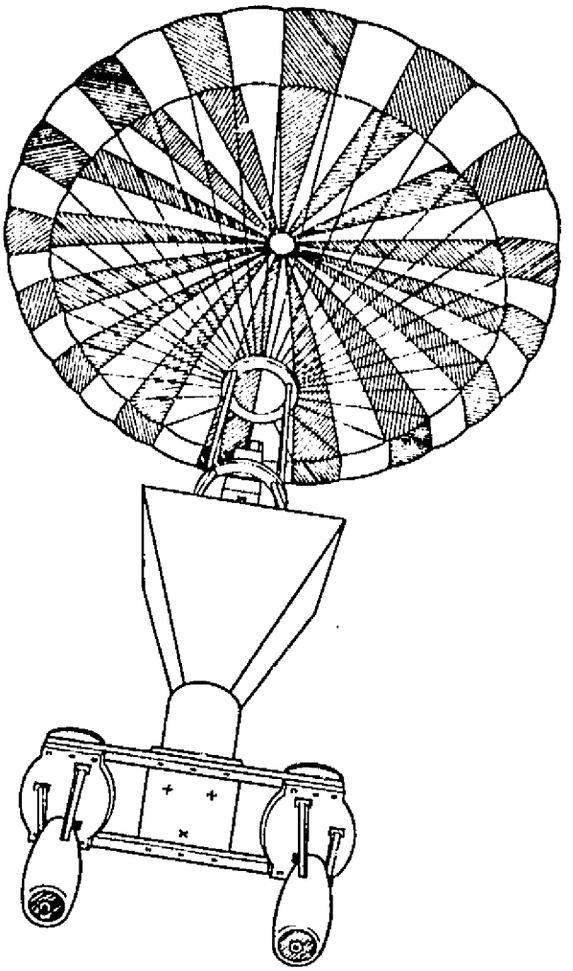

Figure 5

NO FLOW RATE (scc/sec)
60
50
40
30
20
10
ct/sec
10,000
5,000
29
28
27
26
ALTITUDE (km)

Figure 6

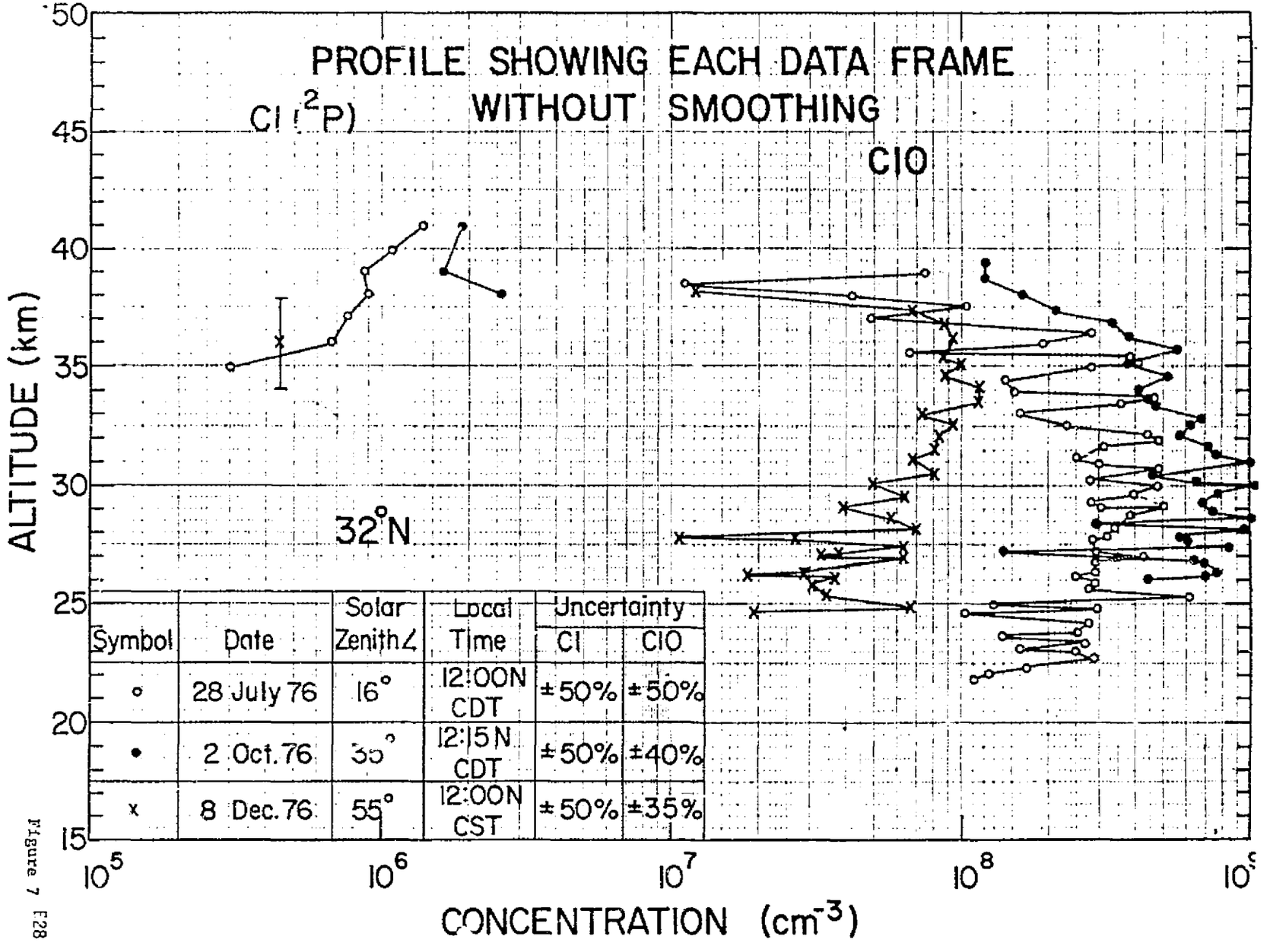
PROFILE SHOWING EACH DATA FRAME
WITHOUT SMOOTHING
Cl (^{2}P)
ClO
32°N
ALTITUDE (km)
CONCENTRATION (cm^{-3})
50
45
40
35
30
25
20
15
10^5
10^6
10^7
10^8
Symbol | Date | Solar Zenith∠ | Local Time | Uncertainty Cl | Uncertainty ClO
○ | 28 July 76 | 16° | 12:00N CDT | ±50% | ±50%
● | 2 Oct. 76 | 35° | 12:15N CDT | ±50% | ±40%
× | 8 Dec. 76 | 55° | 12:00N CST | ±50% | ±35%

Figure 7 F28

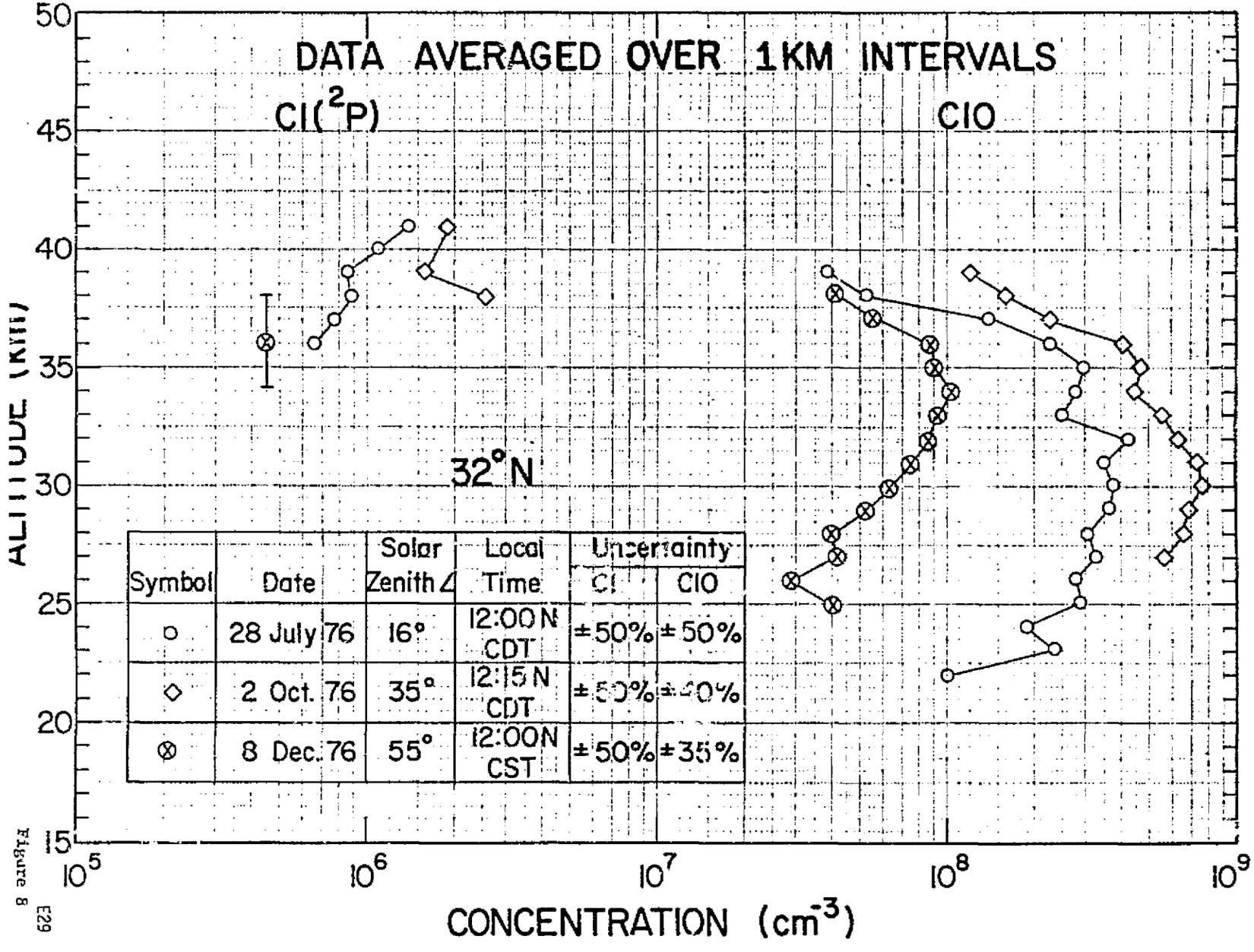
DATA AVERAGED OVER 1KM INTERVALS
Cl(^{2}P)
ClO
32°N
ALTITUDE (KM)
CONCENTRATION (cm^{-3})
50
45
40
35
30
25
20
15
10^5
10^6
10^7
10^8
10^9
Symbol | Date | Solar Zenith ∠ | Local Time | Uncertainty Cl | Uncertainty ClO
○ | 28 July 76 | 16° | 12:00 N CDT | ±50% | ±50%
◇ | 2 Oct. 76 | 35° | 12:15 N CDT | ±50% | ±50%
⊗ | 8 Dec. 76 | 55° | 12:00N CST | ±50% | ±35%

Figure 8

E29

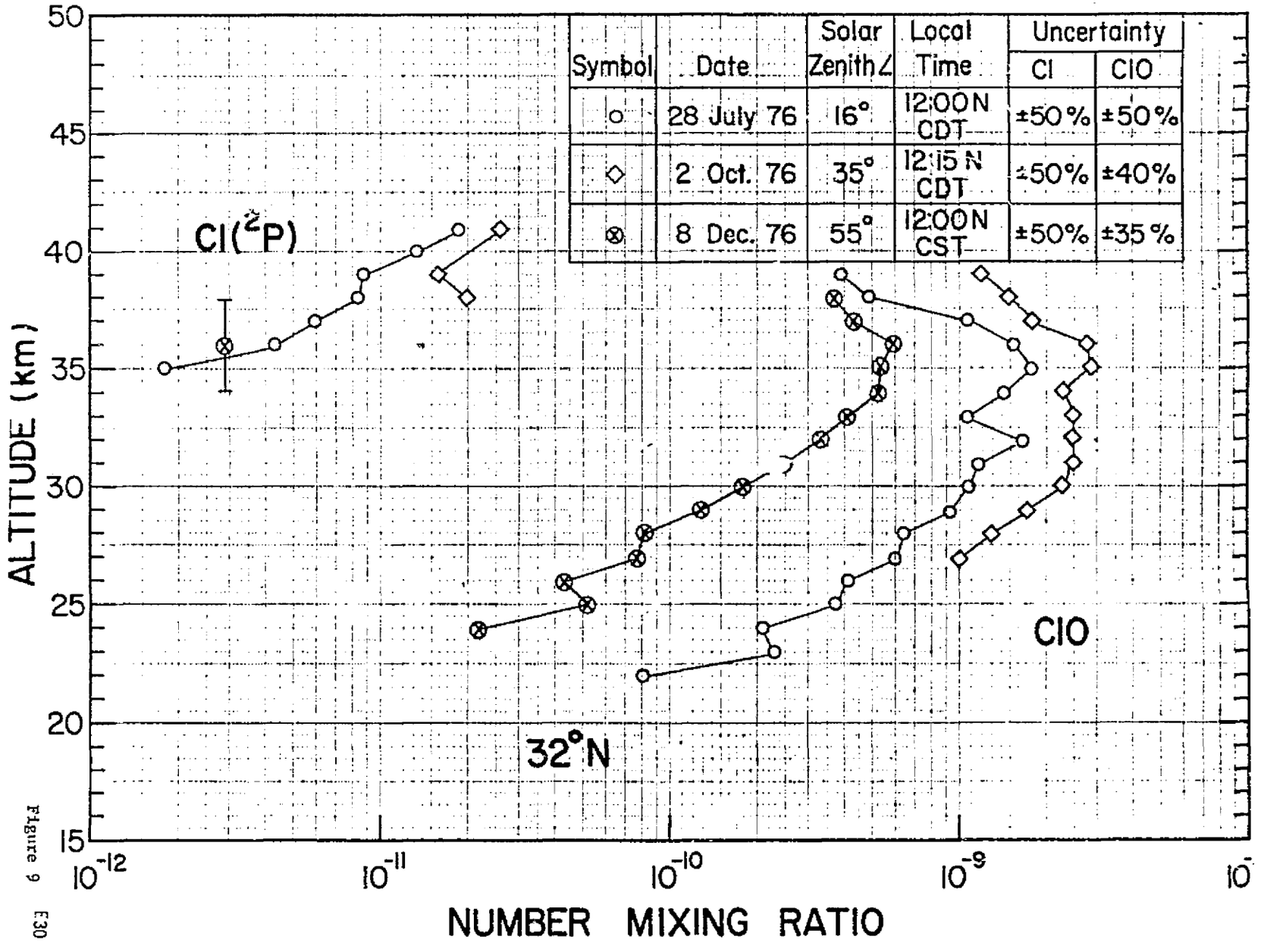
Symbol
Date
Solar Zenith ∠
Local Time
Uncertainty
Cl
ClO
○ 28 July 76 16° 12:00 N CDT ±50% ±50%
◇ 2 Oct. 76 35° 12:15 N CDT ±50% ±40%
⊗ 8 Dec. 76 55° 12:00 N CST ±50% ±35%
Cl(²P)
ClO
32°N
ALTITUDE (km)
NUMBER MIXING RATIO
50
45
40
35
30
25
20
15
10⁻¹²
10⁻¹¹
10⁻¹⁰
10⁻⁹

Figure 9

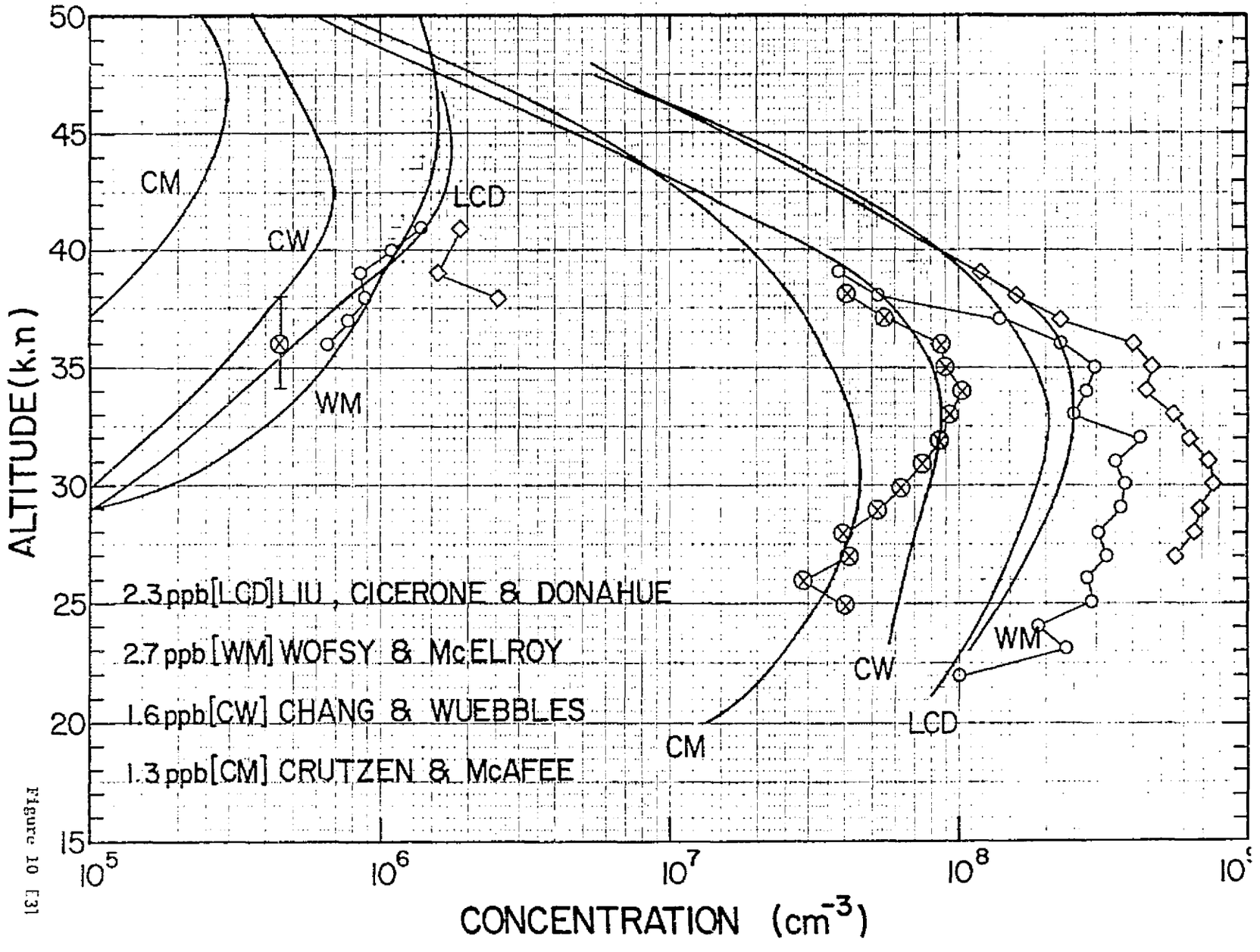
ALTITUDE(k.m)
CONCENTRATION (cm^{-3})
50
45
40
35
30
25
20
15
10^5
10^6
10^7
10^8
CM
CW
LCD
WM
2.3 ppb[LCD] LIU, CICERONE & DONAHUE
2.7 ppb [WM] WOFSY & McELROY
1.6 ppb[CW] CHANG & WUEBBLES
1.3 ppb[CM] CRUTZEN & McAFEE

Figure 10 [31]

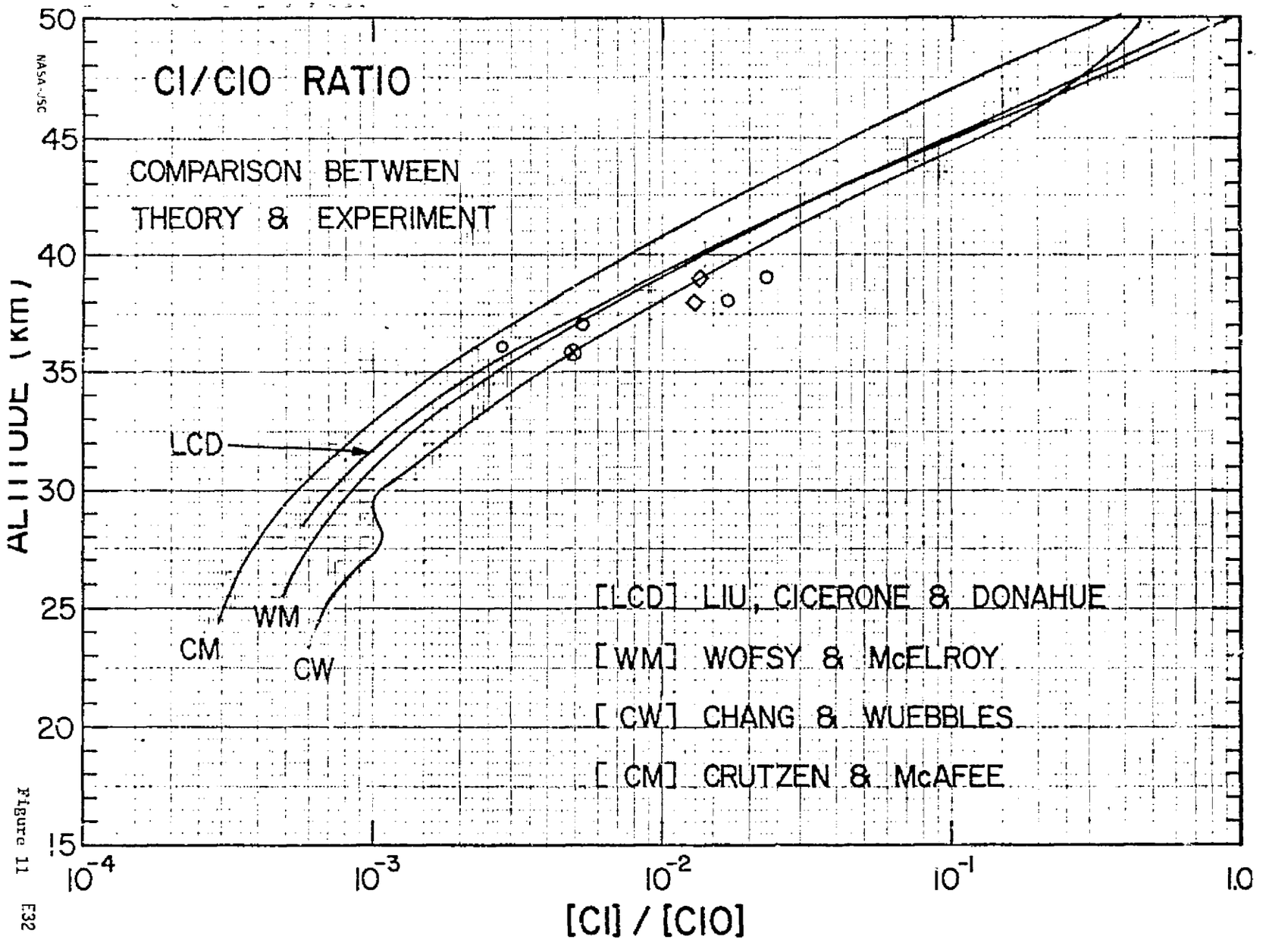

NASA-JSC

Figure 11

E32